INFORMATION TO USERS

This manuscript has been reproduced from the microfilm master. UMI films the text directly from the original or copy submitted. Thus, some thesis and dissertation copies are in typewriter face, while others may be from any type of computer printer.

The quality of this reproduction is dependent upon the quality of the copy submitted. Broken or indistinct print, colored or poor quality illustrations and photographs, print bleedthrough, substandard margins, and improper alignment can adversely affect reproduction.

In the unlikely event that the author did not send UMI a complete manuscript and there are missing pages, these will be noted. Also, if unauthorized copyright material had to be removed, a note will indicate the deletion.

Oversize materials (e.g., maps, drawings, charts) are reproduced by sectioning the original, beginning at the upper left-hand corner and continuing from left to right in equal sections with small overlaps. Each original is also photographed in one exposure and is included in reduced form at the back of the book.

Photographs included in the original manuscript have been reproduced xerographically in this copy. Higher quality 6" x 9" black and white photographic prints are available for any photographs or illustrations appearing in this copy for an additional charge. Contact UMI directly to order.

UMI

A Bell & Howell Information Company
300 North Zeeb Road, Ann Arbor MI 48106-1346 USA
313/761-4700 800/521-0600

Regulation of the Ste4p G protein beta Subunit Activity in the Pheromone Response Pathway of *Saccharomyces cerevisiae*

by

Jinah Kim

A dissertation submitted to the Graduate Faculty in Biomedical Sciences in partial fulfillment of the requirements for the degree of Doctor of Philosophy, The City University of New York.

1998

Approval Page

This manuscript has been read and accepted for the Graduate Faculty in Biomedical Sciences in satisfaction of the dissertation requirement for the degree of Doctor of Philosophy.

July 21, 1998
Date

Paul B. Lazarow
Chair of Examining Committee

July 22, 1998
Date

Terry A. Krulwich
Executive Officer

Avrom Caplan

Jeanne Hirsch

James Konopka

Gianni Piperno

Supervisory Committee

The City University of New York

Regulation of the Ste4p G protein beta Subunit Activity in the Pheromone Response Pathway of *Saccharomyces cerevisiae*

Abstract

Advisor: Professor Jeanne P. Hirsch

The pheromone response in *Saccharomyces cerevisiae* is activated by the binding of pheromone to its receptor, which belongs to the G protein-coupled receptor family. The Gβγ complex transduces the signal in the pheromone response, which results in arrest in the G_1 phase of the cell cycle, transcriptional activation of mating-specific genes, and cellular morphogenesis.

The mechanism of receptor-mediated heterotrimeric G-protein activation has been thoroughly investigated. However, the regulatory mechanisms controlling Gβγ complex activity subsequent to dissociation from Gα-GTP are not well-understood. The goal of this work was to investigate mechanisms of regulating Gβγ activity in the pheromone response pathway through 1) characterization of Ste4p-mediated receptor inhibition and 2) identification of the mating function of *SSF1*.

The $STE3^{DAF}$ mutation results in the inappropriate expression of **a**-factor receptor (Ste3p) in *MAT***a** cells. Expression of this receptor inhibits

pheromone-induced cell cycle arrest, a phenomenon termed receptor inhibition. *STE4*^{SD} alleles were isolated which were able to reverse receptor inhibition. The Ste4p^{SD} was capable of restoring both pheromone-mediated cell cycle arrest and transcriptional activation in *STE3*^{DAF} cells. To identify the mechanism of Ste4p-mediated receptor inhibition the localization of Ste4p was observed in *STE3*^{DAF} cells. The Ste4p-GFP fusion protein appeared to be differentially localized in *STE3*^{DAF} cells compared to wild type cells after pheromone exposure. The results suggest that G-protein signaling may be controlled through regulating the Gβγ localization in response to different signals from the cell surface.

Characterization of the mating function of *SSF1* was also examined. *SSF1* and *SSF2* are redundant essential genes, which when overexpressed, results in increased mating efficiency in a strain containing a defective Gβ subunit. Overexpression of *SSF1* resulted in increased mating projection formation. Cells depleted of Ssfp proteins were defective in projection formation. These results suggested that Ssf1p may increase mating efficiency through regulating cellular morphogenesis. A Ssf1p-GFP fusion demonstrated nucleolar localization, which suggested that Ssf1p may indirectly promote projection formation.

Acknowledgments

First, I would like to thank my advisor, Dr. Jeanne Hirsch, for supporting me and giving me the opportunity to explore science under her guidance. Jeanne has been an excellent advisor and scientist from whom I have learned so many things.

I would especially like to thank Dr. Avrom Caplan, Dr. Gillian Small, Dr. Serafín Piñol-Roma, Dr. Scott Henderson, and Dr. Gianni Piperno for the knowledge they shared with me during this period. I would also like to thank all of the members of the Department of Cell Biology and Anatomy for constantly teaching me and creating a supportive environment. In particular, I would like to thank my lab mates Yong Xue and Montserrat Batlle for all the help and interesting discussions.

Finally, I would like to thank my best friends, Daphna Eisenberg and Dan Eisenberg, without whose constant support and encouragement my work would never have been completed.

Table of Contents

List of Tables

List of Figures

I. Introduction

A. Heterotrimeric G protein signal transduction

Diverse stimuli including hormones, photons, neurotransmitters, phospholipids, peptides and odorants activate members of the G-protein coupled receptor (GPCR) family. The extracellular activation of a GPCR, promotes intracellular responses by activation of effector proteins through heterotrimeric G proteins. Members of the G protein-coupled receptor family share common structural characteristics, including seven hydrophobic transmembrane domains and a hydrophilic carboxy-terminal tail (reviewed in (41)). The intracellular domains of the serpentine receptors mediate interaction with the heterotrimeric G proteins, which in turn activate the appropriate effectors. Heterotrimeric G proteins are composed of α, β and γ subunits and are encoded by many genes, which includes at least 20 Gα, 6 Gβ, and 12 Gγ mammalian genes (reviewed in (59)).

The heterotrimer is associated with the receptor in the inactive state in which the α subunit is bound to GDP. Ligand-mediated activation causes a conformational change in the receptor that results in GDP release. The high intracellular concentration of GTP results in its rapid binding to the α subunit, which causes a conformational shift and dissociation of the α from

the βγ complex. The Gβγ complex is effectively a single functional unit and can only be separated by denaturing conditions. Downstream effectors may be activated by Gα-GTP or free Gβγ complexes.

Effectors of Gα and Gβγ

The many Gα subunits can be categorized into four main classes based on the cellular response elicited as follows: $G\alpha_s$, which activates adenylate cyclase, $G\alpha_i$, which inhibits adenylate cyclase, $G\alpha_q$, which activates phospholipase C-β, and $G\alpha_{12}$, which has largely unknown function. The amino acid sequence of the Gβ subunit contains seven WD repeats which form a seven-bladed propeller structure composed of repeating β-sheets. The Gβγ complex does not undergo a conformational change upon dissociation from Gα which suggests that Gα confers negative regulation by binding to and blocking the Gβγ effector interface (20, 135). In mammalian systems the Gβγ complex is responsible for activation of a variety of effectors, including phospholipase C-β, phospholipase A_2, G protein-gated inward rectifier K^+ channels, adenylyl cyclase, and G protein- coupled receptor kinases (reviewed in (26)).

Regulators of Gα and Gβγ signaling

Signal deactivation is dependent on the intrinsic rate of hydrolysis of GTP by Gα. The Gα-GDP complex induces dissociation of Gα from effectors

and reassociation with Gβγ. The slow catalytic activity of Gα may be modulated by a growing family of regulators of G protein signaling (RGS proteins) (reviewed in (8)). RGS proteins are GTPase activating proteins (GAPs) for Gα subunits, conferring negative regulation on G protein signaling. The first RGS gene, *SST2*, was identified in *S. cerevisiae* by a mutation that prevents recovery from pheromone-induced growth arrest (16, 17, 39). A characteristic 120-residue RGS core is present in at least 19 mammalian genes (8), therefore RGS protein-mediated regulation of GTPase activity will likely prove to be a widespread mechanism of regulating G protein signaling.

Phosducin is thought to regulate G protein signaling by binding to the Gβγ complex and preventing the reassociation with Gα-GDP (5, 87). It has been demonstrated that a region of the carboxy terminus of phosducin is sufficient for high affinity interactions with the Gβγ complex (9). In addition, it has recently been demonstrated that an interaction between phosducin and Gα may increase the extent of inhibition on G protein signaling (4). Protein kinase A-dependent phosphorylation of phosducin prevents the inhibitory effects of phosducin on G protein signaling (5), however the biological significance of this finding is not known.

B. The pheromone response pathway signal transduction

Cells respond to their external environment by recognizing an extracellular signal, transmitting the signal across the cell membrane, and

eliciting a response through activation of the appropriate signal transduction pathway. The pheromone response in the budding yeast *Saccharomyces cerevisiae* is initiated by the binding of a secreted peptide pheromone to its cell surface receptor. Mating occurs between haploid cells of opposite mating types, which are either **a** or α mating type. The differential expression of mating type specific genes is controlled by regulatory proteins encoded by the mating-type (*MAT*) locus (reviewed in (137)). The *MAT*α gene encodes two proteins, Matα1p and Matα2p which regulate the transcription of the mating-type specific genes. In *MAT*α cells, expression of α-specific genes, such as the α-factor structural genes and the **a**-factor receptor is positively regulated by Matα1p. Transcription of **a**-specific genes, such as the **a**-factor structural genes and the α-factor receptor is repressed by Matα2p. *MAT***a** cells do not express either Matα1p or Matα2p. Therefore, they express only **a**-specific genes, because α-specific genes are not induced and **a**-specific genes are not repressed.

Signal transduction of the pheromone response pathway

Haploid *MAT***a** and *MAT*α cells produce the secreted peptide pheromones **a**-factor and α-factor, respectively. These pheromone ligands bind to the appropriate receptor located on the surface of cells of the opposite mating type; the **a**-factor receptor (encoded by *STE3*) is present on the surface of *MAT*α cells and the α-factor receptor (encoded by *STE2*) is present on the cell surface of *MAT***a** cells (reviewed in (138))(See Table 1- Gene List). The pheromone receptors are members of the G protein-coupled receptor family and are coupled to a heterotrimeric G-protein composed of α, β, and γ

subunits (encoded by *GPA1*, *STE4*, and *STE18*). The yeast pheromone response pathway utilizes two common eukaryotic signaling modules, a heterotrimeric G protein and a mitogen-activated protein (MAP) kinase cascade (49) (Figure 1-1). The G protein βγ complex transduces the signal to the downstream kinase cascade most likely through the p21-activated kinase (PAK) homologue, Ste20p (89, 94). The serine-threonine kinase Ste20p phosphorylates the mammalian MEKK homolog, Ste11p (155). Ste11p then phosphorylates and activates the MEK homolog, Ste7p (101). The dual specificity kinase, Ste7p, in turn phosphorylates the MAP kinases Fus3p and Kss1p, which have partially redundant function (48).

Initial epistasis experiments suggested that Ste5p acts at a step between Ste20p and Ste11p (61, 85, 139). However, more recent results demonstrate that the pheromone pathway signal transduction is not a simple linear pathway. Ste5p forms a molecular scaffold by interacting with each of the components of the MAP kinase cascade (25, 95, 112). In addition, Ste5p contains a cysteine-rich domain similar to the LIM-type zinc-finger which has been demonstrated to mediate dimerization and signal transduction (70, 156). Therefore, Ste5p may act as a scaffold protein to maintain specificity of the many cellular kinases or may act in a manner analogous to receptor tyrosine kinases to promote cross-phosphorylation of the associated kinases.

Figure 1-1. Schematic representation of the pheromone response pathway in *Saccharomyces cerevisiae*.

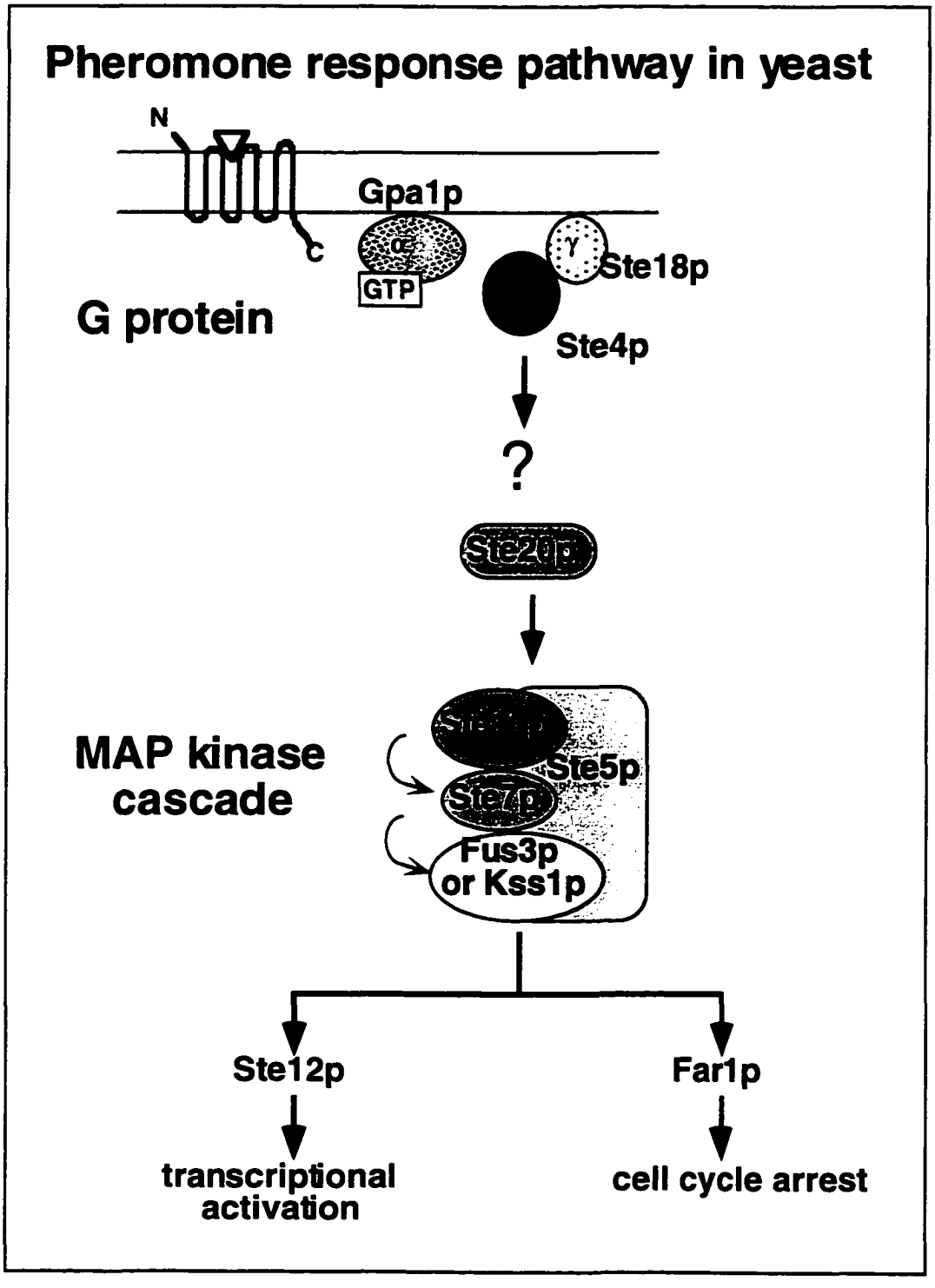

C. Major responses of pheromone pathway activation

Mating pathway signaling results in transcription of mating-specific genes and arrest in the G_1 phase of the cell cycle. Activated MAP kinase phosphorylates Ste12p which is the transcription factor required for mating specific transcriptional activation (43, 46, 47). The Ste12p transcription factor promotes transcription of mating-specific genes by binding to the pheromone-response elements (PRE) located in the upstream regulatory regions of pheromone-regulated genes (43, 47). Mating-specific genes are required for functions including G_1 arrest, polarized morphogenesis, cell adhesion, cell fusion, karyogamy, and desensitization of the signal (reviewed in (83)).

The other target of the MAP kinases is Far1p, the cyclin-dependent kinase inhibitor. The activated MAP kinase phosphorylates Far1p and promotes the association of Far1p with the Cln-Cdc28p kinase complex (105, 106, 145). Cdc28p is the budding yeast homologue of $p34^{cdc2}$ and is the catalytic subunit of the cyclin-dependent kinase (CDK) that promotes progression through the cell cycle (154). G_1 cyclins (encoded by *CLN1*, *CLN2*, and *CLN3*) are the regulatory components of the CDK required for the G_1 to S transition (121, 154). The binding of Far1p to the G_1 cyclin-dependent kinase results in inactivation of the complex, and thus arrest in the G_1 phase of the cell cycle (106). Arrest in the G_1 phase of the cell cycle prior to initiation of Start prevents initiation of a new cycle of DNA synthesis and budding. Therefore, conjugating yeast cells arrest in the G_1 phase of the cell cycle at a stage when

both mating partners contain haploid nuclear content. Nuclear fusion during zygote formation results in formation of a nucleus with diploid nuclear content.

In addition to pheromone-induced transcriptional activation and cell cycle arrest, morphological changes are also induced in response to pheromone stimulation. The cell undergoes morphological changes by promoting projection formation towards the direction of the highest pheromone concentration (127). The ability to sense the pheromone gradient, create polarity within the cell, and form a projection towards the highest pheromone gradient is important for high efficiency mating. Cells that are not capable of projection formation are characterized with weak mating defects when mated to wild type cells and severe mating defects when both partners contain defects in polarized morphogenesis (22, 81).

Cell polarization and projection formation

Cells undergo polarized morphogenesis during bud formation and mating projection formation, however differences exist between these two processes. Bud formation occurs in haploid or diploid cells during the vegetative life cycle, whereas mating projection formation occurs in haploid cells, which are preparing for conjugation, after exposure to pheromone. Cells forming mating projections are morphologically dissimilar from budding cells (Figure 1-2). Conjugating yeast lack the tight constriction present at the bud neck, a junction between the mother and daughter cell (See arrowhead,

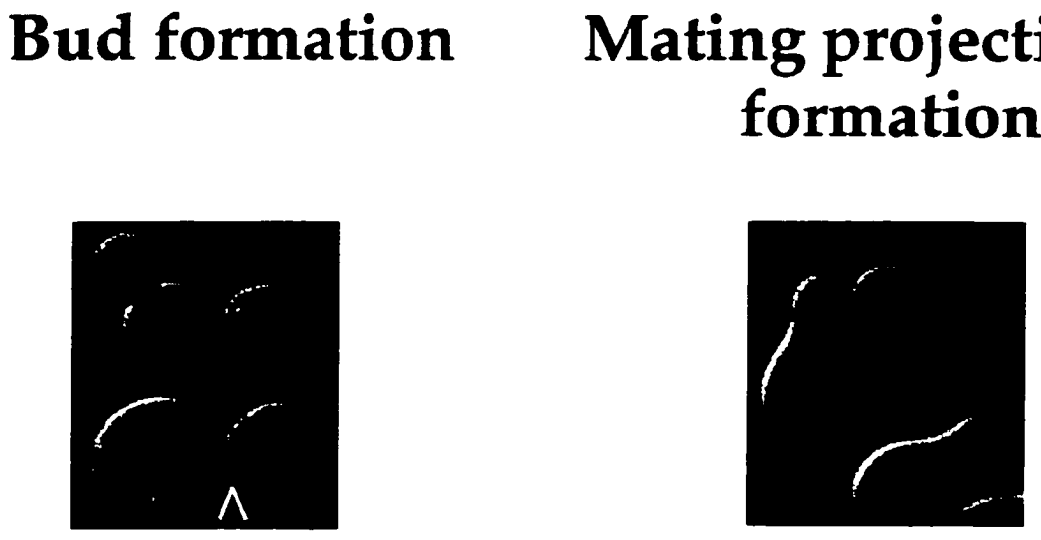

Figure 1-2. Morphology of cells undergoing bud formation and mating projection formation.

Morphology of vegetative cells undergoing bud formation (left) as compared to cells preparing for conjugation undergoing projection formation (right). Live cells were photographed using differential interference optics.

Figure 1-2). Vegetative yeast undergo bud formation in late G_1 which progresses through the cell cycle, whereas, haploid mating yeast are arrested in the G_1 phase of the cell cycle. Finally, bud site selection is genetically predetermined, whereas mating projection site selection is dependent on external cues. Mating cells must sense and respond to the pheromone gradient by polarizing towards a mating partner; the cell must override its intrinsic polarity and repolarize the cytoskeleton and secretory apparatus to deliver proteins involved in secretion and fusion to the mating projection tip.

Despite the differences mentioned above, significant similarities also exist between bud formation and projection formation. Both of these processes require a spatially restricted growth in the plasma membrane and rearrangement of the cell wall. Polarized morphogenesis of mating projection formation and bud formation both require similar events involving the following steps: 1) site selection, 2) polarity establishment, and 3) organization of the cytoskeleton toward the region of polarized growth. In addition, certain proteins have conserved functions during bud and projection formation.

Site selection

The first step in cellular morphogenesis is site selection, which requires recognition of a landmark to promote the localization of polarity establishment proteins to the site of cell growth (23). The pheromone receptor genes, *STE2* and *STE3*, encode proteins that are thought to be

involved in site selection during projection formation. Cells expressing a mutation of the *STE2* gene (*ste2-T326*), which encodes a C-terminal truncation of the α-factor receptor, do not form projections; however, they are still capable of signaling (81). Receptor clustering is observed in cells exposed to pheromone (72). The intracellular domains of receptors may cluster in response to pheromone binding and act as the spatial cue for the recruitment of polarity establishment proteins.

Polarity establishment

The next step in cellular morphogenesis is polarity establishment (Figure 1-3). *CDC42*, *CDC24*, and *BEM1* are three genes known to be required for polarized axis formation. Cells containing mutations in these polarity establishment genes enlarge isotropically and are unable to localize cell-surface growth to form projections. The polarity establishment proteins Cdc42p, Cdc24p and Bem1p localize to the bud tip, a region of polarized cell growth during bud formation (1, 19, 22, 24). Polarity establishment during mating projection formation also requires the same set of proteins: Cdc42p, Cdc24p, and Bem1p with the addition of Spa2p (22, 51). These polarity establishment genes encode a diverse group of proteins required for polarized axis formation. Cdc42p is a Rho-type GTPase, and Cdc24p is its associated guanine nucleotide exchange factor (GEF). The human homologue of Cdc42p (Cdc42Hs) regulates formation of filopodia (102). Spa2p is predicted to form a coiled-coil structure, which may promote filament formation required for interaction with cytoskeletal elements (51). Bem1p contains two src-

homology 3 (SH3) domains which may be important for interaction with the cytoskeleton (22, 51).

Organizing the cytoskeleton

The final event in projection formation is organization of the cytoskeleton and secretory apparatus toward the region of polarized growth. Actin is thought to be required during bud formation to orient the secretory pathway towards the presumptive bud tip (3). The actin cytoskeleton is essential for polarized growth, however, there are actin-dependent and actin-independent processes that serve to define a functional order for proteins involved in establishment of cell polarity. Cdc42p and Bem1p are the first polarity establishment proteins that localize to the incipient bud tip in an actin-independent manner (3). After Cdc42p and Bem1p mark the incipient bud site, Spa2p and cytoskeletal elements called septins (Cdc10p, Cdc11p, Cdc12p) are targeted to the incipient bud site independently of actin (3). During projection formation, it is probable that Cdc42p localizes to the projection tip early and promotes the organization of the actin cytoskeleton.

It has been suggested that proteins essential for signal transduction form a signaling complex which activates a group of proteins called the morphology complex. Bem1p was shown to interact with Ste5p, Ste20p, actin and Far1p (88, 92). The finding that Bem1p associates with signaling molecules and cytoskeletal elements suggests a role in bridging the signaling complex to the morphology complex. Therefore, the morphology complex is

composed of proteins that promote localized and polarized growth of the cell and links the signaling complex to the cytoskeletal network.

Mutations in two genes, *SPA2* and *FAR1*, define two different classes of defects in projection formation. Spa2p is a polarity establishment protein that restricts cell growth to the bud tip in vegetatively growing cells (133). A strain containing a null allele of *SPA2* enlarges in a uniform manner and has a rounder appearance compared to wild type cells due to the inability to properly polarize and restrict growth (133). Strains containing null alleles of *SPA2* are defective in projection formation (51).

In addition to its role as a cyclin-dependent kinase inhibitor, Far1p also regulates polarity during mating. The carboxy-terminal domain of Far1p is involved in regulating cellular morphology (146). Cells containing the *far1Δc* allele, which encodes a protein lacking the carboxy terminus, form normal pheromone-dependent projections. However, the cells are defective in orienting the projection towards the highest pheromone concentration and instead form projections in the direction of the incipient bud site (146). Cells exposed to pheromone must ignore internal cues that promote bud formation to reestablish polarity and direct the secretory apparatus in the direction of the highest pheromone gradient to promote mating. This mutation identified a novel function for Far1p in regulating the orientation of the mating projection toward the mating partner, however, the mechanism by which Far1p controls polarity is still unknown (146).

D. Adaptation to pheromone signaling

A characteristic of biological signaling systems is the ability to undergo adaptation by decreasing the response to a prolonged stimulus. Haploid yeast exposed to pheromone undergo cell cycle arrest and prepare for fusion. However, if conjugation does not occur it is essential to terminate signaling and resume vegetative growth. Adaptation from pheromone response pathway signaling occurs at many levels including, pheromone, receptor, and G proteins. Mutations in genes that act as negative regulators of pheromone pathway signaling display increased sensitivity to pheromone and define different steps in adaptation.

Degradation of pheromones

α-factor is produced by *MAT*α cells and binds to the α-factor receptor present on the cell surface of *MAT***a** cells. *MAT***a** cells produce a secreted endopeptidase, encoded by *SST1* (*BAR1*) (93). The **a**-specific *SST1* gene product cleaves α-factor and promotes recovery of *MAT***a** cells from pheromone pathway signaling. In addition, a membrane-associated **a**-factor degrading activity has been demonstrated in *MAT*α cells (96). Therefore, the concentration of pheromone in the environment is regulated by production of pheromone-specific peptidases.

Receptor desensitization

In mammalian systems, the decreased response to exposure of a specific agonist, termed homologous desensitization, involves phosphorylation of

receptors by second messenger-dependent kinases and G protein-coupled receptor kinases (reviewed in (50)). The GRKs are targeted to the plasma membrane by free Gβγ complexes (109). As a result of receptor phosphorylation by GRKs, an inhibitory protein of the arrestin family is targeted to the receptor (reviewed in (50)), which stimulates the endocytic uptake of receptors from the cell surface.

Pheromone receptor phosphorylation and ubiquitination

The hydrophilic C-terminal tail of members of the GPCR family has been demonstrated to be important to receptor desensitization. In *S. cerevisiae*, deletion of the C-terminal hydrophilic domain of the pheromone receptors results in increased sensitivity to pheromone, which suggests that the carboxy terminal domain serves as an important regulatory domain for receptor function (10, 81, 119). Analysis of receptor truncation mutations is complicated by the fact that the C-terminal cytoplasmic tail is required for several cellular functions. Cells containing a mutation in *STE2* (*ste2-T326*), which encodes a carboxy terminally truncated receptor, display increased sensitivity to pheromone and defects in the morphological response to pheromone (81).

Both the α-factor receptor (Ste2p) and the **a**-factor receptor (Ste3p) are subject to phosphorylation within their C-terminal domains (119, 158). It is apparent that phosphorylation of Ste2p is a regulatory modification, as mutation of the distal phosphorylation sites in the C-terminal tail of Ste2p resulted in an increase in sensitivity to pheromone. These results

demonstrated that receptor phosphorylation results in pheromone pathway desensitization (21). Determination of the exact role of phosphorylation in receptor function is complicated by the fact that the receptor kinase has not been identified.

In addition to pheromone-stimulated phosphorylation, the pheromone receptors are subject to constitutive phosphorylation (158). It has been proposed that constitutive phosphorylation of receptors may serve as a molecular tag to identify old receptors destined for degradation (21, 72). The ability to differentiate old and new receptors may suggest a means of promoting polarity within the cell and signaling may initiate from newly synthesized receptors (21, 72).

The pheromone receptors are also subject to ligand-dependent and constitutive ubiquitination (65, 124). Strains containing mutations in ubiquitin conjugating enzymes display defects in Ste2p internalization, suggesting that ubiquitination is required for endocytosis (65). In addition, incorporation of a single lysine to arginine mutation in the C terminus of Ste2p results in complete inhibition of ubiquitination and internalization (65). Ubiquitination targets the receptors for endocytosis and subsequent degradation in the vacuole (65). Vacuolar targeting of the receptors does not permit recycling to the plasma membrane. Therefore, it is apparent that ligand-dependent ubiquitination is an important mechanism for regulating receptor activity on the cell surface.

Regulating Gα and Gβ activity in the yeast pheromone response

Sst2p, a member of the RGS family, has been demonstrated to be a negative regulator of Gpa1p signaling, as described above. Strains containing mutations in *SST2* display an increased sensitivity to pheromone, suggesting a role in adaptation (16, 17, 39).

The Gβ subunit is phosphorylated in response to pheromone induction (28). Expression of a phosphorylation defective Gβ subunit resulted in an enhanced sensitivity to pheromone (28). This supersensitivity to pheromone suggested that phosphorylation is involved in an adaptive response to pheromone. The residues required for phosphorylation of Gβ are located within a region which is not conserved in mammalian Gβ subunits. Phosphorylation of Ste4p is not required for signaling since deletion of the residues that are essential for pheromone-dependent phosphorylation (Δ310-346) does not abrogate signaling or mating (28). Results have also been obtained demonstrating that phosphorylation does not result in adaptation (91). The biological significance of Gβ subunit phosphorylation is undetermined, but it is possible that phosphorylation of Gβ may serve as molecular tag to identify subunits destined for pheromone-dependent degradation.

MAP kinase dephosphorylation

MSG5 was isolated in a screen for genes which when overexpressed resulted in suppression of the constitutive activation of the pheromone response pathway in a strain containing a null allele of *GPA1* (42). In addition, a strain containing a null allele of *MSG5* displayed supersensitivity to pheromone (42). The predicted protein sequence of Msg5p contained sequence similarity with a protein phosphatase and was able to dephosphorylate Fus3p (42). These results suggested that Msg5p serves an adaptive function in the pheromone response pathway. Other negative regulatory phosphatases may exist that modulate the activity of the pheromone response pathway at the level of the MAP kinase module.

Hormone destruction and receptor down regulation are adaptive mechanisms conserved from yeast to mammals. Adaptative mechanisms are present at many levels in the pheromone response pathway, as described above. The apparent redundancy in negative regulatory mechanisms may be required to balance the amplified stimulatory signal. In addition, negative regulation of signal transduction at different levels permits greater responsiveness and control over signaling.

E. Significance

G-protein coupled receptors (GPCR) sense the outside world through extracellular ligand binding surfaces and promote the appropriate response through cytoplasmic interfaces with the G-proteins. Multicellular organisms require GPCRs and heterotrimeric G-proteins for neurotransmission, taste, smell, vision, and many hormonal responses. Mutations in GPCRs demonstrate the importance of proper receptor function. Truncations in the vasopressin 2 receptor results in congenital nephrogenic diabetes insipidus (123). Autosomal dominant mutations in the lutropin receptor and thyrotropin result in familial male precocious puberty and thyroid adenomas, respectively (104, 130). In addition, G protein activity mediates cellular differentiation and altered activity results in oncogenesis (38, 62). Therefore, understanding the regulatory mechanisms of GPCR and heterotrimeric G protein signaling may provide clues toward the elucidation of targets of therapy for human diseases resulting from receptor mutations.

In this work the pheromone response pathway of *Saccharomyces cerevisiae* is utilized as a model system to better understand the regulatory mechanisms required for G protein mediated signaling. An obvious advantage of using yeast is the ease of genetic manipulation. Additionally, in molecular terms pheromone response signaling is one of the best understood pathways, which utilizes a heterotrimeric G protein linked to a MAP kinase cascade. The mechanism of heterotrimeric G protein activation through

serpentine receptors is conserved between yeast and mammals. Therefore, examination of the regulatory mechanisms of G_β signaling will likely provide relevant information for understanding higher eukaryotic G protein signaling.

The focus of this work was to better understand in molecular terms the regulation of the Ste4p G-protein β subunit activity. The goals of the project include 1) investigation of the mechanism of Ste4p-mediated receptor inhibition and 2) identification of the mating function of *SSF1*, a gene which when overexpressed suppresses mutations in *STE4*.

Table 1. Gene List

Gene name	Product	Reference
SIGNAL TRANSDUCTION		
STE2	α-factor receptor (present in *MAT***a** cells)	(12, 100)
STE3	**a**-factor receptor (present in *MAT*α cells)	(58, 100)
GPA1	G protein α- subunit	(40, 99)
STE4	G protein β-subunit	(60)
STE18	G protein γ-subunit	(150)
STE20	PAK kinase homologue	(114)
STE5	scaffold protein	(60)
STE11	MEKK	(60, 143)
STE7	MEK	(14, 60)
FUS3	MAPK	(45)
PROJECTION FORMATION		
CDC42	rho-type GTPase	(118)
	polarity establishment protein	
SPA2	polarity establishment protein	(134)
BEM1	polarity establishment protein	(22)
FAR1	cyclin-dependent kinase inhibitor	(18)

II. Pheromone pathway signaling is inhibited in *STE3*^{DAF} cells

A. Introduction

1. Receptor inhibition

Haploid *MAT***a** cells normally express Ste2p, the α-factor receptor, and undergo cell cycle arrest and transcriptional induction in response to α-factor stimulation. However, *MAT***a** cells containing the *STE3*^{DAF} mutation, inappropriately express the **a**-factor receptor and exhibit resistance to pheromone induced cell cycle arrest; these cells undergo a phenomenon termed receptor inhibition (66) (See Figure 2-1).

The *STE3*^{DAF} mutation, originally named *DAF2* (dominant alpha-factor resistance) was isolated in a screen for mutations that resulted in resistance to α-factor-induced cell cycle arrest in *MAT***a** cells (33). The *STE3*^{DAF} allele contains a rearrangement in the 5′ flanking region which permits expression of wild type *STE3* in all cell types, but does not alter the level of *STE3* RNA as compared to its level in *MAT*α cells. The inappropriate expression of the **a**-factor receptor in *MAT***a** cells prevents signaling, however, the biological function of this mutation is not known. It has been suggested that the *STE3*^{DAF} mutation may be important during mating-type switching or recovery from zygote formation, a situation in which both receptors are transiently present on one cell surface (66). In these situations it would be favorable to suppress the pheromone response pathway.

Figure 2-1. Schematic representation of the *STE3*^{DAF} phenotype.

Expression of the **a**-factor receptor (Ste3p) in *MAT***a** cells results in resistance to pheromone-induced cell cycle arrest and transcriptional activation at late timepoints.

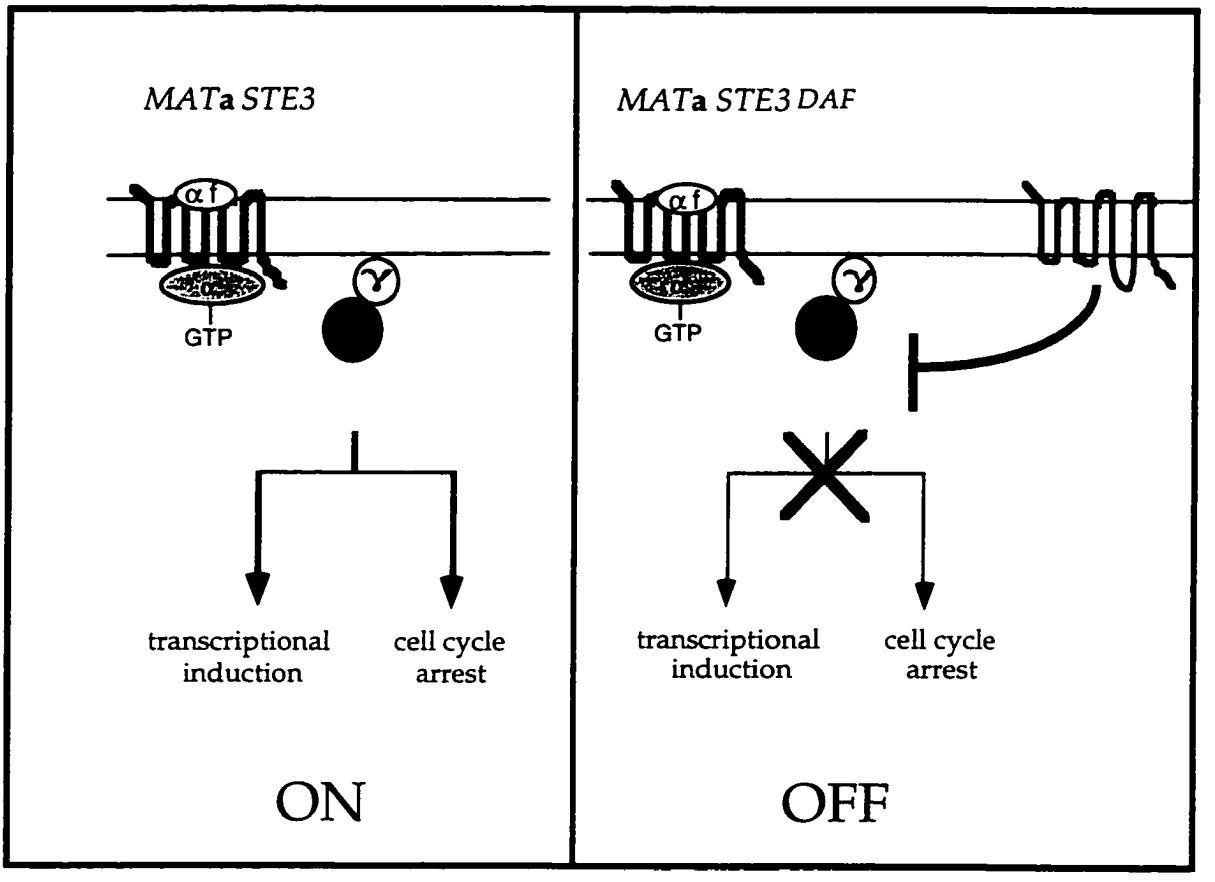

STE3^{DAF}- mediated receptor inhibition can suppress the constitutive cell cycle arrest caused by deletion of *GPA1*, the G protein α subunit gene, and thus does not require the α subunit for function (33, 66). Expression of *STE2*, which encodes the α-factor receptor, is not required for receptor inhibition; deletion of the *STE2* gene does not affect the ability of *STE3*^{DAF} cells to suppress the constitutive cell cycle arrest in cells containing null alleles of *GPA1* (66). Also, deletion of the carboxy terminus of Ste2p, which results in increased pheromone sensitivity, does not suppress the *STE3*^{DAF} phenotype (33, 81). *SST2* encodes a protein of the RGS family (regulators of Gα signaling) and strains containing mutations in *SST2* display an increased sensitivity to pheromone, suggesting a role in adaptation (16, 17, 39). However, *STE3*^{DAF} does not required Sst2p; a *MAT***a** *STE3*^{DAF} *sst2* strain displays the phenotype of receptor inhibition (66).

Initial characterization of the *STE3*^{DAF} phenotype demonstrated that *MAT***a** *STE3*^{DAF} strains displayed increased basal levels of *FUS1* RNA (33, 66). The *STE3*^{DAF} mutation resulted in the expression of the **a**-factor receptor in *MAT***a** cells, which secrete **a**-factor encoded by the *MFA1* and *MFA2* genes. The constitutive binding of **a**-factor to the **a**-factor receptor (Ste3p) on the cell surface was suggested to form an autocrine loop that functioned to desensitize the cellular response to α-factor as a mechanism of mediating receptor inhibition (66). However, this autocrine loop-mediated desensitization did not affect the *STE3*^{DAF} phenotype, as deletion of *MFA1* and *MFA2* did not

abrogate *STE3*^{DAF}-mediated resistance to α-factor (66). Since *MAT***a** *STE3*^{DAF} *mfa1 mfa2* strains displayed the *STE3*^{DAF} phenotype, but did not display the high level of basal signaling, strains with this genotype were used in this work (See Table 2).

In addition to inhibition of cell cycle arrest, cells containing the *STE3*^{DAF} mutation exhibit a block in pheromone-mediated signaling at late time points after pheromone treatment (32). In *STE3*^{DAF} cells, initial activation of the pheromone response pathway is similar to that observed in wild type cells, as measured by Fus3p MAP kinase activity and *FUS1* RNA levels (32). However, at later time points after pheromone induction, *STE3*^{DAF} cells display a decrease in signaling compared to wild type levels (32). Overexpression of a hyperactive allele of *STE5*^{Hyp} is able to suppress the *STE3*^{DAF} phenotype, whereas overexpression of *STE4* did not appear to suppress the *STE3*^{DAF} phenotype (32). This result demonstrated that the mutation acts upstream of *STE5*. Furthermore, overexpression of *STE20* in the presence of pheromone was able to suppress the *STE3*^{DAF} phenotype, which suggested that receptor inhibition acted at a step between *STE5* and *STE4* (32). Taken together, the epistasis results demonstrated that the *STE3*^{DAF} mutation acts at the level of or downstream of *STE4*.

2. Identification of *STE4*^{SD} alleles

*MAT***a** *STE3*^{DAF} cells exposed to α-pheromone do not undergo cell cycle arrest and do not display pheromone-dependent transcriptional activation. Epistasis results suggested that *STE3*^{DAF} may act at the level of the G-protein β subunit. Therefore, a screen was undertaken to identify mutations in *STE4*, which encoded an altered protein capable of reversing receptor inhibition (31). The goal was to isolate *STE4*^{SD} (termed *STE4*^{SD} for suppressor of *STE3*^{DAF}) alleles which were able to restore signal transduction in *STE3*^{DAF} cells exposed to pheromone (Figure 2-2). To test the hypothesis that *STE4* mediates receptor inhibition, an error-prone polymerase chain reaction (PCR) mutagenic screen was undertaken (31). PCR mutagenesis was used to introduce random changes in *STE4*, then the library of mutagenized *STE4* was transformed into a *MAT***a** Δ*ste4* *STE3*^{DAF} strain with a plasmid containing a gapped *STE4* gene under the control of the *STE4* promoter (31). Expression of the *STE4* alleles was achieved by *in vivo* recombination of the PCR fragment and the gapped vector. To assay for pheromone-dependent transcriptional induction, a reporter plasmid containing a *FUS1*-β-galactosidase gene fusion was present in the strain which permitted visual screening of colonies that responded to pheromone (31).

The isolation of *STE4*^{SD} mutations that encode Ste4 proteins capable of inducing both pheromone-mediated cell cycle arrest and transcriptional activation in *STE3*^{DAF} cells suggested that the mutations isolated were

Figure 2-2. Schematic representation of *STE4*^{SD} suppression of the *STE3*^{DAF} phenotype.

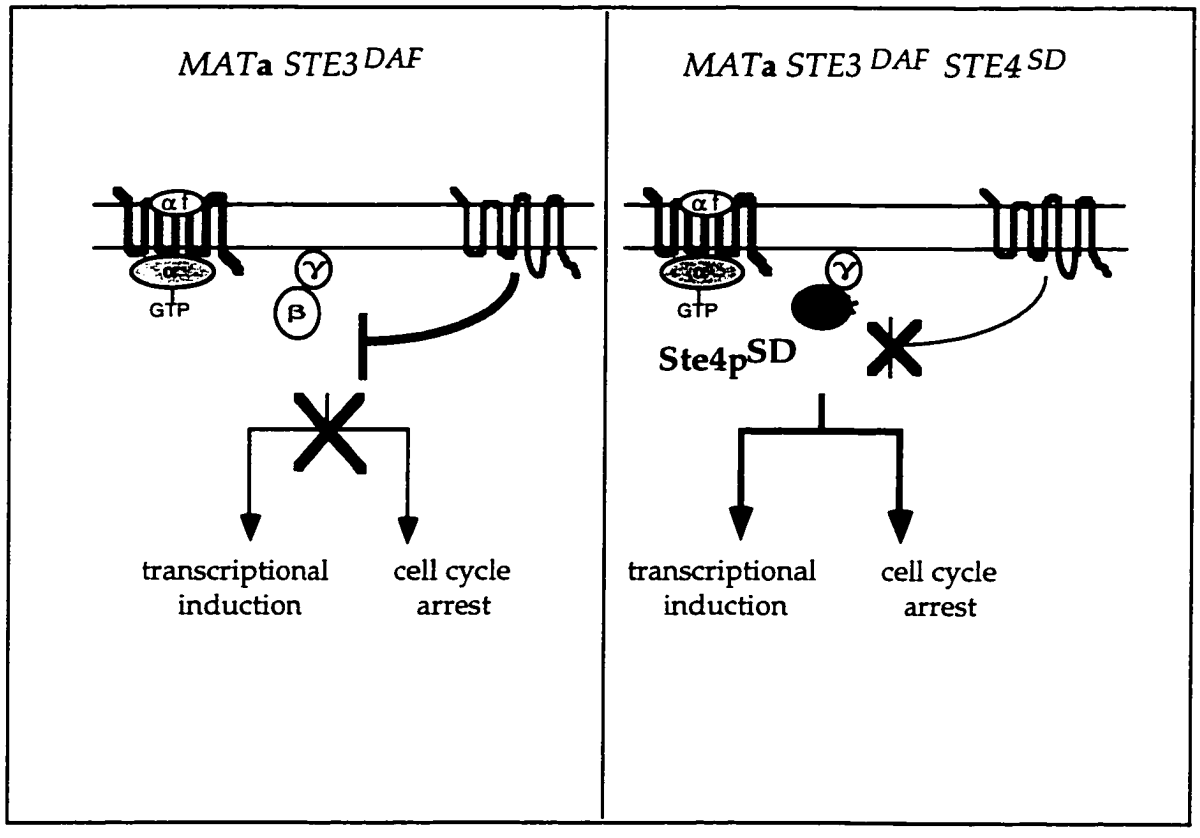

able to reverse receptor inhibition (31). Three *STE4*^{SD} alleles were isolated in the screen, which contained multiple point mutations and were able to reverse the *STE3*^{DAF} phenotype to variable degrees as measured by halo assay. The halo assay entails spreading a lawn of cells onto an agar plate, a filter disc is placed in the center of the lawn, and pheromone is added onto the disc and diffuses from the center. Cells undergo pheromone-dependent arrest in the center of the plate where concentrations of pheromone are higher. Cells on the outer regions of the plate are not arrested since the concentration of pheromone is lower with increasing distance from the pheromone source. This threshold response to pheromone produces the characteristic halo of arrested cells.

Initial characterization of the *STE4*^{SD} alleles

STE4^{SD1} suppressed receptor inhibition to the greatest extent as measured by halo assay (31). The *STE4*^{SD1} allele contained the following three mutations: R162G, C182R, and I195V (31). The mutation R162G was located between WD repeats 2 and 3 and C182 and I195V were located within WD repeat 3. The fraction of unbudded cells in a culture after the addition of α-factor is a quantifiable assay for pheromone sensitivity (110). Cells exposed to pheromone undergo arrest in the G_1 phase of the cell cycle and do not initiate bud formation which begins at the advent of START. Therefore, the percentage of cells present in the G_1 phase of the cell cycle is quantifiable by the percentage of unbudded cells. *MAT***a** *STE3*^{DAF} cells containing the *STE4*^{SD1} allele were 92% unbudded, as compared to *STE3*^{DAF} cells containing wild type

STE4 which were 60% unbudded (31). The results suggest that $STE3^{DAF}$ cells expressing the $STE4^{SD1}$ allele appeared to undergo pheromone-dependent cell cycle arrest.

The other two alleles, $STE4^{SD2}$ and $STE4^{SD3}$, resulted in incomplete suppression of receptor inhibition, i.e. partial halos were formed (31). The $STE4^{SD2}$ allele contained three mutations Q17L, Q21R, and M283V, which were located within the N-terminus of Ste4p and within WD repeat 4 (31). *MAT***a** $STE3^{DAF}$ cells containing $STE4^{SD2}$ were 70% unbudded (31). The $STE4^{SD3}$ allele also contained three mutations: L132I, N155D, and D270G (31). The mutations were located within WD repeat 2, WD repeat 5. The budding index of this allele in a $STE3^{DAF}$ strain was 66% (31). Since this allele had the weakest phenotype as measured by halo assay and budding index, it was not studied further.

The mutations in the $STE4^{SD}$ alleles described above were created by random PCR mutagenesis. Because there were multiple changes in each allele, it was necessary to determine the relative contribution of each point mutation present in the $STE4^{SD}$ alleles to the suppression of receptor inhibition. To accomplish this aim, the individual point mutations and combinations of point mutations were isolated and tested for the ability to reverse receptor inhibition. The percentage of unbudded cells was measured to quantify the level pheromone-dependent G_1 arrest attributable to each of the alleles containing individual point mutations and combinations of point mutations (data not shown). Many of the individual point mutations in

STE4 obtained in the screen did not demonstrate an obvious phenotype in $STE3^{DAF}$ cells, therefore, these mutations were disregarded. Point mutations which resulted in an ability to reverse receptor inhibition were constructed into a single allele which is able to reverse receptor inhibition to the greatest extent, as assayed by cell cycle arrest and pheromone-dependent transcriptional activation.

The goal of this work was to isolate an allele of $STE4^{SD}$ that was capable of reversing receptor inhibition to the greatest extent. This allele should be able to specpfically reverse receptor inhibition, which is assayed by the sustained transcription of pheromone-inducible genes at late time points. In addition, expression of the $STE4^{SD}$ allele in wild type cells should not demonstrate increased basal or pheromone-induced transcriptional activation. Therefore, initial steps were taken to characterize the regulatory mechanisms of Ste4p activity in the context of the $STE3^{DAF}$ mutation.

B. Materials and methods

1. Plasmid construction

A centromeric plasmid containing the *STE4* gene was constructed by cloning the 5 kb *Sph*I-*BamH*I fragment from plasmid M81p12 (27) to produce YCpSTE4. The 5 kb *Sph*I-*BamH*I fragment from plasmid M81p12 was cloned into pUC19 to produce pUC-STE4.1. A centromeric plasmid containing *STE4* was constructed by subcloning the 5 kb *Sph*I-*BamH*I fragment from plasmid M81p12 into YCplac111 (52) to create YCpLSTE4. Centromeric *LEU2* plasmids containing $STE4^{SD}$ alleles were constructed by cloning the 5 kb *Sph*I-*BamH*I fragment from pUC-STE4.1 constructs that had been subjected to site-directed mutagenesis (Transformer Site Directed Mutagenesis kit, Clontech) into YCplac111. The *FUS1-lacZ* reporter plasmid was constructed by cloning the 6 kb *Pst*I fragment from pSB234 (kindly provided by E. Elion) into YCplac111 to create YCpF1-LZ.

A construct that fuses *STE3* to the green fluorescent protein (GFP) gene was made by first incorporating a *Not*I site immediately before the stop codon of an allele of $STE3^{DAF}$ through PCR-mediated (36) site-directed mutagenesis (Stratagene) with oligonucleotide primers oSTE3N1, 5′ - GAAAATACTGCAGGCGGCCGCCACAAGTGTGTC-3′ and oSTE3N2, 5′-GACACACTTGTGGCGGCCGCCTGCAGTATTTTC-3′ using as a template pDAF2m-4 (66). Next, a 0.7 kb fragment encoding the GFP gene containing

flanking *Not*I sites was subcloned into the *Not*I site to produce pDAF2m-4GFP. A high copy plasmid containing the *STE3*-GFP fusion was constructed by cloning the 3 kb *Sph*I- *Sac*I fragment from pDAF 2m-4GFP into YEplac112 to make YEpSTE3-GFP. A construct encoding a truncated version of *STE3* ΔC, which removes 107 residues from the carboxy-terminus of *STE3* and also incorporates a *Not*I site immediately prior to a stop codon, was constructed by PCR-mediated site-directed mutagenesis with oligonucleotide primers oSTE3C1, 5′ - CATTTCTATGGCGGCCGCTGAATTCCAGATGATCC - 3′ and oSTE3C2, 5′ - GGATCATCTGGAATTCAGCGGCCGCCATAGAAATG - 3′ using as a template pDAF2m-4 (66). A 0.7 kb fragment encoding the GFP gene was subcloned into the *Not*I site. A high copy plasmid containing the *STE3*ΔC-GFP fusion was constructed by cloning the 2.7 kb *Sph*I- *Sac*I fragment from pDAF 2m-4GFP into YEplac112 to make YEpSTE3ΔC-GFP.

Incorporation of point mutations into *STE4* to create $STE4^{SD10}$ was constructed by *in vitro* mutagenesis (Clontech) using oligonucleotide primers oBETA4 5′-CTTTCGAAACTCCATAAATGGTACAG-3′ and oBETA7 5′-GTATATACTGTAGGGTGACATTAT-3′ using pUCSTE4.1 as a template to produce pUC-SD10. A 2.1 kb *BamH*I-*Sac*I from pUC-SD10 cloned into BTL49 (kindly provided by Thomas Leeuw) to produce YCpSD10.

2. Strains and Media

Strains used in this study are listed in Table 4 and were derived from W3031A (obtained from R. Rothstein). The *gpa1::TRP1* null allele was made by transformation of a strain that contained a *gpa1::URA3* (40) with a 3.8 kb *Sma*I fragment from a marker swap plasmid pUT11 (34). The *FAR1* gene was disrupted by transformation with a 3.8 kb *Xho*I-*Sac*I fragment from pfar1-U1 (32) to create *far1::URA3*. The *ste2::LEU2* alleles was made by transformation with a *BamH*I fragment from pAB506. The $STE3^{DAF}$-*LEU2* allele present in two strains was made by transformation of each strain that contained a $STE3^{DAF}$-*TRP1* with a 4.4 kb *Sma*I-*Xho*I fragment from a marker swap plasmid pTL7 (34). All strain constructions involving transformations were confirmed by Southern blot.

Strains were grown on YEPD (2% glucose) or YEP-Gal (3% galactose), and strains under selection were grown on synthesis dropout media, as described (132).

3. Yeast methods

Yeast transformations were performed by the lithium acetate method (71) modified as described previously (66). Yeast RNA was extracted from cells as described previously (35). Halo assays were performed by spreading a lawn of cells onto a plate and placing a filter disk containing 5 µl α-factor onto the plate. Plates were incubated at 30°C for 1 -2 days.

4. Northern blots

RNA was transferred to a nitrocellulose membrane after formaldehyde-agarose gel electrophoresis as described (90). The membranes were UV cross-linked using a Stratalinker UV box. Prehybridization and hybridization were done at 65°C in a buffer containing 0.9 M NaCl, 0.09 M sodium citrate, 0.1% Ficoll, 0.1% polyvinylpyrrolidone, 0.1% bovine serum albumin, 33 mM sodium pyrophosphate, 50 mM sodium phosphate monobasic. The probes used were gel-purified DNA restriction fragments ^{32}-P labeled by random primer labeling using a Prime-It kit (Stratagene). The fragments used were: *FUS1*, a 1.4 kb *Eco*RI-*Hin*DIII fragment from pSL589 (97); ribosomal protein gene *TCM1* (126), a 0.8 kb *Hpa*I-*Sal*I fragment from plasmid pAB309Δ; phosphoglycerate kinase gene *PGK1*, a 0.5 kb *Bam*HI-*Xba*I fragment from pPGK1.

5. Immunoblots

For immunoblotting, cells were grown to early log phase, pelleted, and washed once in TE (10 mM tris-HCl and 1 mM EDTA). Cells were resuspended in synthetic medium and α-factor was added to a final concentration of 3 μM and aliquots were removed at 1 and 6 hr after α-factor addition. Cell lysates were prepared by harvesting 10 ml of log phase cells, washing once with cold TE and resuspending in 350 μl of lysis buffer (50 mM tris-HCl [pH 8.0], 1% SDS, 1 mM PMSF, 1 μg of [apoprotein, leupeptin, chymostatin, and pepstatin] per ml). The mixture was added to acid-washed

beads (0.5 mm) and vortexed at high speed for 10 min. Glass beads and cell debris were separated from the lysate by centrifugation in a microfuge for 2 min. Protein concentration of the samples was determined using a bicinchoninic protein assay kit (Pierce) and equal amounts were loaded onto SDS polyacrylamide gels (10% polyacrylamide). Separated proteins were transferred to nitrocellulose and the blot was probed with anti-Ste4p rabbit polyclonal antiserum (67) at a dilution of 1:1000, anti-Pma1p monoclonal antiserum at a dilution of 1:10,000 (2), or anti-Pgk1p polyclonal antibody at a dilution of 1:300,000. Donkey anti-rabbit immunoglobulin conjugated to horseradish peroxidase (Amersham) or goat anti-mouse immunoglobulin conjugated to horseradish peroxidase (Amersham) were used at dilutions of 1:10,000. Immune complexes were detected with an enhanced chemiluminescence kit (Amersham).

6. Differential centrifugation

For crude membrane preparations, approximately 4 x 10^9 cells were grown to mid-log phase and α-factor was added to a final concentration of 0.1 μM and incubated at 30°C for 3 hr. Cells were pelleted for 5 min at 1500 x*g* then resuspended in 15 ml of buffer A (50 mM Tris-HCl [pH 7.5], 5 mM EDTA, 1.0 M NaCl, 1 mM PMSF. The mixture was added to acid-washed glass beads (0.5 mm) and vortexed for 2 min using a Bead-Beater (Biospec Products). Unlysed cells and cell debris were removed from the lysate by centrifugation at 700*g* for 5 min. To obtain a crude membrane fraction, the supernatant (S20) was

subjected to centrifugation at 20,000 *g* for 20 min. The membrane pellet (P20) was resuspended in 1 ml buffer A. Protein concentration of the samples was determined using a bicinchoninic protein assay kit (Pierce) and equal amounts were loaded onto SDS polyacrylamide gels (10% polyacrylamide). Immunobloting was accomplished as described above.

7. Microscopy

*MAT***a** *STE3* or *MAT***a** $STE3^{DAF}$ cells containing a GFP-STE4 gene fusion plasmid under the control of the *STE4* promoter, were grown to log phase and α-factor was added to a final concentration of 0.1 μM. *MAT***a** cells containing either a STE3-GFP plasmid or a STE3ΔC-GFP plasmid were grown to log phase and α-factor was added to a final concentration of 0.1 μM. Aliquots were taken at the indicated times and the fusion was observed directly on a Zeiss Axioskop using a FITC filter.

Table 2. Strain List: Chapter II

Strain	Genotype	Source
W303-1A	*MATa leu2-3,112 trp1-1 can1-100 ura3-1 ade2-1 his3-11,15*	R. Rothstein
W303-1B	*MATα leu2-3,112 trp1-1 can1-100 ura3-1 ade2-1 his3-11,15*	R. Rothstein
The following strains are isogenic to W3031A:		
H67-9D.Ba	*MATa mfa1-Δ3::HIS3 mfa2- Δ 2::HIS3 sst1::hisG STE3*	(32)
H67-6C.Ba	*MATa mfa1-Δ3::HIS3 mfa2- Δ 2::HIS3 sst1::hisG* $STE3^{DAF2.5}$*-TRP1*	(32)
AC17-7B	*MATa mfa1-Δ3::HIS3 mfa2- Δ 2::HIS3 sst1::hisG ste4::HIS3 STE3*	(30)
AC17-2B	*MATa mfa1-Δ3::HIS3 mfa2- Δ 2::HIS3 sst1::hisG ste4::HIS3* $STE3^{DAF}$	(30)
K39-23B	*MATa mfa1-Δ3::HIS3 mfa2- Δ 2::HIS3 sst1::hisG ste4::HIS3 gpa1::TRP1* $STE3^{DAF2.5}$*-TRP1*	this study
K39-23Bf	*MATa mfa1-Δ3::HIS3 mfa2- Δ 2::HIS3 sst1::hisG ste4::HIS3 gpa1::TRP1* $STE3^{DAF2.5}$*-TRP1 far1::URA3*	this study
K39-23B.s2	*MATa mfa1-Δ3::HIS3 mfa2- Δ 2::HIS3 sst1::hisG ste4::HIS3 gpa1::TRP1* $STE3^{DAF2.5}$*-TRP1 ste2::LEU2*	this study
K39-23Df	*MATα ste4::HIS3* $STE3^{DAF2.5}$*-TRP1 gpa1::TRP1 far1::URA*	this study

Table 3. ***STE4*** **alleles**

STE4 allele	mutation position	mutant phenotype/reference
STE4	**none**	**wild type**
$STE4^{SD13}$	Q17L, Q21R, R162G	suppressor of $STE3^{DAF}$ /this study
$STE4^{SD10}$	Q17L, R162G	suppressor of $STE3^{DAF}$ /this study
$STE4^{\Delta 310\text{-}346}$	Δ310-346	phosphorylation defective/ (28)

C. Results

Receptor inhibition of mating pathway signaling is mediated by Ste4p

*MAT***a** cells containing the *STE3*^{DAF} mutation, which results in the inappropriate expression of *STE3*, do not arrest in response to pheromone stimulation. The following lines of evidence suggest that the *STE3*^{DAF} mutations acts at the level of the G protein β subunit: 1) *STE3*^{DAF} is unable to suppress the constitutive activation that results from overexpression of *STE5*^{Hyp}; 2) the *STE3*^{DAF} mutation is able to suppress the constitutive activation that results from overexpression of *STE4*; and 3) *STE4*^{SD} alleles were obtained which were able to cause cell cycle arrest in *STE3*^{DAF} cells (31, 32). Individual *STE4*^{SD} mutations did not result in complete suppression of *STE3*^{DAF}. Therefore, it was necessary to construct combinations of individual point mutations to identify an allele that was able to reverse receptor inhibition to the greatest extent. Expression of this *STE4*^{SD} allele should be able to reverse receptor inhibition by increasing pheromone-induced transcription only at late time points in *STE3*^{DAF} cells. In addition, expression of the *STE4*^{SD} allele should demonstrate normal basal and pheromone-dependent transcriptional activation.

1. *STE4*^{SD13} allele is capable of reversing receptor inhibition

The goal was to identify the combination of mutations in *STE4* that encoded a mutant protein capable of suppressing the *STE3*^{DAF} phenotype to the highest level. To find the allele with the greatest ability to reverse receptor inhibition, different combinations of individual point mutations were subjected to halo assay, as a measure of pheromone-dependent cell cycle arrest.

Expression of individual point mutations resulted in partial reversion of the phenotype (31). Therefore, combinations of individual point mutations were constructed to isolate the *STE4*^{SD} allele that resulted in the highest level of signaling. The individual point mutation that resulted in the greatest ability to reverse receptor inhibition, as measured by halo assay and budding index, was *STE4*^{SD4} which encodes the point mutation R162G. The mutations located in the N-terminus of *STE4*^{SD2}, which encoded mutations Q17L and Q21R also resulted in relatively high level of suppression of receptor inhibition. Therefore these three point mutations were introduced into one allele, *STE4*^{SD13}.

Pheromone-dependent cell cycle arrest was assayed in a *MAT***a** *STE3*^{DAF} Δ*ste4* strain containing a low copy plasmid encoding the *STE4*^{SD13} allele under the control of the *STE4* promoter. This *STE3*^{DAF} *STE4*^{SD13} containing cell displayed a partially filled halo (Figure 2-3, bottom). Wild type *MAT***a** cells exposed to α-factor produce a clear halo of arrested cells and *MAT***a** *STE3*^{DAF} cells that contain a wild type *STE4* allele do not arrest in response to

pheromone, therefore, do not produce a halo (Figure 2-3, left and right). Therefore, expression of the $STE4^{SD13}$ allele in the $STE3^{DAF}$ strain resulted in the highest level of cell cycle arrest, albeit partial suppression of the $STE3^{DAF}$-mediated receptor inhibition was observed. This $STE4^{SD13}$ allele contained the following mutations: Q17L, Q21R, and R162G. The mutations were located in the amino terminus and between WD repeats 2 and 3 (Figure 2-4 and Table 3- *STE4* alleles).

Figure 2-3. Mutations in *STE4* suppress receptor inhibition.

Halo assays were performed with 5 µl of 1 mM α-factor. Top left, a *MAT***a** *STE3 ste4::HIS3* strain (AC17-7B) containing a low copy wild type *STE4* plasmid (YCpLSTE4); a *MAT***a** $STE3^{DAF}$ *ste4::HIS3* (AC17-2B) strain containing either a low copy wild type *STE4* plasmid (YCpLSTE4; top right) or a low copy plasmid containing the allele $STE4^{SD13}$ (YCpLSD13; bottom).

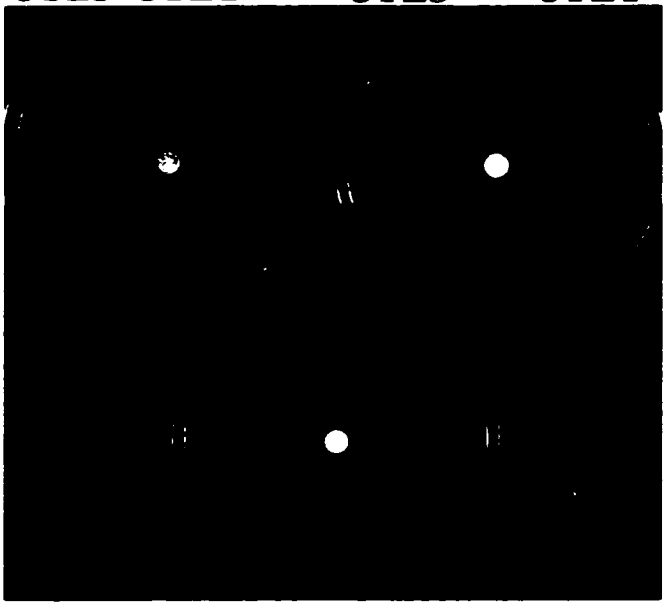

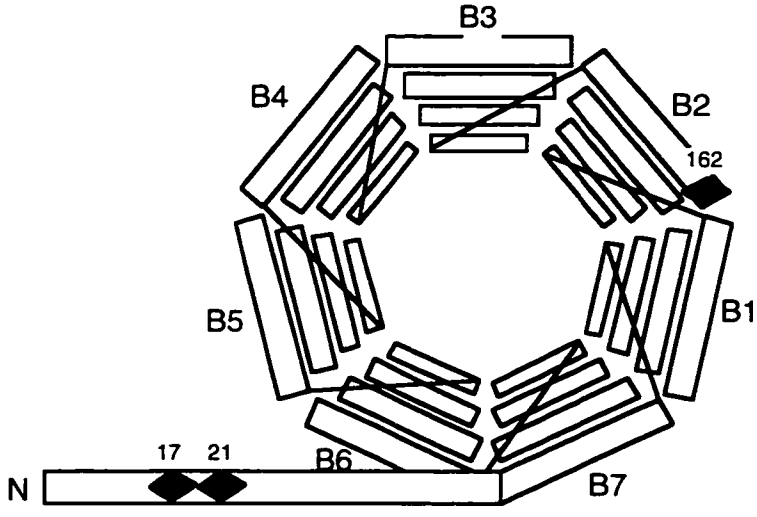

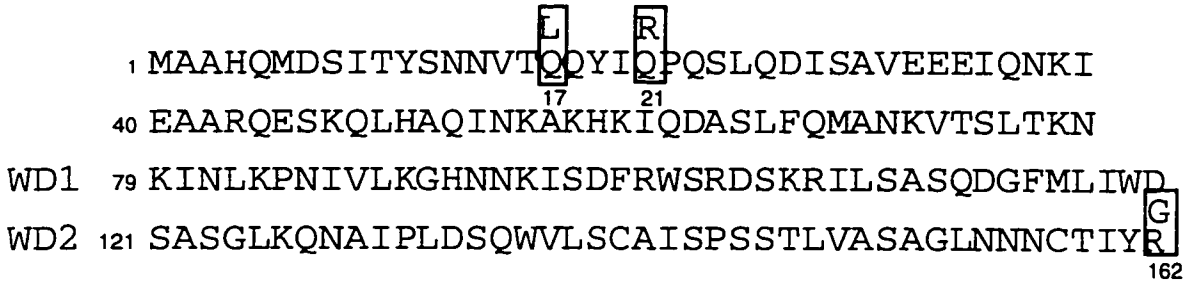

Figure 2-4. Locations of mutations on Ste4p Gβ stucture.

The Ste4p sequence is depicted as a seven-bladed β-propeller structure. The *STE4*^{SD13} allele contains the following mutations: Q17L and Q21R and R162G, which are represented by diamonds in the diagram. The sequence of amino acids 1-162 of Ste4p is displayed above.

2. *STE4*^{SD13} promotes sustained transcriptional activation in *STE3*^{DAF} cells

*MAT***a** cells containing the *STE3*^{DAF} mutation inappropriately express the **a**-factor receptor and exhibit a decrease in transcriptional activation at late time points after pheromone treatment (32). Transcriptional induction of many genes is required for cell adhesion, cell cycle arrest, cell fusion, and karyogamy during mating. *FUS1* RNA is a useful marker for pheromone-dependent transcriptional activation as it is induced up to 100-fold in response to α-factor treatment (97, 144). To test the ability of Ste4p^{SD13} to increase signaling at late timepoints, the *STE3*^{DAF} cells expressing the *STE4*^{SD13} allele as the sole source of Gβ subunits were treated with α-pheromone, and RNA was isolated to determine the level of *FUS1* RNA induction. Wild type *MAT***a** cells treated with α-factor displayed a significant increase in *FUS1* RNA levels that remained high for three hours (Figure 2-5, lanes 1-4). In *MAT***a** *STE3*^{DAF} cells treated with α-factor, the *FUS1* RNA levels increased at one hour, but displayed a dramatic decrease by three hours (Figure 2-5, lanes 5-8), as previously described (32). *STE3*^{DAF} cells expressing the *STE4*^{SD13} allele displayed a similar increase in *FUS1* RNA levels at 1 hour, but demonstrated sustained expression of *FUS1* RNA at three hours (Figure 2-5, lanes 9-12). The

Figure 2-5. Effect of $STE4^{SD13}$ on pheromone-induced transcription.

(A) The following strains were treated with α-factor (0.1 μM) for the indicated periods of time: a *MAT***a** *STE3 ste4::HIS3* (AC17-7B) strain containing a wild type *STE4* plasmid (YCpLSTE4; lanes 1-4); a *MAT***a** $STE3^{DAF}$ *ste4::HIS3* (AC17-2B) strain containing either wild type *STE4* (YCpLSTE4, lanes 5-8) or the mutant allele $STE4^{SD13}$ (YCpLSD13; lanes 9-12). RNA was isolated, transferred to nitrocellulose, and hybridized with a *FUS1* probe. The blot was rehybridized with *PGK1* to determine the amount of RNA per lane. (B) The data were quantified by PhosphorImager analysis and the level of *FUS1* RNA was normalized to the control *PGK1* RNA level. Values from the *STE3 STE4* strain are represented by the open bars; values from the $STE3^{DAF}$ $STE4^{SD13}$ strain are represented by the shaded bars. The graph shows the average values from duplicated experiments.

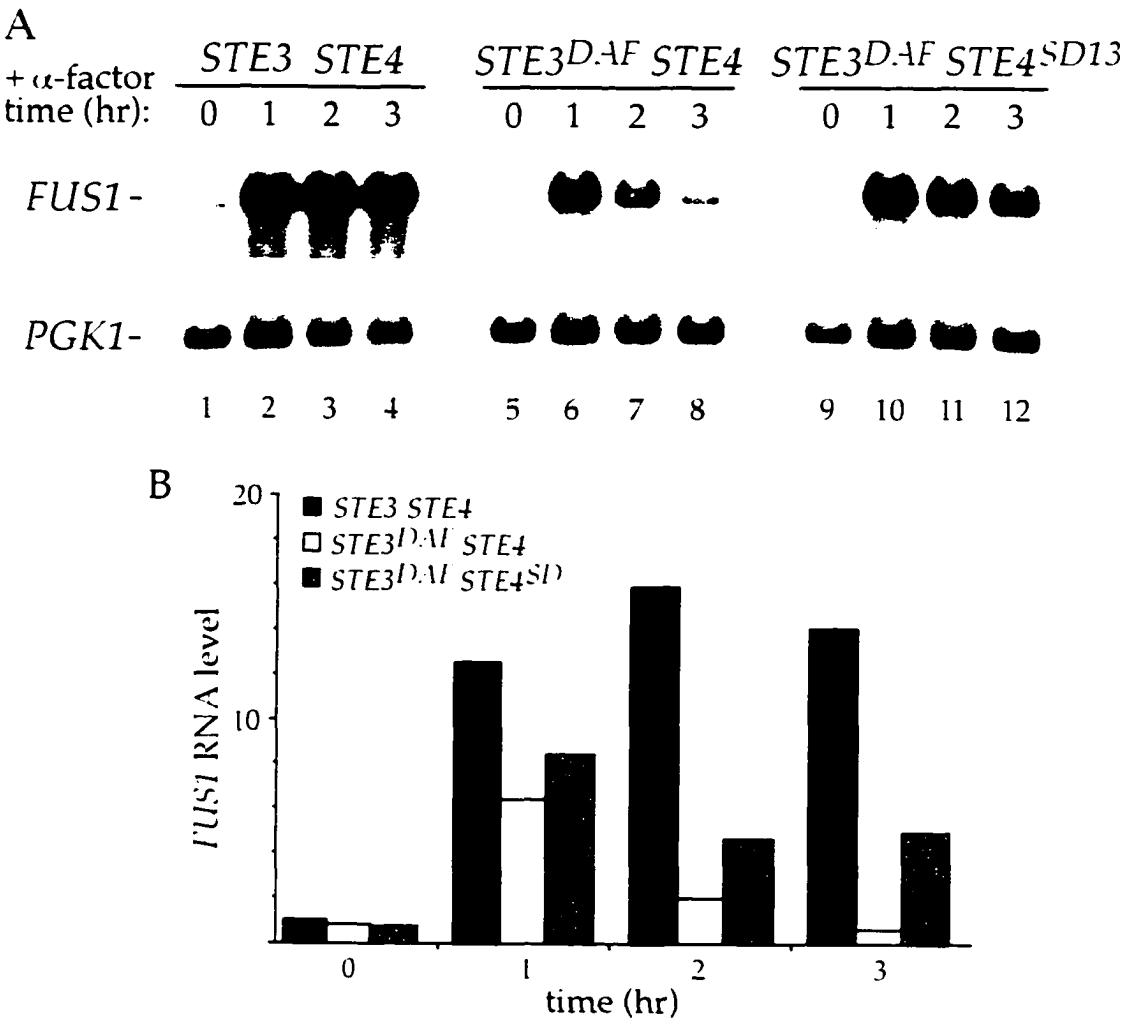

level of *FUS1* RNA was quantified by PhosphorImager Analysis (Molecular Dynamics) and normalized to *PGK1* RNA levels. The normalized *FUS1* RNA levels were averaged from two independent experiments and calculated to be approximately 7-fold increased in $STE3^{DAF}$ cells containing $STE4^{SD13}$ as compared to $STE3^{DAF}$ cells containing wild type *STE4* (Figure 2-5B). Therefore, $STE3^{DAF}$ cells containing $STE4^{SD13}$ display a partial reversal of receptor inhibition, as measured by halo assay and pheromone-induced transcriptional activation.

3. In *MAT***a** cells $STE4^{SD13}$ does not confer supersensitivity to pheromone

$STE4^{SD5}$ encodes an altered G protein β-subunit that resulted in supersensitivity to pheromone and caused enhanced suppression of receptor inhibition most likely by disrupting the interaction with Gα subunit (31). This result suggested that expression of mutant $Ste4p^{SD}$ proteins that cause constitutive signaling may increase signal transduction in a manner not specific to receptor inhibition. To test whether the $STE4^{SD13}$ gene product would cause supersensitivity to pheromone, cell cycle arrest was assayed in wild type *MAT***a** cells expressing the $STE4^{SD13}$ allele. The level of signaling in a *MAT***a** Δ*ste4* strain transformed with a low copy plasmid containing either wild type *STE4* or the $STE4^{SD13}$ allele was assayed for cell cycle arrest. Wild type *MAT***a** cells containing *STE4* responded to pheromone and produced a halo of arrested cells (Figure 2-6, left). Wild type *MAT***a** cells expressing the

Figure 2-6. Effect of $STE4^{SD13}$ on cell cycle arrest in *MAT***a** cells.

Halo assays were performed with 5 µl of 1 mM α-factor. A *MAT***a** strain containing either a wild type *STE4* plasmid (YCpLSTE4; left) or a plasmid containing $STE4^{SD13}$ allele (YCpLSD13; right).

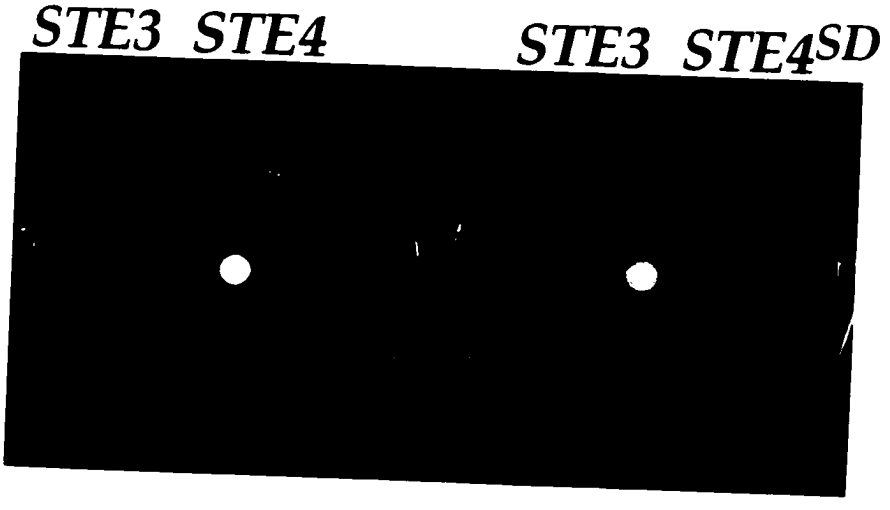

STE4^{SD13} allele produced a halo of arrested cells indistinguishable in size from a strain containing the wild type *STE4* allele (Figure 2-6, right). Strains displaying increased sensitivity to pheromone produce a larger zone of arrested cells, as compared to a wild type strain, since the cells are able to respond to the lower concentration of pheromone present at distances further from the pheromone source. Therefore, the *STE4*^{SD13} allele does not encode a Gβ subunit that results in increased sensitivity to pheromone.

4. Signaling in wild type cells is not affected by *STE4*^{SD13}

Expression of the *STE4*^{SD13} allele in wild type *MAT***a** cells did not result in increased sensitivity to pheromone, demonstrating specificity for receptor inhibition. To test whether the *STE4*^{SD13} allele has any effect on signaling in cells that do not express *STE3*^{DAF}, the basal and pheromone-induced levels of *FUS1* RNA were measured in wild type *MAT***a** cells expressing *STE4*^{SD13} as the only copy of *STE4*. The level of *FUS1* RNA induction in *MAT***a** cells containing *STE4*^{SD13} (Figure 2-7A, lanes 5-8) or *STE4* (Figure 2-7A, lanes 1-4) was not significantly different in pheromone treated cells at all time points. The *FUS1* RNA levels were quantified and normalized to *PGK1* RNA levels by PhosphorImager analysis (Molecular Dynamics). The level of *FUS1* RNA differed in *MAT***a** containing either *STE4*^{SD13} or *STE4* by less than 20% after treatment with pheromone for 3 hr (Figure 2-7B). In addition, the basal level of pheromone pathway signaling as measured by *FUS1* RNA levels was unaltered in wild type *MAT***a** cells expressing *STE4* or *STE4*^{SD13} left untreated

Figure 2-7. Ability of *STE4*^{SD13} to signal in wild type *MAT***a** and *MAT*α cells. (A) A *MAT***a** *STE3 ste4::HIS3* strain (AC17-7B) containing either a wild type *STE4* plasmid (YCpLSTE4, lanes 1-4) or a plasmid containing the *STE4*^{SD13} allele (YCpLSD13, lanes 5-8) was treated with α-factor (0.1μM) for the indicated periods of time and RNA was isolated. RNA blots were prepared and hybridized as described in legend Figure 2-5. (B) The data from the experiment shown in (A) were quantified by PhosphorImager analysis and the level of *FUS1* RNA was normalized to the control *PGK1* RNA level. Values from the *STE4* strain are represented by the filled bars; values from the *STE4*^{SD13} strain are represented by the shaded bars.

(C) A *MAT*α *STE3 ste4::HIS3* strain (AC18-9C) containing either a wild type *STE4* plasmid (YCpLSTE4, lanes 1-4) or a plasmid containing the *STE4*^{SD13} allele (YCpLSD13, lanes 5-8) was treated with **a**-factor (40ng/ml) for the indicated periods of time and RNA was isolated. RNA blots were prepared and hybridized as described in legend Figure 2-5. (D) The data from the experiment shown in (C) were quantified by PhosphorImager analysis and the level of *FUS1* RNA was normalized to the control *PGK1* RNA level. Values from the *STE4* strain are represented by the filled bars; values from the *STE4*^{SD13} strain are represented by the shaded bars.

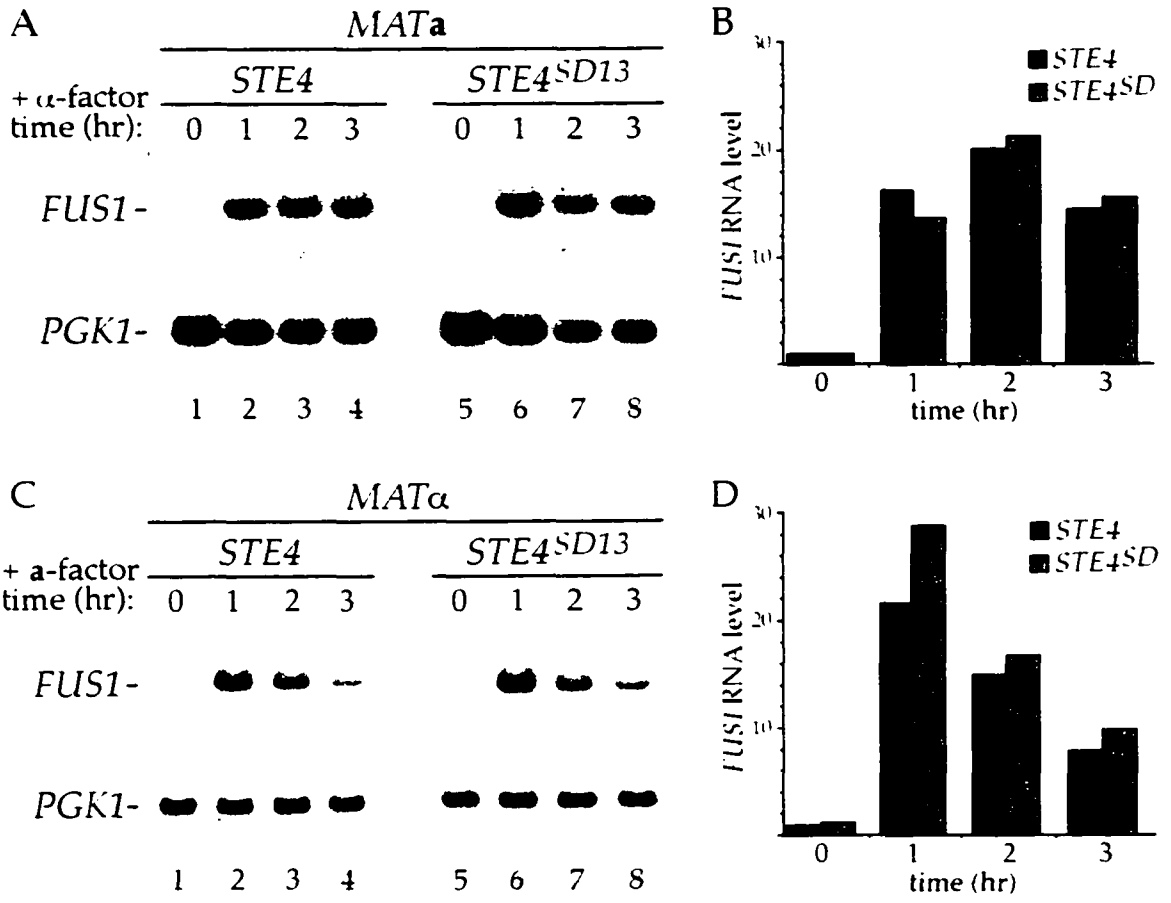

(Figure 2-7A, compare lanes 1 and 5). Constitutive activation of the pheromone response pathway is observed by an increase in the basal level of *FUS1* RNA. Therefore, these results demonstrate that the *STE4*^{SD13} allele encodes a protein that does not affect either basal or pheromone-induced signaling in wild type *MAT***a** cells.

The *STE4*^{SD13} allele appears to have an effect on signaling in *MAT***a** cells that inappropriately express the **a**-factor receptor (Ste3p), but this allele does not appear to have an effect on signaling in wild type *MAT***a** cells that lack the **a**-factor receptor. Therefore, it was of interest to test the ability of the mutant Ste4p^{SD13} to signal in wild type *MAT*α cells, which normally express Ste3p (**a**-factor receptor). A wild type *MAT*α Δ*ste4* strain was transformed with a low copy plasmid containing either the *STE4* or *STE4*^{SD13} allele, treated with **a**-factor, and the level of *FUS1* RNA was measured. In *MAT*α cells expressing the *STE4*^{SD13} allele as the only copy of *STE4*, the *FUS1* RNA levels were induced at 1 hr and declined gradually for the next two hours (Figure 2-7C, lanes 5-8). Wild type *MAT*α cells expressing the wild type *STE4* allele also demonstrated a similar trend of *FUS1* RNA induction (Figure 2-7C, lanes 1-4). The *FUS1* RNA levels were quantified and normalized, as described above. The relative *FUS1* RNA levels in *MAT*α *STE4* and *MAT*α *STE4*^{SD13} strains differed by less than 1.35-fold at 1 hr (Figure 2-7D). The apparent decrease in signaling in *MAT*α cells may reflect decreased sensitivity to **a**-factor due to degradation of **a**-factor by an extracellular protease (96). These results suggest

that pheromone pathway signaling is not greatly affected by the expression of the *STE4*^{SD13} allele in *MAT*α cells.

5. *STE4*^{SD13} suppression of receptor inhibition is independent of *GPA1*

The G-protein α subunit acts as a negative regulator of Gβγ signaling. Deletion of *GPA1* in wild type cells results in constitutive activation of the pheromone pathway due to the presence of free Gβγ complexes. *GPA1* null cells arrest as large unbudded cells in the G_1 phase of the cell cycle and contain high levels of pheromone-inducible transcripts resulting from the constitutive activation of pheromone signaling. *MAT***a** *STE3*^{DAF} cells containing a null allele of *GPA1* are able to suppress this constitutive activation, demonstrating that the *STE3*^{DAF} mutation is independent of *GPA1* (33, 66). If *STE4*^{SD13} encodes a protein that acts to specifically reverse the *STE3*^{DAF} phenotype, then expression of *STE4*^{SD13} should be able to increase signaling in a *MAT***a** *STE3*^{DAF} strain containing a null allele of *GPA1*. To test this hypothesis, the level of pheromone signaling was measured in a *MAT***a** *STE3*^{DAF} strain containing a null allele of *GPA1*. Wild type strains lacking *GPA1* do not require addition of pheromone to induce pheromone pathway signaling, as the pathway is constitutively activated, therefore, these strains also contained a null allele of *FAR1*, which encodes the cyclin-dependent kinase inhibitor, to circumvent the constitutive growth arrest resulting from Δ*gpa1*. *MAT***a** *STE3*^{DAF} cells containing wild type *STE4* (Figure 2-8A, lane 3) were able to block the constitutive signaling resulting from deletion of *GPA1*,

Figure 2-8. Effect of *STE4*^{SD13} in cells lacking the Gα and α-factor receptor genes.

(A) RNA was isolated from the following strains: a *MAT*α *STE3*^{DAF} *ste4::HIS3 gpa1::TRP1 far1::URA3* strain (K39-23Df) containing either a wild type *STE4* plasmid (YCpLSTE4, lane 1) or a plasmid containing the *STE4*^{SD1} allele (YCpLSD13, lane 2), and a *MAT***a** *STE3*^{DAF} *ste4::HIS3 gpa1::TRP1 far1::URA3* strain (K39-23Bf) containing either a wild type *STE4* plasmid (YCpLSTE4, lane 3) or a plasmid containing the *STE4*^{SD13} allele (YCpLSD13, lane 4). (B) RNA was isolated from the following strains: a *MAT***a** *STE3*^{DAF} *ste4::HIS3 gpa1:TRP1* strain (K39-23B) containing either a wild type *STE4* plasmid (YCpLSTE4, lane 1) or a plasmid containing the *STE4*^{SD13} allele (YCpLSD13, lane 2), and a *MAT***a** *STE3*^{DAF} *ste4::HIS3 gpa1::TRP1 ste2::LEU2* strain (K39-23B.s2) containing either a wild type *STE4* plasmid (YCpLSTE4, lane 3) or a plasmid containing the *STE4*^{SD13} allele (YCpLSD13, lane 4). RNA blots were prepared and hybridized as described in the legend to Figure 2-5. The data were quantified by PhosphorImager analysis and the level of *FUS1* RNA was normalized to the control *PGK1* RNA level. The relative level of *FUS1* RNA is shown below each lane.

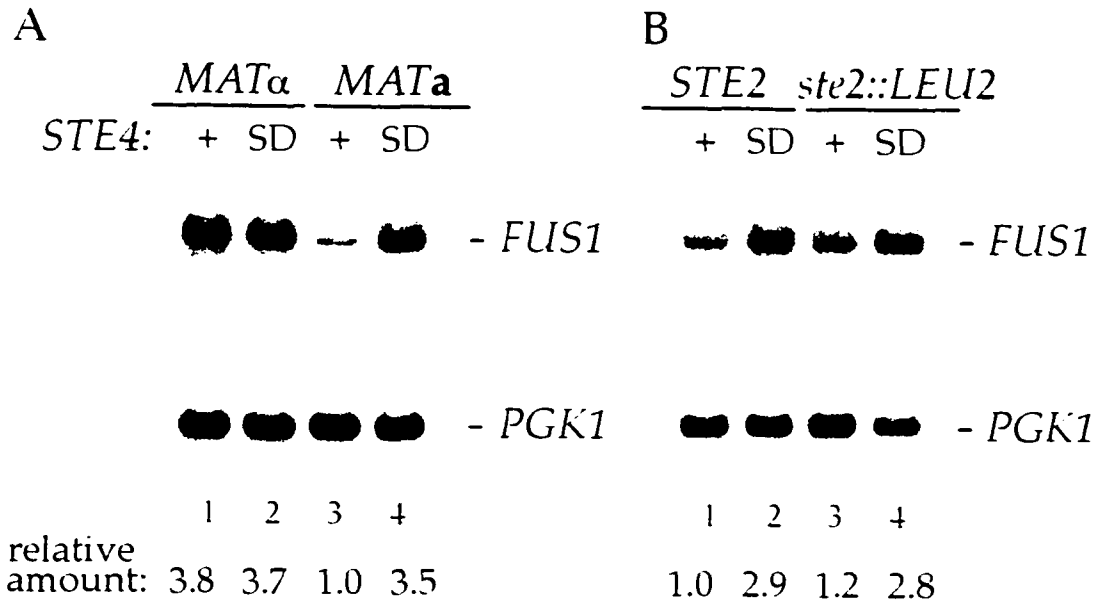

as previously described (33, 66). Expression of *STE4*^{SD13} increased the *FUS1* RNA levels by approximately 3.5-fold compared to *STE4* in the same strain (Figure 2-8A, compare lanes 3 and 4). The ability of the *STE4*^{SD13} allele to reverse the *STE3*^{DAF} phenotype in Δ*gpa1* cells demonstrates that Ste4p^{SD13} does not mediate receptor inhibition through the direct interaction with the Gα subunit (Gpa1p), as *STE4*^{SD13} is capable of reversing the *STE3*^{DAF} phenotype in the absence of *GPA1*. The results described above further support the theory that *STE4*^{SD13} is able to specifically reverse the *STE3*^{DAF} phenotype.

6. *STE4*^{SD13} suppression of receptor inhibition is cell-type specific

*MAT***a** *STE3*^{DAF} Δ*gpa1* cells containing the *STE4*^{SD13} allele displayed increased signaling. Therefore, it was of interest to test whether expression of the *STE4*^{SD13} allele in *MAT*α Δ*gpa1* cells can affect signaling. The *FUS1* RNA levels were measured in *MAT*α Δ*gpa1* cells containing the *STE3*^{DAF} mutation. The strains also contained a null allele of *FAR1* to prevent cell cycle arrest as a result of Δ*gpa1*, as described above. Since deletion of *GPA1* results in ligand and receptor independent pheromone response pathway signaling, this situation provided a means of testing whether unoccupied Ste3p could likewise have an inhibitory function on signaling. The level of transcriptional activation in a *MAT*α Δ*gpa1* strain containing the *STE3*^{DAF} allele was measured. The *MAT*α Δ*gpa1* *STE3*^{DAF} strain contained

approximately 3.8 fold greater *FUS1* RNA than a *MAT***a** Δ*gpa1* $STE3^{DAF}$ strain (Figure 2-8, lanes 1 and 3). Expression of the $STE4^{SD13}$ allele in either the *MAT*α or the *MAT***a** strain resulted in similar levels of *FUS1* induction (Figure 2-8A, lanes 2 and 4). Expression of $Ste3p^{DAF}$ in *MAT***a** cells has an inhibitory effect, whereas expression of $Ste3p^{DAF}$ in *MAT*α cells does not inhibit signaling in *GPA1* null strains. $STE4^{SD13}$ was able to increase the basal level of *FUS1* RNA in a *MAT***a** Δ*gpa1* $STE3^{DAF}$ strain, whereas expression of $STE4^{SD13}$ did not alter the basal level of *FUS1* RNA in a *MAT*α Δ*gpa1* $STE3^{DAF}$ strain. These results demonstrate that $STE4^{SD13}$ is able to specifically reverse the $STE3^{DAF}$-mediated suppression of constitutive signaling in a *MAT***a** Δ*gpa1* strain. This ability to increase signaling was cell-type dependent, as the level of signaling in the *MAT*α Δ*gpa1* strain expressing either $STE4^{SD13}$ or *STE4* was essentially identical. The results may suggest that a *MAT***a**- specific gene is required for receptor inhibition and $Ste4p^{SD13}$ is able to inhibit the function of this cell-type specific protein.

7. *STE2* is not required for $STE4^{SD13}$phenotype

The results presented above suggest that a cell-type specific gene acts downstream of $STE3^{DAF}$ to mediate receptor inhibition. *STE2* is an obvious *MAT***a**- specific gene which could mediate receptor inhibition. However, it has previously been demonstrated that deletion of *STE2* does not affect $STE3^{DAF}$- mediated receptor inhibition (66). An experiment was performed to

test whether expression of *STE2* affects *STE4*^{SD13}-mediated suppression of receptor inhibition. Basal *FUS1* levels were measured in the presence of either wild type *STE4* or the *STE4*^{SD13} allele in a *MAT***a** *STE3*^{DAF} Δ*gpa1* strain containing either *STE2* or a Δ*ste2* allele. Expression of *STE4*^{SD13} alleles in either *MAT***a** Δ*gpa1* *STE2* or *MAT***a** Δ*gpa1* Δ*ste2* strains resulted in an approximately 3-fold increase in basal *FUS1* RNA levels compared to the same strains containing wild type *STE4* (Figure 2-8B, lanes 1-4). The results suggest that deletion of *STE2* does not affect the ability of Ste4p^{SD13} to reverse receptor inhibition.

The results presented thus far indicate that expression of the *STE4*^{SD13} allele in a *MAT***a** *STE3*^{DAF} strain confers the ability to specifically reverse receptor inhibition, as assayed by pheromone-dependent transcriptional activation. The allele did not result in either supersensitivity to pheromone or constitutive activation of the pheromone response pathway in wild type *MAT***a** or *MAT*α cells. The *STE4*^{SD13} allele was able to reverse the *STE3*^{DAF} phenotype independently of *GPA1* and *STE2*. In addition, the ability to reverse receptor inhibition was demonstrated to be cell-type specific. Isolation of an allele of *STE4* that was able to specifically reverse the *STE3*^{DAF} phenotype supported the theory that receptor inhibition is mediated by the Gβ subunit Ste4p. Therefore, it was of interest to determine the regulatory mechanisms that affect wild type Ste4p activity in the context of receptor inhibition, which will be described below.

8. Electrophoretic mobility and relative abundance of Ste4p in *STE3*^{DAF} cells

Overexpression of Ste4p results in activation of the pheromone pathway due to an increase in the amount of free Gβγ complexes (29, 103, 151). Therefore, one mechanism of pheromone pathway signaling downregulation may involve regulation of the total cellular abundance of Ste4p. It is plausible that *STE3*^{DAF} cells may downregulate Ste4p activity through decreasing the concentration of free Gβγ complexes by decreasing the total cellular abundance of Ste4p as compared to wild type cells. To test this theory, the abundance of Ste4p was observed in wild type and *STE3*^{DAF} cells. Total cell lysates were isolated in wild type and *STE3*^{DAF} cells after treatment with pheromone for the indicated time points, and equivalent amounts of total protein were subjected to immunoblot analysis using polyclonal anti-Ste4p antiserum (67). Wild type *MAT***a** cells treated with α-factor for 1 hr and 2 hr appeared to contain the same amount of Ste4p as cells left untreated (Figure 2-9A, lanes 1-3). After treatment for 4 hr with pheromone, the amount of Ste4p in wild type cells appeared to increase slightly, compared to Ste4p levels in cells left untreated (Figure 2-9A, lanes 1 and 4). This difference in abundance of Ste4p may reflect an increase in the pheromone-induced transcription of *STE4*. The amount of Ste4p did not appear to be significantly altered in *STE3*^{DAF} cells after treatment with pheromone for up to 2 hr, as compared to wild type cells (Figure 2-9A, lanes 1-3 and lanes 5-8). In contrast, the level of

Figure 2-9. Electrophoretic mobility and relative abundance of Ste4p in *STE3*^{DAF} cells.

The following strains were treated with α-factor (0.1 μM) for the indicated periods of time: (A) A *MAT***a** *STE3* strain (H67-9D.Ba) (lanes 1-4), a *MAT***a** *STE3*^{DAF} strain (H67-6C.Ba) (lanes 5-8), and a strain containing a null allele of *ste4* (AC17-7B) (lane 9). (B) A *MAT***a** *STE3* *ste4::HIS3* strain (AC17-7B) containing a *STE4*$^{\Delta 310\text{-}346}$ plasmid (YCpΔ36, lanes 1-4) and *MAT***a** *STE3*^{DAF} *ste4::HIS3* strain (AC17-2B) containing a *STE4*$^{\Delta 310\text{-}346}$ plasmid (YCpΔ36, lanes 5-8). Cell extracts were prepared and resolved by SDS-PAGE. Western blots were probed with an anti-Ste4p antiserum.

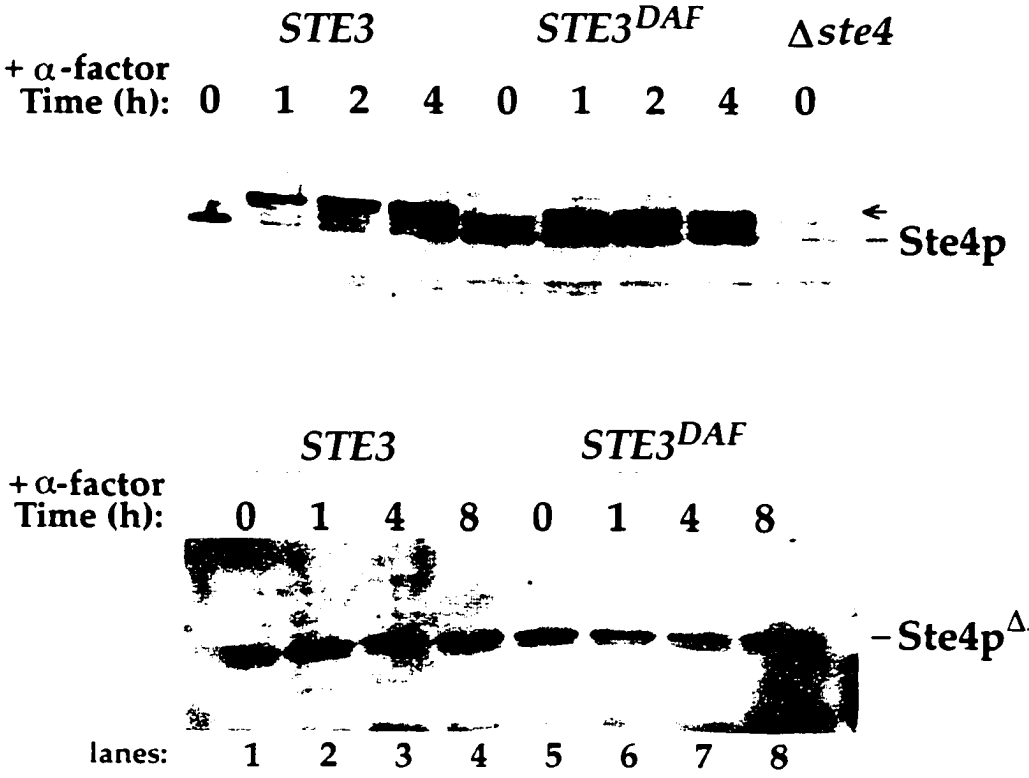

Ste4p in *STE3*^{DAF} cells exposed to pheromone for 4 hr did not appear to increase as observed in wild type cells (Figure 2-9A, lanes 4 and 8). This finding is consistent with previous results showing that an increase in pheromone-induced transcription is not observed at late time points in *STE3*^{DAF} cells. The immunoblot of cells containing a null allele of *STE4* did not contain an observable band that corresponds to Ste4p (Figure 2-9, lane 9). These results suggest that Ste4p protein levels are not significantly altered in wild type or *STE3*^{DAF} cells after treatment with pheromone. Signaling in *STE3*^{DAF} cells has been demonstrated to decrease after 1 hr of pheromone treatment, therefore, the effects of *STE3*^{DAF}-mediated receptor inhibition most likely occur prior to 4 hr. Therefore, the absence of an increase in Ste4p levels in *STE3*^{DAF} cells may reflect the absence of signaling in *STE3*^{DAF} cells that prevents transcriptional induction of Ste4p.

Post-translational modification may be a mechanism of regulating the activity of Ste4p. There was an observable difference in the electrophoretic mobility of Ste4p in wild type cells as compared to *STE3*^{DAF} cells after pheromone treatment. The predominant species of Ste4p in wild type and *STE3*^{DAF} cells prior to pheromone treatment is a species of approximately 47 kD (Figure 2-9A, lane 1 and 5). Treatment with pheromone for up to 4 hr in wild type strains resulted in the appearance of several slower migrating species, which most likely represent phosphorylated species (Figure 2-9A, lanes 2-4). Pheromone-induced phosphorylation of the Gβ subunit has been described previously (28). In *STE3*^{DAF} cells, the predominant species of Ste4p

appeared to be a slower migrating band after exposure to pheromone for 1 hr, but at 4 hr the predominant species of Ste4p appeared to be a faster mobility band that may represent a hypophosphorylated form of Ste4p (Figure 2-9A, lanes 5-8). Taken together, these results demonstrate that Ste4p abundance is not significantly altered in wild type and *STE3*^{DAF} cells after 2 hr of pheromone treatment. After treatment of wild type cells for 4 hr, there is a slight increase in the level of Ste4p most likely due to sustained transcription of *STE4*, which is not apparent in *STE3*^{DAF} cells that undergo receptor inhibition at the same time point (32). However, Ste4p is differentially post-translationally modified in *STE3*^{DAF} cells, as compared to wild type cells. The role of phosphorylation in receptor inhibition will be further discussed below.

9. A region of Ste4p subject to phosphorylation is not essential for receptor inhibition

The crystal structure of the $G_{t\beta\gamma}$ complex demonstrated that the G_{β} subunit contains seven WD repeats and has a seven-bladed propeller structure (135). The structure of the Ste4p Gβ subunit is predicted to form a similar seven-bladed propeller structure based on the predicted protein sequence. However, in contrast to metazoan Gβ subunits, the yeast β subunit contains two non-homologous regions; the first is located at the extreme amino terminus (corresponding to Ste4p residues 1- 35) of the protein and the second is located within WD repeat 6 (corresponding to Ste4p residues 310-346). It was shown previously that deletion of the second non-homologous region resulted in an

altered protein, Ste4p$^{\Delta 310\text{-}346}$, has previosuly been demonstrated to be defective in pheromone-induced phosphorylation and resulted in supersensitivity to pheromone (28). Phosphorylation of Ste4p is not essential for signal transduction, but has been reported to have a role in adaptation to pheromone (28). However, the exact function of phosphorylation in recovery from pheromone is not understood (28). Other alterations within this region, which was demonstrated to be subject to phosphorylation, may also be subject to other post-translational modifications not tested here. To test the requirement for this region of Ste4p on receptor inhibition, transcriptional activation was measured in *STE3*^{DAF} cells containing the *STE4*$^{\Delta 310\text{-}346}$ allele. Wild type and *STE3*^{DAF} cells containing a low copy plasmid containing the *STE4*$^{\Delta 310\text{-}346}$ allele were treated with pheromone for the indicated times. The *FUS1* RNA levels in wild type cells containing the *STE4*$^{\Delta 310\text{-}346}$ allele increased approximately 10-fold compared to basal levels after 1 hr treatment with pheromone and remained high for 3 hr (Figure 2-10, lanes 2-4). *STE3*^{DAF} cells containing the *STE4*$^{\Delta 310\text{-}346}$ allele displayed a 4-fold increase in *FUS1* RNA levels at 1 hr and decreased to basal levels by 2 hr (Figure 2-10, lanes 5-8). These results demonstrate that expression of the phosphorylation-defective Ste4p$^{\Delta 310\text{-}346}$, as the sole source of G_β subunits, did not result in sustained *FUS1* RNA transcription after pheromone treatment at late time points. In fact, the *FUS1* level after treatment with pheromone for 1 hr in *STE3*^{DAF} cells containing the *STE4*$^{\Delta 310\text{-}346}$ allele was significantly reduced compared to *STE3*

Figure 2-10. Effect of *STE4*$^{\Delta 310\text{-}346}$ on signaling.

A *MAT***a** *STE3* *ste4::HIS3* strain (AC17-7B) was transformed with a plasmid containing the *STE4*$^{\Delta 310\text{-}346}$allele (YCpΔ36, lanes 1-4) and a *MAT***a** *STE3*^{DAF} *ste4::HIS3* strain (AC17-2B) was transformed wtih a plasmid containing the *STE4*$^{\Delta 310\text{-}346}$ allele (YCpΔ36, lanes 5-8) were treated with α-factor (0.1μM) for the indicated periods of time and RNA was isolated. RNA blots were prepared and hybridized as described in legend Figure 2-5. The data were quantified by PhosphorImager analysis and the level of *FUS1* RNA was normalized to the control *PGK1* RNA level.

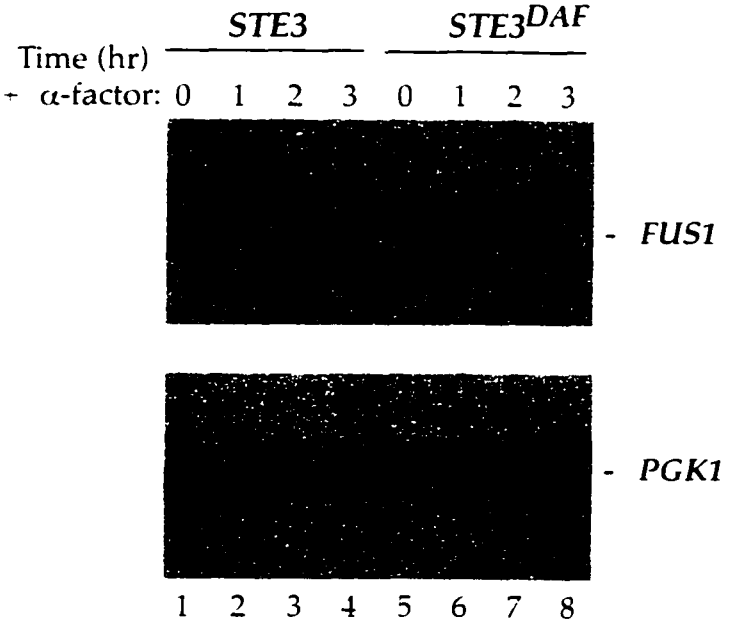

cells containing the *STE4*$^{\Delta 310\text{-}346}$ allele (Figure 2-10, lanes 2 and 6). This observation suggested that expression of the *STE4*$^{\Delta 310\text{-}346}$ allele in *STE3*^{DAF} cells appeared to promote receptor inhibition to a greater degree that cells expressing *STE4*. The mechanism by which this allele promotes receptor inhibition is unknown. These results support the previous finding that expression of this allele does not suppress the *STE3*^{DAF} phenotype, as measured by halo assay (30). Taken together, these results demonstrate that expression of a phosphorylation defective Ste4p$^{\Delta 310\text{-}346}$ does not inhibit receptor inhibition in *STE3*^{DAF} cells. However, other alterations within residues 310-346 of Ste4p may be subject to other post-translational modifications not tested here. Therefore, deletion of the domain of Ste4p that has previously been demonstrated to be essential for phosphorylation does not appear to be required for *STE3*^{DAF}-mediated receptor inhibition.

Ste4p$^{\Delta 310\text{-}346}$ abundance is not altered in *STE3*^{DAF} cells

In wild type cells exposed to pheromone, the predominant species of Ste4p appears as several slower migrating, presumably hyperphosphorylated species (Figure 2-9A, lanes 2-4). Whereas at late time points, in *STE3*^{DAF} cells treated with pheromone, the predominate form of Ste4p appeared to be a faster mobility species, which is presumably hypophosphorylated (Figure 2-9A, lanes 6-8). To better assess the abundance of Ste4p in wild type and *STE3*^{DAF} cells, Ste4p$^{\Delta 310\text{-}346}$ was observed by immunoblot analysis in wild type and *STE3*^{DAF} cells. Total cell lysates were isolated in wild type and *STE3*^{DAF}

cells after treatment with pheromone for the indicated time points and equivalent amounts of total protein for each sample were loaded and subjected to immunoblot analysis using polyclonal anti-Ste4p antiserum (67). The amount of Ste4p$^{\Delta 310\text{-}346}$ does not appear to be significantly altered in *STE3*^{DAF} cells treated with pheromone for up to 8 hr, as compared to wild type cells (Figure 2-9B, lanes 1-8). The Ste4p$^{\Delta 310\text{-}346}$ species identified by immunoblot displays a faster mobility than wild type Ste4p consistent with *STE4*$^{\Delta 310\text{-}346}$ encoding an altered protein containing a deletion. No slower migrating species were observed after pheromone treatment, which supports the theory that deletion of the domain within WD repeat 6 creates an altered Ste4p (Figure 2-9B, lanes 1-8). It is apparent that the levels of Ste4p are not significantly altered in *STE3*^{DAF} cells as compared to wild type cells treated with pheromone, demonstrating that the mechanism by which *STE3*^{DAF} inhibited signaling does not involve changes in the abundance of Ste4p.

10. Localization of a GFP-Ste4p fusion protein in wild type and *STE3*^{DAF} cells

The *STE4*^{SD13} mutation characterized above was demonstrated to specifically reverse receptor inhibition, which suggested that receptor inhibition is mediated through Ste4p. However, regulation of the total cellular abundance of Ste4p is probably not the primary mechanism of regulating Ste4p activity during receptor inhibition. Therefore, it was of interest to determine whether the subcellular localization of Ste4p is

differentially regulated in *STE3*^{DAF} cells treated with pheromone as compared to wild type cells. To observe the localization of Ste4p, wild type or *STE3*^{DAF} cells containing a chromosomal deletion of *STE4* were transformed with a low copy plasmid containing a green fluorescent protein (GFP)- *STE4* gene fusion under the control of the *STE4* promoter. The strains were grown to log phase then treated with pheromone for the indicated amounts of time. The fusion protein in live cells was subjected to direct observation using a Zeiss Axioskop with a FITC filter.

In cells left untreated, the GFP-Ste4p fusion appeared to reside partially at the plasma membrane and also diffusely in either internal membranes or the cytoplasm (Figure 2-11A). This observation is consistent with cell fractionation results obtained previously that describe approximately 40% of Ste4p associated tightly with the plasma membrane, 30% of Ste4p associated with internal membranes, and 30% of Ste4p associated with non-membrane fractions as measured by density gradient centrifugation of cell fractions (67). After treatment with pheromone, wild type *MAT***a** cells initiated projection formation at 1 hr and appeared to form full-length projections by 2 hr (Figure 2-11, A - D). In *MAT***a** cells treated with pheromone for 1 hr, the GFP-Ste4p fusion had a polarized distribution and appeared to associate with the plasma membrane at a position that corresponds to the presumptive projection tip (Figure 2-11B). The fusion protein signal remained highly concentrated at the projection tip and the plasma membrane in cells exposed to pheromone for 2

and 3 hr (Figure 2-11C and 3-11D). Cells containing a vector alone did not display an observable signal (data not shown).

The localization of the GFP-Ste4p fusion in untreated *MAT***a** $STE3^{DAF}$ cells was essentially identical to that seen in untreated wild type *MAT***a** cells left untreated (compare Figure 2-11A and Figure 2-12A). The GFP-Ste4p fusion signal appeared to have a polarized distribution toward the presumptive projection tip in $STE3^{DAF}$ cells exposed to pheromone for 1 hr (Figure 2-12B); the signal appeared to be similar to that seen in wild type cells exposed to pheromone for the same amount of time (Figure 2-12B). After $STE3^{DAF}$ cells were treated for 2 hr with pheromone, the fusion protein signal appeared to remain predominately localized to the projection tips (Figure 2-12C). However, after treatment for 3 hr with pheromone, the GFP-Ste4p fusion in $STE3^{DAF}$ cells did not appear to be associated predominately with the plasma membrane (Figure 2-12D). The $STE3^{DAF}$ cells resumed budding, which is consistent with these cells undergoing receptor inhibition of cell cycle arrest, as compared to wild type cells which formed projections in response to pheromone under the same conditions (compare Figure 2-11D and 2-12D).

In *MAT***a** $STE3^{DAF}$ cells exposed to pheromone for 3 hr, the GFP-Ste4p protein did not appear to be associated with the plasma membrane. Instead it appeared to be associated within an internal compartment as the signal did not appear diffusely present throughout the cytoplasm, which is observed in cells expressing GFP alone (data not shown). However, the exact localization of the fusion protein has not yet been determined. In addition, at an

Figure 2-11. Localization of GFP-Ste4p in wild type cells.

A *MAT***a** *STE3 ste4::HIS3* strain (AC17-7B) containing a low copy GFP-*STE4* plasmid (BTL49) was treated with α-factor (0.1μM) for the indicated times. The live cells were subjected to direct microscopic observation using a Zeiss Axioskop and FITC filter.

STE3

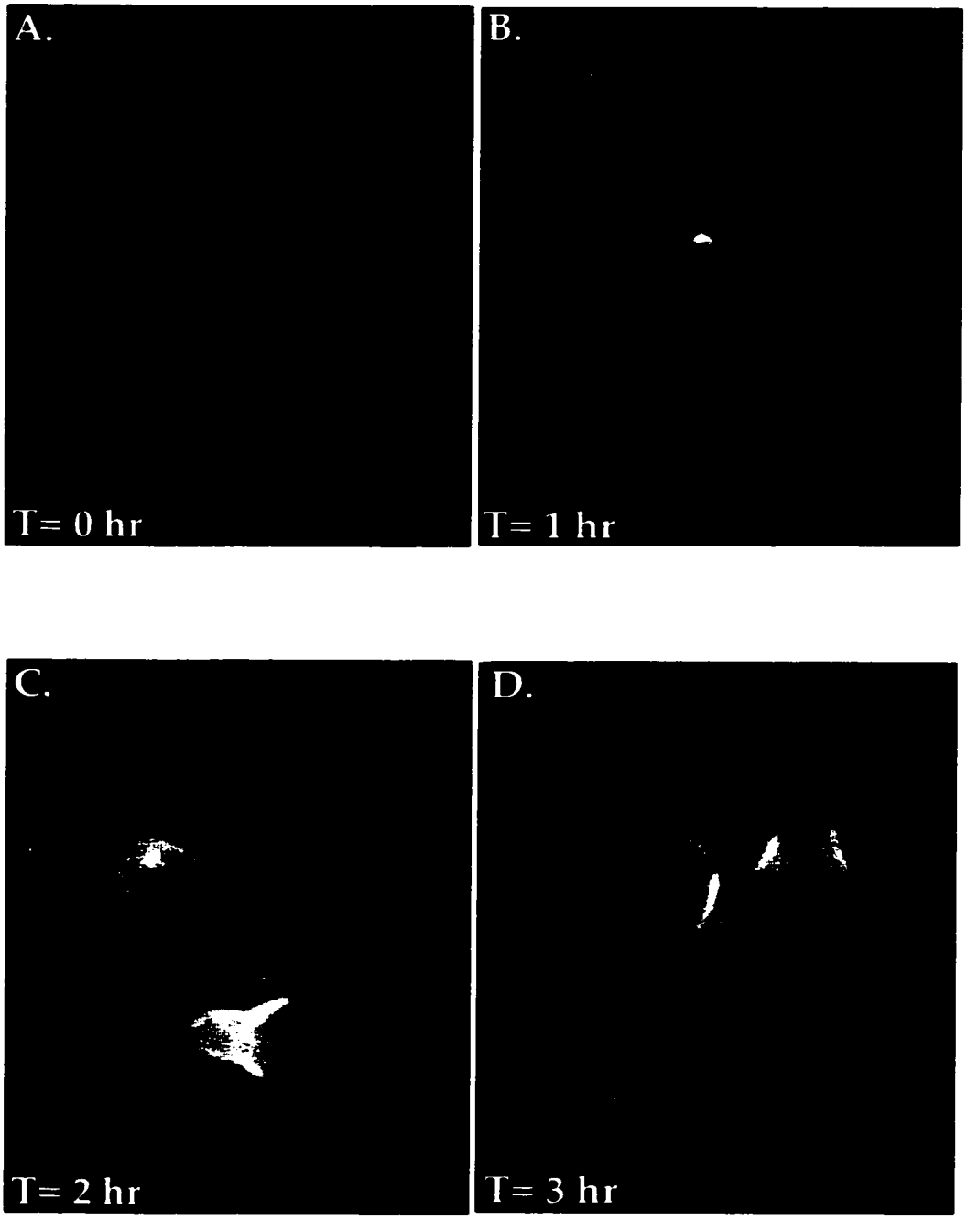

Figure 2-12. Localization of GFP-Ste4p in *STE3*^{DAF} cells.

A *MAT***a** *STE3*^{DAF} *ste4::HIS3* strain (AC17-7B) containing a low copy GFP-*STE4* plasmid (BTL49) was treated with α-factor (0.1μM) for the indicated times. The live cells were subjected to direct microscopic observation using a Zeiss Axioskop and FITC filter.

STE3DAF

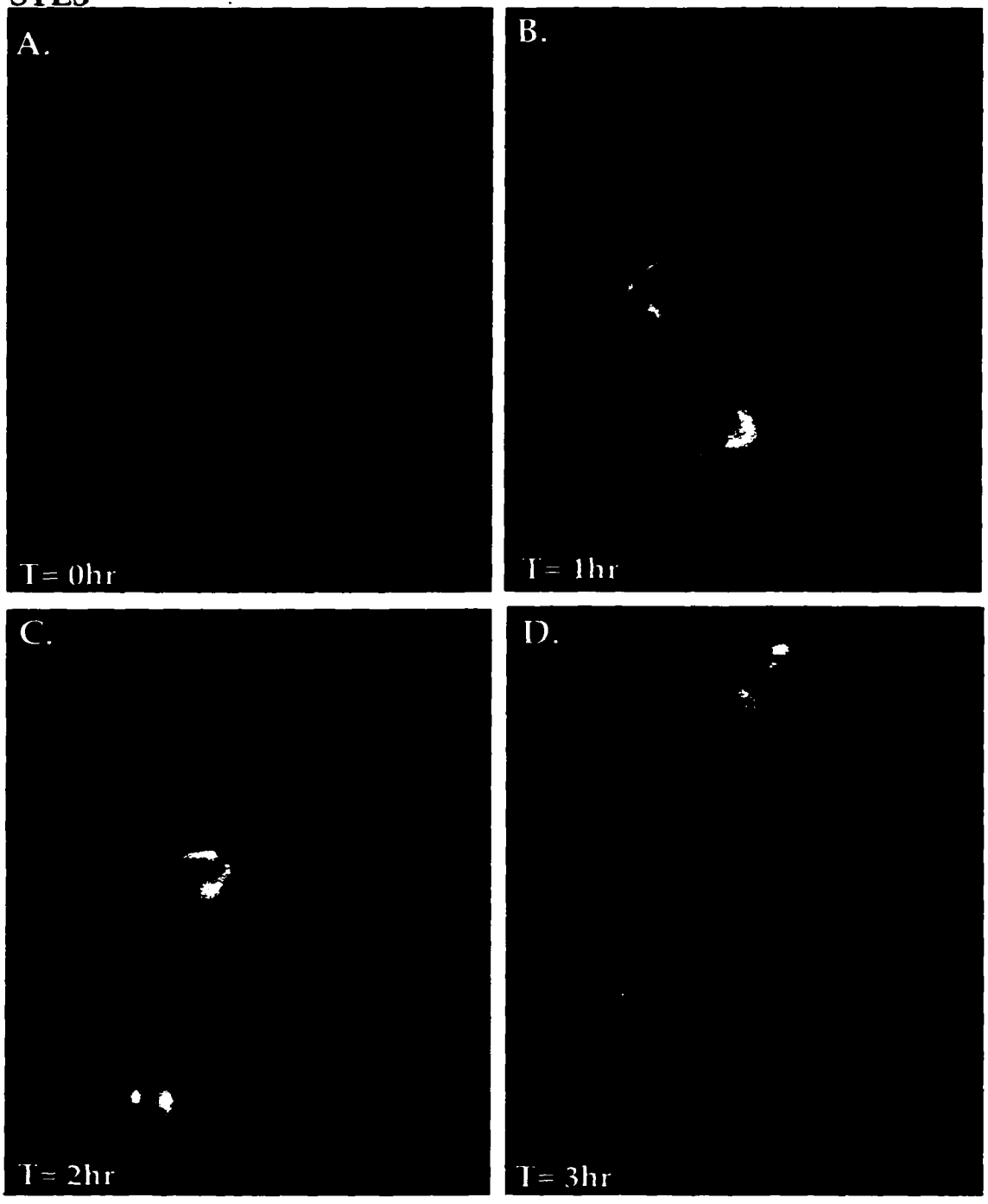

intermediate time point of 2.5 hr, a *STE3*^{DAF} cells appeared to be composed of a mixture of cells either undergoing projection formation or budding. The fusion protein appeared to reside at the plasma membrane in cells undergoing projection formation and the fusion protein appeared to reside with the plasma membrane and an internal fraction in cells undergoing bud formation (data not shown). The results demonstrate that after exposure to pheromone for 3 hr, *MAT***a** *STE3*^{DAF} and wild type cells did not have the same pattern of localization of GFP-Ste4p. One
interpretation of these results is that one mechanism of controlling the activity of Ste4p is through regulation of the localization of Ste4p. Wild type cells may be competent to signal by the continued association of Ste4p with the plasma membrane.

11. Ste4p- and Ste4p^{SD}- GFP fusions differentially localize in *STE3*^{DAF} cells

The wild type Ste4p localized predominately with the plasma membrane in *MAT***a** cells exposed to pheromone, however, the GFP-Ste4p fusion protein did not appear to be associated with the plasma membrane in *STE3*^{DAF} cells at late time points. These results suggested that regulation of Gβ subunit activity in the pheromone response pathway may include a mechanism of regulating the localization of Ste4p. The *STE4*^{SD} mutations obtained previously were capable of specifically reversing receptor inhibition. Therefore, it was of interest to observe the localization of the altered protein

in *STE3*^{DAF} cells. This aim was accomplished by first introducing the *STE4*^{SD} point mutations within the coding region of *STE4* in the GFP fusion construct. An allele of *STE4*^{SD10} (See Table 3) containing two of the three mutations (Q17L and R162G) that comprise the *STE4*^{SD13} allele were introduced by site-directed mutagenesis. Expression of the *STE4*^{SD10} allele in a *STE3*^{DAF} strain was capable of reversing receptor inhibition as assayed by cell cycle arrest (data not shown). The relative contribution of the third point mutation (Q21R) toward reversing the receptor inhibition phenotype was less significant, therefore, it was not introduced into this allele. The GFP constructs containing gene fusions with either wild type *STE4* or *STE4*^{SD10} were introduced into *STE3*^{DAF} cells containing chromosomal deletions of *STE4* and the fusion proteins were subjected to direct microscopic observation in live cells, as described above.

The mutant protein GFP-Ste4p^{SD10} signal appeared similar to the wild type GFP-Ste4p fusion signal in untreated *STE3*^{DAF} cells (Figure 2-13, top panels). Both the GFP-Ste4p^{SD10} and wild type GFP-Ste4p signals appeared polarized toward the presumptive projection tip in *STE3*^{DAF} cells exposed to pheromone for 1 hr (Figure 2-13 middle panels). After treatment for 3 hr with α-factor, the wild type GFP-Ste4p fusion in *STE3*^{DAF} cells did not appear to be primarily plasma membrane associated, as described above (Figure 2-13, bottom left panel). In contrast, the GFP-Ste4p^{SD10} fusion signal in *STE3*^{DAF} cells exposed to α-factor for 3 hr appeared to be predominately plasma membrane associated (Figure 2-13, bottom right panel). The pattern of localization of the

Figure 2-13. Localization of GFP-Ste4p^{SD10} in *STE3*^{DAF} cells.

A *MAT***a** *STE3*^{DAF} *ste4::HIS3* strain (AC17-7B) containing either a GFP-*STE4* plasmid (BTL49) (left panels) or a GFP-*STE4*^{SD10} plasmid (YCpGFP-SD10) (right panels) were treated with α-factor (0.1μM) for the indicated times. The live cells were subjected to direct microscopic observation using a Zeiss Axioskop and FITC filter.

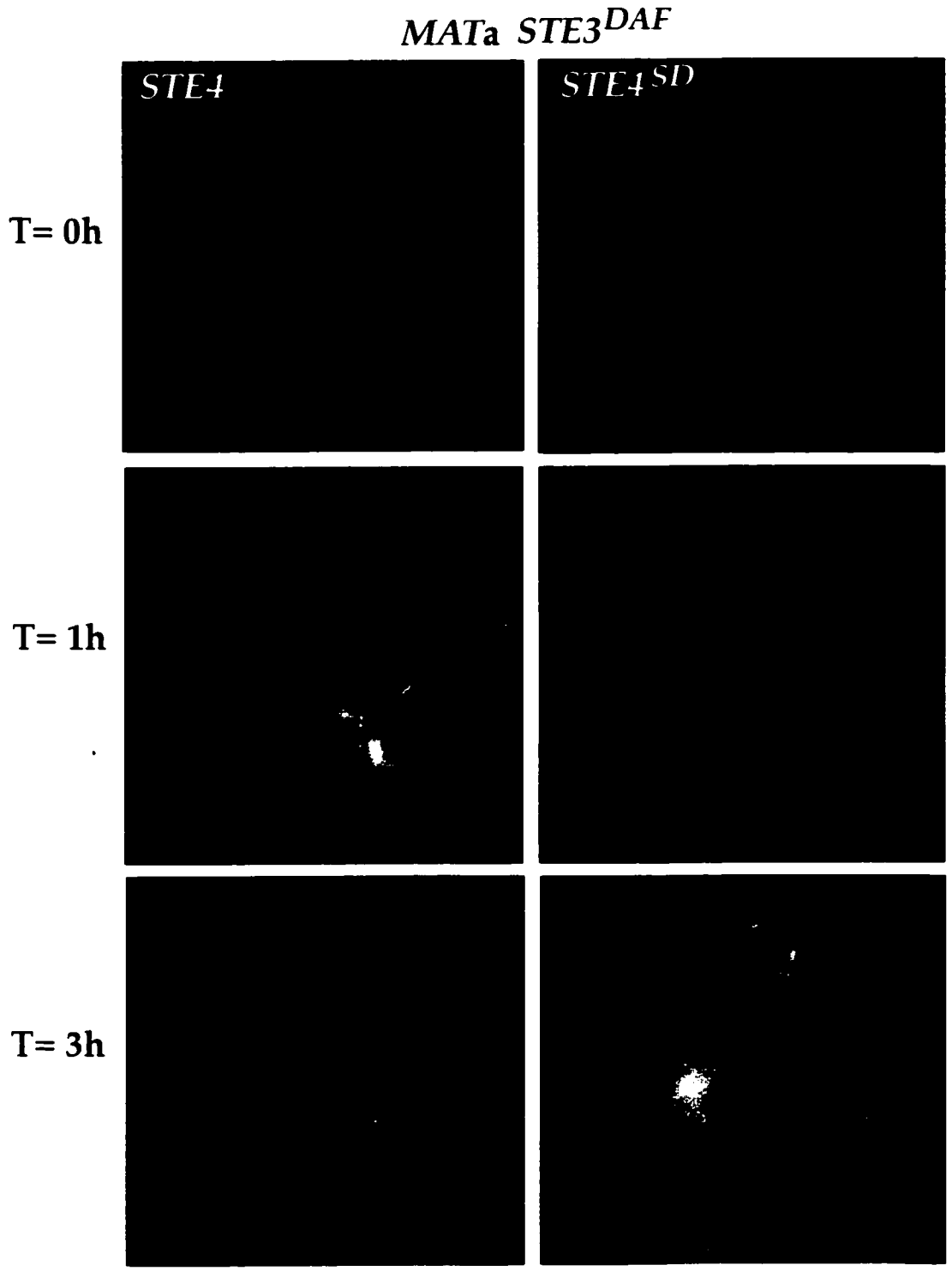

GFP-Ste4p and GFP-Ste4p^{SD10} fusion proteins appeared similar in wild type cells treated with pheromone or left untreated (data not shown), consistent with the function of this allele to specifically reverse receptor inhibition.

The localization of a GFP-Ste4p fusion protein appeared differentially regulated in wild type and *STE3^{DAF}* cells at late time points after pheromone treatment. Expression of the *STE4^{SD10}* allele in *MAT***a** *STE3^{DAF}* cells demonstrated that alteration of residues of Ste4p can specifically reverse receptor inhibition. In addition, the observation that the GFP-Ste4p^{SD10} fusion displayed an altered localization specifically in *STE3^{DAF}* cells at late time points demonstrated that the ability to reverse receptor inhibition is also associated with an increase in Ste4p association with the plasma membrane. Ste4p^{SD10}-mediated suppression of receptor inhibition displayed altered localization as compared to wild type Ste4p in *STE3^{DAF}* cells and appeared to become more plasma membrane localized. The ability to localize to the plasma membrane at late timepoints after pheromone treatment is also seen in wild type cells exposed to pheromone. Therefore, it is plausible that control of Ste4p activity may entail a mechanism of regulating the localization of Ste4p.

12. Ste3p internalization is not required for receptor inhibition

The results described above suggest that a GFP-Ste4p fusion protein becomes internalized in response to pheromone in *STE3^{DAF}* cells. The evidence also suggests that Ste4p is not diffusely localized within the cytoplasm, but may remain associated with an internal membrane. Recent

evidence has demonstrated that the Gβγ complex in other systems may interact directly with GPCRs, perhaps as a mechanism to promote ligand-induced conformational changes in Gα or to promote the association between the Gα subunit and its receptor (107, 141, 142). If the Gβγ complex directly binds to the **a**-factor receptor (Ste3p), then it is plausible that **a**-factor receptor endocytosis promotes Gβ internalization during receptor inhibition. To test whether endocytosis of Ste3p is essential for receptor inhibition, a *STE3ΔC363* allele, which removes 107 amino acids from the carboxy terminus of Ste3p, was constructed. It has been demonstrated previously that cells containing the mutation *STE3Δ365*, which encodes a carboxy terminally truncated receptor, do not display constitutive endocytosis of Ste3p (37). The halo assay was used to measure cell cycle arrest in *MAT***a** cells containing the *STE3ΔC* allele. A plasmid containing either a wild type *STE3* allele or the *STE3ΔC* allele, both under the control of the $STE3^{DAF}$ promoter, was introduced into *MAT***a** cells. A *MAT***a** strain containing vector alone was also tested and as expected, these cells arrested and produced a halo (Figure 2-14, bottom). *MAT***a** cells expressing *STE3* were resistant to pheromone-induced cell cycle arrest and did not form a halo (Figure 2-14, top left). Likewise, *MAT***a** cells containing the *STE3ΔC* allele were resistant to pheromone-inducible arrest (Figure 2-14, top right). These results demonstrate that constitutive endocytosis of Ste3p is not essential for receptor inhibition.

Figure 2-14. Receptor inhibition is not altered by preventing Ste3p endocytosis.

Halo assays were performed with 5 µl of 1mM α-factor. *MAT***a** strains containing the following plasmids: Bottom, control vector (YEplac112); top left, plasmid containing $STE3^{DAF}$ allele (YEpGFP-STE3); Top right, plasmid containing $STE3\Delta C^{DAF}$ allele (YEpGFP-STE3ΔC).

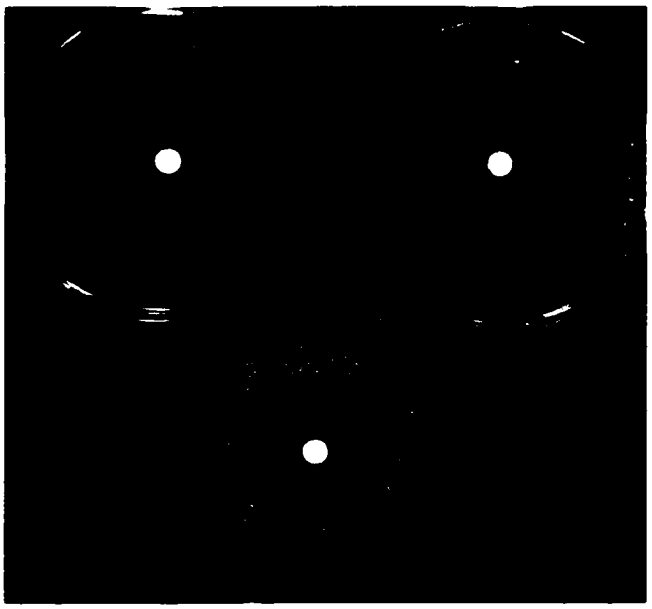

Figure 2-15. Localization of Ste3p in *MAT***a** cells.

The following strains were treated with α-factor (0.1 μM) for the indicated times: (A-C) a *MAT***a** *STE3* strain (H67-9D.Ba) containing a $STE3^{DAF}$ plasmid (YEpSTE3-GFP); (D-E) *MAT***a** *STE3* strain (H67-9D.Ba) containing a $STE3\Delta C^{DAF}$ plasmid (YEpSTE3ΔC-GFP).

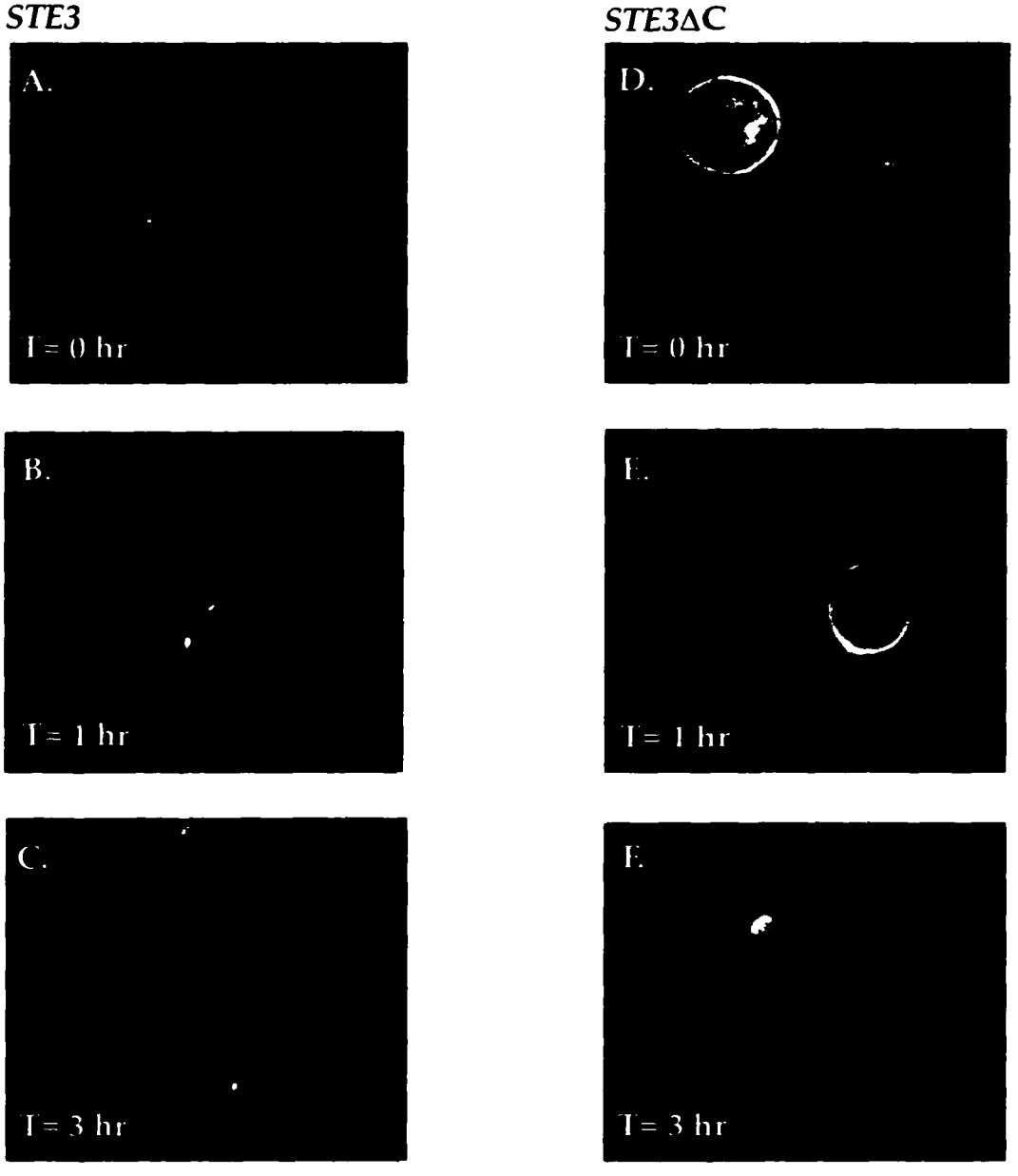

To test further the hypothesis that receptor endocytosis is not a requirement for receptor inhibition, the subcellular localization of Ste3p receptor was observed in *MAT***a** $STE3^{DAF}$ cells. A *STE3*-GFP gene fusion under the control of a $STE3^{DAF}$ promoter and was introduced into *MAT***a** cells. Cells expressing Ste3p-GFP were grown to log phase and treated with α-factor for 3 hr, then were subjected to direct microscopic observation. In the absence of pheromone, the localization pattern of the Ste3p-GFP fusion appeared faintly at the plasma membrane with punctate foci, which may represent endocytic vesicles transporting Ste3p from the plasma membrane to the vacuole or secretory vesicles delivering Ste3p-GFP to the plasma membrane (Figure 2-15A). After α-factor treatment for 1 hr, the signal appeared largely plasma membrane associated with some foci still observable (Figure 2-15B). The Ste3p-GFP fusion pattern appeared largely punctate with some cell surface signal after treatment with pheromone for 3 hr (Figure 2-15C). The results suggest that Ste3p is not restricted to the plasma membrane in *MAT***a** $STE3^{DAF}$ cells treated with pheromone. The pattern of localization of Ste3p in *MAT***a** cells was not reminiscent of the pattern of localization of Ste4p in $STE3^{DAF}$ cells (compare Figure 2-15C to Figure 2-12D).

In contrast, the pattern of localization of the endocytosis-defective Ste3ΔCp-GFP fusion protein appeared primarily associated with the cell surface in untreated cells. Small foci were also observed which may represent secretory vesicles delivering Ste3ΔCp-GFP to the plasma membrane (Figure 2-

15D). The intensity of the signal appeared increased compared to the wild type Ste3p-GFP signal, which may be due to increased cell surface receptor number due to inhibition of endocytosis. Treatment with α-factor for 1 hr appeared to result in a slight increase in plasma membrane association of the fusion protein (Figure 2-15E). After treatment with α-factor for 3 hr, the cells containing the Ste3ΔCp-GFP fusion protein appeared to contain more punctate foci than cells treated for 1 hr, however the predominant signal appeared localized to the plasma membrane (Figure 2-15F). The results suggest that in *MAT***a** cells exposed to pheromone, Ste3p-GFP is not primarily plasma membrane associated and Ste3ΔCp-GFP is primarily plasma membrane associated. The genetic and fluorescence results demonstrate that endocytosis of Ste3p is not required for receptor inhibition.

13. Endocytosis is not essential for receptor inhibition

The previous results demonstrate that a truncated version of Ste3p, which is defective in endocytosis, is capable of promoting receptor inhibition. If Ste4p is targeted to an internal membrane, another protein may promote endocytosis of Ste4p during receptor inhibition. To test whether endocytosis is essential for receptor inhibition, a strain containing a mutation in *END4*, a gene required for endocytosis, was assayed. *END4* (also called *SLA2*) is required for endocytosis, actin cytoskeleton polarization, and growth at high temperatures (68, 147). *END4* is also required for viability in a strain deleted

Figure 2-16. Effect of *end4* on receptor inhibition.

Halo assays were performed with 5 µl of 1 mM α-factor. Right, a *MAT***a** *end4::LEU2* strain containing either a low copy $STE3^{DAF}$ plasmid (pDAF2m-8, left), or a control vector (YCp50, right).

end4 STE3 *end4 STE3^{DAF}*

for the gene encoding actin-binding protein 1 (*ABP1*) (147). To test the ability of a strain containing *end4* to suppress the $STE3^{DAF}$ phenotype, either a plasmid containing $STE3^{DAF}$ or vector alone was transformed into *end4* cells and cell cycle arrest was measured by the halo assay. The results demonstrate that *end4* cells arrested in response to pheromone (Figure 2-16, left), whereas *end4* cells containing $STE3^{DAF}$ displayed resistance to cell cycle arrest (Figure 2-16, right). The binding of α-factor to its receptor normally results in internalization by receptor-mediated endocytosis (73, 125). Strains containing*end4* mutations display defects in receptor clearance and internalization, however, endocytosis is not required for signal transduction (116, 119). In fact, cells containing *end4* mutations display an increased sensitivity to pheromone compared to *END4* cells (116). Therefore, inhibition of endocytosis does not appear to have an effect on receptor inhibition.

14. Abundance of soluble Ste4p is not altered in $STE3^{DAF}$ cells

Direct observation of the GFP-Ste4p fusion suggested Ste4p is differentially localized in wild type as compared to $STE3^{DAF}$ cells exposed to pheromone. A plausible mechanism of downregulation of Ste4p activity in $STE3^{DAF}$ cells may entail sequestration of Ste4p away from the plasma membrane. Ste4p was hypothesized to be targeted to an internal compartment rather than to a soluble cytoplasmic pool. This hypothesis is based on the observation that the GFP-Ste4p signal (See Figure 2-12F) did not

Figure 2-17. Abundance of soluble Ste4p.

A *MAT***a** *STE3* strain (H67-9D.Ba) and a *MAT***a** $STE3^{DAF}$ strain (H67-6C.Ba), both containing a $STE4^{\Delta 310\text{-}346}$ plasmid (YCpΔ36). The strains were grown to log phase and treated with α-factor for 3 hr and cell extracts were separated into soluble (S20) and pellet (P20) fractions. Equal amounts of protein were subjected to SDS-PAGE, and the proteins were detected by using immunoblotting using anti-Ste4p antibodies and antibodies specific for Pgk1p (cytosolic) and Pma1p (plasma membrane).

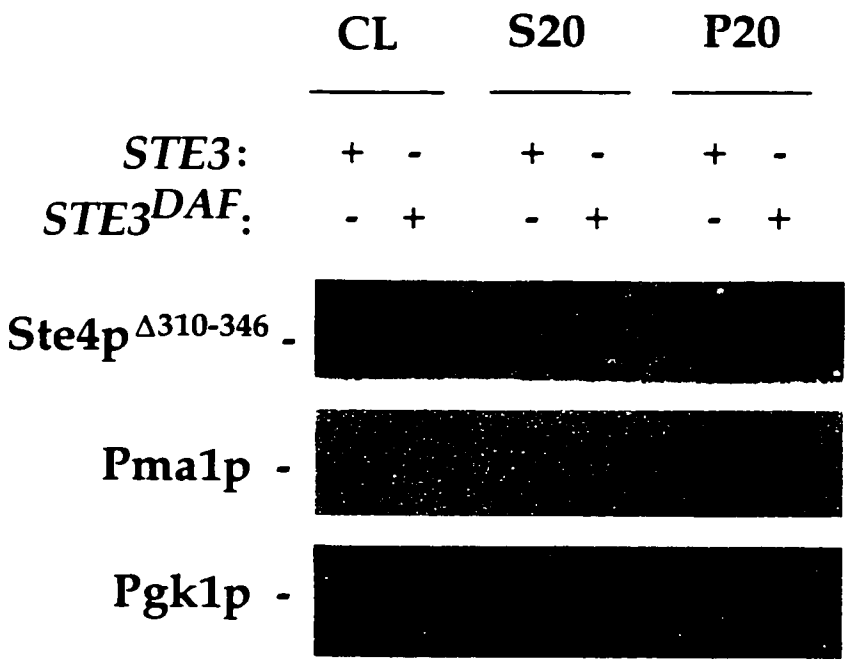

become diffusely localized within the cytoplasm but appeared vesicular or particulate at late time points after pheromone treatment in *STE3*^{DAF} cells. To test whether Ste4p in *STE3*^{DAF} cells exposed to pheromone was re-localized from the plasma membrane to a soluble fraction in *STE3*^{DAF} cells, the soluble and insoluble fractions of *STE3*^{DAF} and wild type cells treated with pheromone were separated and subjected to immunoblot analysis with anti- Ste4p antiserum. Post-translational modification of Ste4p in wild type cells exposed to pheromone appeared to complicate the determination of Ste4p abundance, therefore, the altered Ste4p$^{\Delta 310\text{-}346}$ protein that does not alter receptor inhibition was used. Wild type and *STE3*^{DAF} cells were grown to log phase, treated with pheromone for 3 hr, mechanically lysed and subjected to a low speed spin to remove nuclei and cellular debris. This cleared cell lysate was then subjected to differential centrifugation at 20,000 x*g*, to produce supernatant (S20) and pellet (P20) fractions. The cleared cell lysate and supernatant (S20) contained cytoplasmic proteins, as observed by the Pgk1p control (Figure 2-17, lanes 1-2 and lanes 3-4). The pellet contained crude cellular membranes, as observed by the presence of Pma1p, which is a plasma membrane ATPase (Figure 2-17, lanes 5 and 6). The pellet did not contain the cytoplasmic protein marker Pgk1p. Cleared cell lysates of wild type and *STE3*^{DAF} cells contained comparable amounts of Ste4p (Figure 2-17, lanes 1 and 2). Wild type and *STE3*^{DAF} cells contained approximately equal amounts of Ste4p in their cytosolic fractions (S20) (Figure 2-17, lanes 3 and 4). Wild type and *STE3*^{DAF} cells also contained approximately equal amounts of Ste4p in the

pellet fractions (P20) (Figure 2-17, lanes 5 and 6). These results suggest that the abundance of soluble Ste4p is not significantly increased in *STE3*^{DAF} cells as compared to WT cells. Therefore, it appears unlikely that Ste4p, which did not appear to be associated with the plasma membrane in *STE3*^{DAF} cells at late time points after pheromone treatment, is localized to a soluble fraction. Therefore, two likely interpretations of these results are as follows: in *MAT***a** *STE3*^{DAF} cells Ste4p is targeted 1) from the plasma membrane to an internal membrane pool or 2) from the plasma membrane to a large protein complex or aggregate, which is not membrane bound, but still pellets with the crude membrane fraction. An alternative interpretation to account for the similarities in abundance of Ste4p in the pellet fraction of *STE3*^{DAF} and wild type cells is that Ste4p is actually not internalized in *STE3*^{DAF} cells after treatment with pheromone, but remains associated with the plasma membrane fraction in both wild type and *STE3*^{DAF} cells. An interpretation of these results may suggest that the fusion of the GFP to the Ste4p may result in alterations of the normal activity and localization of Ste4p. However, the fusion protein activity is not significantly altered as measured by mating in wild type cells and receptor inhibition in *STE3*^{DAF} cells (data not shown). The findings that the fusion protein is functional for both signal transduction and receptor inhibition may be interpreted to suggest that the localization of the GFP-Ste4p accurately reflects wild type Ste4p localization during receptor inhibition.

The abundance of Ste4p in the pellet fraction was not altered in *STE3*^{DAF} cells as compared to wild type cells. It is unknown whether Ste4p remains membrane-associated during receptor inhibition-dependent internalization and, if so, the identity of this putative membrane also remains to be elucidated. Further experiments are required to determine whether Ste4p changes localization in wild type and *STE3*^{DAF} cells and whether Ste4p associates with membranous structures.

D. Discussion

*MAT***a** cells expressing Ste3p are resistant to pheromone-induced cell cycle arrest (33). Epistasis experiments suggested that $STE3^{DAF}$ acts at a level between *STE4* and *STE5* (32). The following results suggest that $STE4^{SD}$ mutations specifically reverse receptor inhibition: 1) the $STE4^{SD13}$ allele increased signaling, as assayed by *FUS1* RNA transcription, at late timepoints after pheromone treatment, 2) expression of $STE4^{SD13}$ in wild type *MAT***a** and *MAT*α cells does not result in either increased basal or pheromone-induced *FUS1* RNA levels, 3) $Ste4p^{SD13}$-mediated reversal of receptor inhibition is independent of the G protein α subunit and the α-factor receptor (encoded by *GPA1* and *STE2*, respectively), and 4) the effect of $STE4^{SD13}$ is cell-type specific.

Location of $STE4^{SD13}$ mutations

The crystal structure of the $G_{t\beta\gamma}$ complex and the G protein heterotrimer has been solved and it demonstrates that, in contrast to the Gα subunit, the Gβγ complex does not undergo significant structural changes during G protein activation (84, 135). These results indicate that the Gα subunit may negatively regulate Gβ activity by blocking the interaction with downstream components which bind to a common interface (135). Residues of the Ste4p Gβ subunit important for interaction with Gpa1p (the Gα subunit) have been mapped genetically (G124, W136, L138, and S151) (148). In addition, residues

of Ste4p important for interaction with potential downstream effectors Ste20p and Ste5p have also been mapped. (69, 89, 153). The mutations present in the *STE4*^{SD13} allele probably do not alter effector interactions since *STE4*^{SD13} allele encodes a protein with three mutations (Q17L, Q21R, R162G) that do not overlap with effector interaction regions. In addition, Ste4p^{SD13} appeared to signal normally in wild type cells, suggesting that effector interactions are not altered. Two of these mutations map to the amino terminus of Ste4p and the third mutation maps to a site within the second blade of the propeller. It is plausible that these mutations are essential for interaction with a novel protein not yet identified, which may promote receptor inhibition.

Subcellular localization of Ste4p Gβ subunit during receptor inhibition

The isolation of mutations in *STE4* that encode an altered protein capable of reversing receptor inhibition supports the view that the *STE3*^{DAF} mutation represents a normal cellular process in *S. cerevisiae*. In addition, it indicates that Ste4p mediates receptor inhibition of mating pathway signaling. Therefore, preliminary characterization of the receptor inhibition function of Ste4p in *STE3*^{DAF} cells was undertaken. Results demonstrated that a GFP-Ste4p fusion appeared differentially localized in wild type and *STE3*^{DAF} cells at late time points after pheromone treatment. Ste4p may be targeted away from the plasma membrane as a mechanism of downregulating Ste4p activity during receptor inhibition. It has been documented previously that G proteins may interact with cytoskeletal elements. However, there was no direct co-localization of the GFP-Ste4p and actin in wild type *MAT***a** cells

expressing the GFP-Ste4p which were incubated with rhodamine-conjugated phalloidin (data not shown). The results suggest that Ste4p may become associated with a protein complex or an internal membrane during receptor inhibition.

Compartmentalization of heterotrimeric G proteins.

Previously, it has been demonstrated that cellular compartmentalization of G proteins and receptors is an important mechanism for regulating signaling. For example, G_i-coupled receptors interact functionally with specific subsets of G proteins (55) and the specificity of signaling in reconstituted systems appears less than that observed *in vivo* (79, 80). These results suggest that although G proteins are capable of interacting with specific receptors to initiate signaling, activation is not observed *in vivo* due to localization constraints. In addition, G protein activity has been observed to be dependent on association with cytoskeletal elements (115, 160). Sequestration of signaling components into cellular compartments may be an important mechanism of regulating G protein activity.

The association of heterotrimeric G proteins with membrane domains may be a mechanism of regulating signaling. The plasma membrane of epithelial cells is organized into easily distinguishable apical and basolateral domains. These smaller membrane domains owe their insolubility in non-ionic detergent to the fact that they are rich in sphingolipids and cholesterol (11). Proteins known to be associated with detergent insoluble membranes

are often linked to lipids, which include GPI anchored proteins and proteins with long saturated acyl chains, such as Src-family kinases (131). The Gα, Gβ, and Gγ subunits of the *S. cerevisiae* pheromone response pathway have been demonstrated to be associated with membranes that are detergent insoluble, however, the biological significance of this finding remains to be elucidated (82). Heterotrimeric G protein α and β subunits have also been documented to be associated with detergent resistant membranes in a human neuroblastoma cell line (117). In support of the theory that sequestration of signaling molecules into specific membrane domains is of physiological significance, an enrichment of Gβγ complexes in these detergent resistant membranes was observed in serum-induced cells as compared to serum-starved cells (117).

The association of G proteins with membranes requires lipid modification of the Gα and Gγ subunits (reviewed in (13)). The yeast Gγ subunit (Ste18p) is required for association of Gβ with cellular membranes (67). It has been demonstrated that residue C107 of the carboxy terminal CAAX box in Ste18p is subject to prenylation, which is essential for membrane association and activity, as introduction of the mutation C107S resulted in sterility (56, 152). Since the Gβγ subunits form a complex that is dissociated only by denaturants, alterations in the lipid modification of Ste18p may be important for specifying interactions with different membranes and may be a mechanism of regulating Gβγ complex localization and activity.

Therefore, cellular compartmentalization of G proteins may be an emerging and important means of controlling G protein activity.

There is increasing evidence that the Gβγ complex may interact directly with G protein-coupled receptors. Fluorescence energy transfer experiments have demonstrated that the $G_{t\beta\gamma}$ complex interacts with rhodopsin (107). Also, regions within the 7th WD repeat interact with a peptide derived from the third intracellular loop of the α2-adrenergic receptor (142). Direct binding of Ste4p (Gβ) to Ste3p (**a**-factor receptor) to prevent Gβ association with effectors is a plausible mechanism of down-regulating Gβ activity. However, the following results do not support this theory: 1) a GFP-Ste4p fusion protein appeared internalized during receptor inhibition, whereas a Ste3p-GFP fusion appeared predominately plasma membrane associated; 2) expression of the *STE3*ΔC allele that encodes an **a**-factor receptor that is defective in endocytosis did not affect receptor inhibition; 3) Ste3p inhibits signaling in *MAT***a** cells, without altering signaling in *MAT*α cells which normally express Ste3p. Therefore, in the model proposed (Figure 2- 18), Ste4p in *MAT***a** $STE3^{DAF}$ cells does not become internalized by direct interaction with Ste3p. Instead, the Ste4p may become internalized by interaction with a regulatory factor (Factor R) which may be an **a**-specific protein activated by Ste3p.

Figure 2-18. Model of receptor inhibition.

Wild type *MAT***a** cells do not express Ste3p. Therefore in this model, these cells would not be capable of activating or inducing Factor R in response to pheromone treatment. In this case the signaling pathway would be active (left). *MAT***a** $STE3^{DAF}$ cells or early zygotes (**a**/α) express both pheromone receptors. In this model Factor R would be induced or activated in response to pheromone treatment. The signaling pathway would be repressed (right).

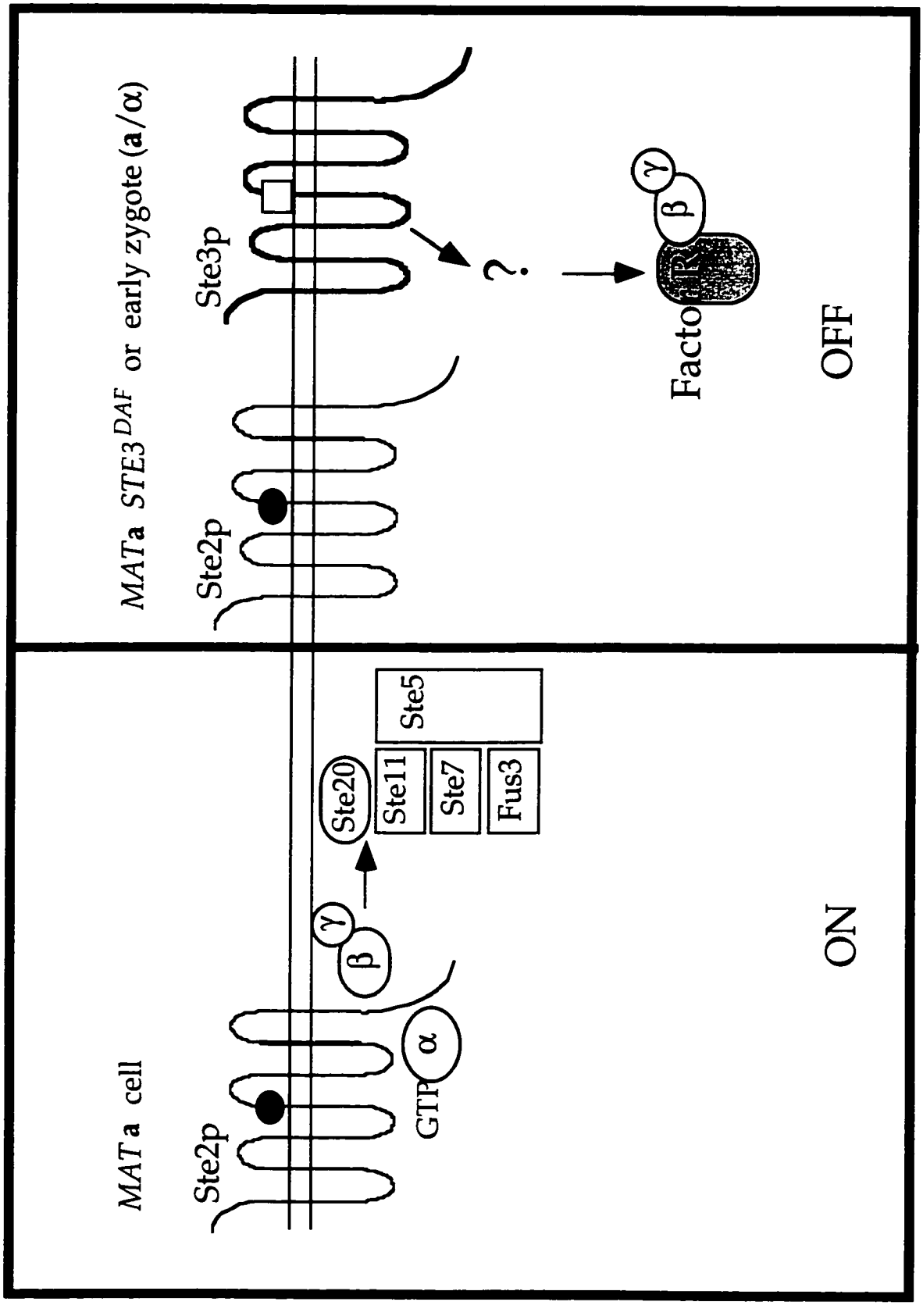

Cell type specific regulators of signaling

The *STE4*^{SD13} allele has an effect in *MAT***a** cells in which Ste3p is expressed, however it does not have an effect in *MAT*α cells that normally express Ste3p. The finding that signaling is inhibited *MAT***a** *STE3*^{DAF} cells at late time points may indicate that an **a**-specific regulatory factor (Factor R) may be subject to pheromone-dependent induction or activation. In the model presented, *MAT*α cells normally express Ste3p, but do not express the **a**-specific inhibitor, therefore signaling is not affected by Ste3p expression. In wild type *MAT***a** cells, Ste3p is not expressed, therefore, Factor R may not be induced or activated. In *MAT***a** *STE3*^{DAF} cells or early zygotes (*MAT***a**/α) that express both pheromone receptors, the **a**-specific Factor R may be present and capable of promoting Ste4p internalization and down-regulation (Figure 2-18). This **a**-specific product cannot be Ste2p since a strain containing a null allele of *STE2* does not suppress receptor inhibition. The model indicates that Factor R may have decreased affinity for Ste4p^{SD13} as a mechanism of increasing the concentration of Gβγ present at the plasma membrane, which reverses receptor inhibition.

Previous studies demonstrated that an **a**-specific product exists that is able to inhibit mating in *MAT***a** cells that express Ste3p (7). The studies showed that expression of different combinations of receptors and pheromones altered mating efficiency. *STE3* and *MFα1* were expressed under the control of heterologous promoters to permit the expression of the **a**-factor

receptor and α-factor in a *MAT***a** *ste2 ste6* strain and a *matα1* strain. (In the *MAT***a** *ste2 ste6* strain, deletion of *ste2* eliminates expression of the α-factor receptor and deletion of *ste6* eliminates the secretion of **a**-factor. *matα1* strains do not express either α- or **a**-specific products.) The *matα1* strain resulted in a 10-fold increase in mating efficiency as compared to the *MAT***a** *ste2 ste6* strain. The strains expressed identical receptor (**a**-factor receptor) and pheromone (α-factor), therefore, the decrease in mating efficiency of the *MAT***a** strain was due to the presence of an **a**-specific product, factor R.

The physiological relevance of the $STE3^{DAF}$ mutation has still not been determined. Since *MAT***a** cells do not express the **a**-factor receptor at any time during the normal life cycle, the $STE3^{DAF}$ mutation probably does not play a role during vegetative growth. Therefore, the ability of the **a**-specific regulatory factor to inhibit pheromone response pathway signaling may be important during early zygote formation when both pheromone receptors are present on the cell surface. Cells expressing Ste3p may activate or induce factor R to inhibit signaling by sequestering Ste4p away from the plasma membrane through either a direct or indirect interaction. $Ste4p^{SD13}$ may specifically reverse receptor inhibition through a decreased interaction with factor R. Inhibition of signaling is likely to be required to promote recovery from mating and cell cycle progression of the newly formed zygote.

E. Future Studies

The regulatory factor which is active in *MAT***a** cells expressing Ste3p remains to be identified. This aim may be accomplished through identification of **a**-specific genes, which contain α2 operator sequences. Alternatively, factor R may be identified through identification of proteins that differentially interact with Ste4p and Ste4p^{SD13} through two-hybrid interaction assays. Genes such as *AKR1*, *SYG1*, and *CDC24*, encode proteins that have been demonstrated to interact with the Ste4p Gβ subunit, as measured by the two-hybrid assay, however the role of these proteins in receptor inhibition has not been examined (74, 113, 136). Another future aim is the determination of the physiological significance of receptor inhibition. The identification of the *STE4*^{SD13} allele which reverses receptor inhibition may provide a means of testing the recovery of mating cells from pheromone response pathway signaling. It is of interest to determine the localization of Ste4p in *MAT***a** *STE3*^{DAF} cells at late time points after pheromone treatment; this aim may be accomplished through cell fractionation experiments. In addition, the fusion protein signal in wild type and *STE3*^{DAF} cells treated with pheromone for 1 hr appears as small punctate foci which did not appear directly associated with the plasma membrane. Identification of proteins that co-localize with these structures may be accomplished through indirect immunofluorescence using known markers. The isolation of the *STE4*^{SD13}

allele demonstrated that receptor inhibition is mediated by Ste4p and supports the view that the $STE3^{DAF}$ mutation represents a cellular event in the yeast life cycle. The observation that the localization of Ste4p is altered in the two cell types suggested that cellular compartmentalization of Ste4p may be a mechanism of regulating G protein activity.

III. *SSF1* Overexpression Increases Mating Efficiency

A. Introduction

SSF1 isolation and initial characterization

The studies presented here were designed to characterize the mating function of the *SSF1* gene. *SSF1* (suppressor of sterile four) was isolated as a multicopy suppressor which increased the mating efficiency of a strain that contained a temperature sensitive G-protein β subunit (*ste4*^{ts})(157). In addition to *SSF1*, other known genes isolated in the screen were *STE18*, which encodes the G-protein γ subunit and *STE5*, which encodes the molecular scaffold that interacts with components of the MAP kinase pheromone response pathway. A closely related homolog, *SSF2*, was identified by hybridization of a *SSF1* probe to yeast genomic DNA (157). Highly similar partial cDNAs of unknown function from *Arabidopsis thialiana* and *Homo sapiens* have been identified; however, Ssf proteins do not share any obvious homology with known proteins (157). Cells containing a deletion in either *SSF1* or *SSF2* do not have an obvious phenotype, but, deletion of both genes is lethal (157). Previously, a strain was constructed that contained null mutations in *SSF1* and *SSF2* and also contained a plasmid with a copy of the *SSF1* gene under the control of the *GAL1* promoter (157). The depletion phenotype was examined by switching the cells to glucose-containing medium. Depletion of *SSF* gene products resulted in growth arrest and decreased mating efficiency; the mating efficiency of cells shifted to glucose for

14 hours decreased by 10-fold and after 18 hours decreased by approximately 100-fold with respect to cells expressing *SSF1* (157). These results demonstrate that depletion of *SSF* gene products results in growth arrest and a decrease in mating efficiency.

The essential and mating functions of Ssf1p are unknown. In addition, it is not known whether the essential function and the mating function of Ssf1p may be attributed to a single cellular process or to separate processes. The dual role of Ssf proteins may be explained by a single function. For example, control of cellular morphology during both vegetative growth and mating requires polarized cell growth. Initial characterization of the mating function was directed at examination of the role of Ssf1p in signal transduction and mating projection formation, which is discussed below.

Part of the work presented here has been published in (77).

B. Materials and methods

1. Plasmid construction

pGAL-SSF1.14 and pSSF1-2 have been described previously (157). The pfar1c-1::*URA3* plasmid, which contains a *URA3* disruption of the carboxyl-terminal domain of *FAR1*, was constructed using a version of the 1.2 kb *Hin*DIII fragment that contains the *URA3* gene in which the *Hin*DIII sites have been converted to *Xba*I sites by filling them in with Klenow polymerase. The 1.2 kb *Xba*I fragment containing *URA3* was cloned into the *Xba*I sites of a 2.4 kb *Xho*I-*Eco*RI fragment containing *FAR1* from pJM306 (98), which had been cloned into pGEM-2 (Promega). The *far1c-1::URA3* allele is predicted to express the amino acids 1-536 of Far1p, which contains the region necessary for its G_1 arrest function (146).

The construct that fuses *SSF1* to green fluorescent protein (GFP) gene was made as follows: first, a *Not*I site was inserted immediately before the stop codon in *SSF1* by performing the polymerase chain reaction (PCR; (36)) with oligonucleotide primers oSSF1-1, 5′-CCGGATCCATCCAGATATAGCAGAC-3′, and oSHA3, 5′-CCGGATCCTAGCGGCCGCATTCGACCTCACTAA-3′ (*SSF1* sequences are underlined) to generate a fragment containing the entire coding region of *SSF1*. This 1.4 kb fragment was cloned into the *BamH*I site of YCplac33 (52), using the terminal *BamH*I sites present in the primers, to create pSSF1r-NotI.

Then, a *Not*I site was inserted at the 5′ end of the GFP gene by performing PCR with oligonucleotides oGFP-1, 5′ - TTAGCGGCCGCAGTAAAGGAGAAGAACTTTTC-3′, (GFP sequences underlined) and the T7 primer, 5′-AATACGACTCACTATAG -3′, using as the template plasmid pBluescript-S65T, which contains the version of GFP that has serine 65 changed to threonine (63). The 0.7 kb fragment generated by PCR was digested with *Not*I and cloned into the *Not*I site of pSSF1r-NotI to create pSF-GP1. The final construct, pSF-GP2, was created by cloning the 1.3 kb *Xba*I fragment from pSF-GP1, containing a 3.4 kb *Hpa*I- *Xba*I fragment, which includes the 5′ end of *SSF1* and 2.8 kb of upstream flanking region, cloned into the *Sma*I-*Xba*I sites of YCplac33. YEpSFGP was constructed by cloning the 3.0 kb *BamH*I fragment from pSF-GP2 into the *BamH*I site of YEp351.

2. Strains and media

Strains used in this study are listed in Table 4. H50-16C.Ba was constructed by transformation of H50-16C with a 5.7 kb *Eco*RI-*Sal*I fragment from pJGSST1 (46). Strain JH8-3510a was constructed using a *GAL-HO* construct to switch the mating type of JH8-3510 (157) to *MAT***a**. Strain JH8-3510a.sp was derived from JH8-3510a by disruption of the *SPA2* gene using a 3.8 kb *Hin*DIII-*Sal*I fragment from plasmid p210 to create the *spa2*-Δ3::*URA3* allele (51). Strain JH8-3510.fc was derived from JH83510 by disruption of the carboxyl-terminal region of the *FAR1* gene using a 2.0 kb *Hin*DIII-*Eco*RI fragment from plasmid

pfar1c-1::URA3 to create the *far1c-1::URA3* allele. Strain JH111-1C was constructed by transformation of strain W3031A (obtained from R. Rothstein) with a 3.8 kb *Sac*I *Sph*I fragment from pJH111 (157) to generate an *ssf1::HIS3* allele. Strain H67-9D.Ba has been described previously (32). Strain AC17-7B is a derivation of H67-9D.Ba in which the *STE4* gene has been replaced with a *ste4::HIS3* allele. Mating assays utilized strain W3031B (obtained from R. Rothstein) as the mating partner. All strain constructions involving transformations were confirmed by Southern blot. Strains were grown on YEPD (2% glucose) or YEP-Gal (3% galactose), and strains under selection were grown on synthetic dropout media, as described (132).

3. Yeast methods

Yeast transformations were performed by the lithium acetate method (71) modified as described previously (66). Yeast RNA was extracted from cells as described previously (35).

4. Northern blots

RNA was transferred to a nitrocellulose membrane after formaldehyde-agarose gel electrophoresis as described (90). The membranes were UV cross-linked using a Stratalinker UV box. Prehybridization and hybridization were done at 65°C in a buffer containing 0.9 M NaCl, 0.09 M sodium citrate, 0.1% Ficoll, 0.1% polyvinylpyrrolidone, 0.1% bovine serum albumin, 33 mM sodium pyrophosphate, 50 mM sodium phosphate monobasic. The probes used were gel-purified DNA restriction fragments ^{32}-P labeled by random

primer labeling using a Prime-It kit (Stratagene). The fragments used were: *FUS1*, a 1.4 kb *EcoRI-HinDIII* fragment from pSL589 (97); ribosomal protein gene *TCM1* (126), a 0.8 kb *HpaI-SalI* fragment from plasmid pAB309Δ; phosphoglycerate kinase gene *PGK1*, a 0.5 kb *BamHI-XbaI* fragment from pPGK1.

5. Mating Assays

Quantitative mating assays were performed essentially as described previously in (57). Briefly, approximately 1.5 x 10^7 cells from log phase cultures of *MAT***a** strains were mixed with an equal number of *MAT*α cells and filtered onto 0.45 mm nitrocellulose filters (Whatman). The filters were placed onto YEPD plates and incubated for 5 hr at 30°C, 34°C, or 37°C. Cells were resuspended in 4 ml of sterile water by vortexing, and the cell suspension was diluted and plated onto one type of selective plate to determine the number of *MAT***a** plus diploid cells and another type of selective plate to determine the number of diploid cells. Mating efficiency was calculated as the percentage of diploid cells divided by the number of *MAT***a** plus diploid cells.

6. Immunoblots

For immunoblotting, cells were grown to early log phase, pelleted, and washed once in TE (10 mM tris-HCl and 1 mM EDTA). Cells were resuspended in synthetic medium and incubated at 30°C, 34°C, or 37°C for 3 hr. For pheromone treated samples, α-factor was added to a final

concentration of 3 μM and aliquots were removed at 1 and 6 hr after α-factor addition. Cell lysates were prepared by harvesting 10 ml of log phase cells, washing once with cold TE and resuspending in 350 μl of lysis buffer (50 mM tris-HCl [pH 8.0], 1% SDS, 1 mM PMSF, 1 μg of [apoprotein, leupeptin, chymostatin, and pepstatin] per ml). The mixture was added to acid-washed beads (0.5 mm) and vortexed at high speed for 10 min. Glass beads and cell debris were separated from the lysate by centrifugation in a microfuge for 2 min. Protein concentration of the samples was determined using a bicinchoninic protein assay kit (Pierce) and equal amounts were loaded onto SDS polyacrylamide gels (10% polyacrylamide). Separated proteins were transferred to nitrocellulose and the blot was probed with anti-Ste4p rabbit polyclonal antiserum (67) at a dilution of 1:1000. Donkey anti-rabbit immunoglobulin conjugated to horseradish peroxidase (Amersham) was used at a dilution of 1:10,000 and immune complexes were detected with an enhanced chemiluminescence kit (Amersham).

7. Microscopy

For projection formation assays, cells were grown at 30°C to log phase, pelleted, and washed once with 10 mM Tris pH 8.0, 1 mM EDTA. The cell pellet was resuspended in 5 ml selective medium to an OD_{600} of 0.3, and α-factor was added to a final concentration of 3 μM for *ste4*^{ts} cells or 6 μM for *ste4*^{ts} *spa2* cells. After a 3 hr incubation, the cells were fixed for 1 hr with 3.7% formaldehyde. Cells were photographed with a 100x objective using

differential interference microscopy on a Zeiss Axiophot microscope using TMAX 3200 film.

For fluorescence microscopy, cells containing the Ssf1p-GFP fusion protein were grown to log phase and incubated in 2 μg/ml 4', 6-diamidine-2-phenylindole-dihydrochloride (DAPI) for 5 min room temperature to stain DNA. Indirect immunofluorescence techniques were essentially as described in (111).

For double-label immunofluorescence, cells were grown to early log phase and fixed for 30 min at room temperature in 3.7% formaldehyde. The cells were washed twice in 1 ml of 1.2 M sorbitol, 0.1 M phosphate buffer pH 7.5 (solution A). Cell walls were removed by resuspending the fixed cells in 1 ml solution A, adding 2 μl β-mercaptoethanol and 3 μl of 15 mg/ml zymolase 20T (Seikagaku), and incubating the samples at 37°C for 15 min. Spheroplasted cells were attached to polylysine-coated wells and further permeabilized by immersion in -20°C methanol for 5 min. Cells were washed with PBS-BSA (PBS +1% BSA) and incubated with a 1:1000 dilution of anti-GFP polyclonal antibody (kindly provided by J. Kahana and P. Silver) and a 1:50 dilution of anti-Nop1p monoclonal antibody (2) for 2 hr. Cells were washed with PBS/BSA and then incubated with Texas-Red-conjugated anti-mouse antibody (1:200) and FITC-conjugated anti-rabbit antibody (1:200) for 1 hr. In control experiments, the Texas-Red-conjugated anti-mouse antibody showed no reactivity with the rabbit primary antibody and the FITC-

conjugated anti-rabbit antibody showed no reactivity with the primary mouse antibody. Cells were incubated with DAPI (1μg/ml) for 5 min at room temperature, then washed with PBS/BSA. Slides were mounted with 90% glycerol containing 1 mg/ml ρ-phenylenediamine and 25 mg/ml NaN_3. cells were photographed with a 100x objective using rhodamine, FITC or UV filters on a Zeiss Axiophot microscope using TMAX 3200 film.

Table 4. Strain List: Chapter III

Strain	Genotype	Source
W303-1A	*MATa leu2-3,112 trp1-1 can1-100 ura3-1 ade2-1 his3-11,15*	R. Rothstein
W303-1B	*MATα leu2-3,112 trp1-1 can1-100 ura3-1 ade2-1 his3-11,15*	R. Rothstein
H50-16C	*MATa ssf1-1::HIS3 ssf2-3::TRP1* [pGAL-SSF1.14]	(157); A
H50-16C.Ba	*MATa ssf1-1::HIS3 ssf2-3::TRP1 sst1 ::HISG* [pGAL-SSF1.14]	this study; A
JH111-1C	*MATa ssf1-1::HIS3*	(157); A
H67-9D.Ba	*MATamfa1-Δ3::HIS3 mfa2- Δ 2::HIS3 sst1::hisG*	(32); A
AC17-7B	*MATamfa1-Δ3::HIS3 mfa2- Δ 2::HIS3 sst1::hisG ste4::HIS3*	(32);A

Strains designated *A* in the reference column are isogenic to W3031A.

Strain	Genotype	Source
SY873	*MATα leu2 trp1 ura3 can1-101 his4-519*	Sprague lab
JH8-3510a	*MATa ste4-ts3510*	(157); B
JH8-3510a.sp	*MATa ste4-ts3510 spa2-Δ3::URA3*	this study; C
JH8-3510a.fc	*MATa ste4-ts3510 far1c-1::URA3*	this study; C

Strains designated *B* in the reference column are isogenic to SY873.

Strains designated *C* in the reference column are isogenic to JH8-3510a.

C. Results

Characterization of the mating function of *SSF1*

SSF1 and *SSF2* encode homologous proteins that share an essential function. In addition, Ssf proteins appear to have a mating function, since depletion of Ssf proteins results in a decrease in mating efficiency, however, the role of Ssf proteins in mating is unknown. To begin characterization of the role of Ssf proteins in mating, pheromone-induced transcriptional activation and mating projection formation, which are two major responses to pheromone response pathway activation, were assayed in cells depleted of *SSF* gene products.

1. *SSF* depletion does not abrogate signal transduction

Pheromone pathway signal transduction results in the activation of the transcription factor Ste12p through a MAP kinase cascade. To determine whether Ssf proteins are required to mediate signal transduction, pheromone-induced transcription was assayed in cells depleted of *SSF* gene products. A *Δssf1 Δssf2* strain containing a copy of *SSF1* under the control of the *GAL1* promoter was grown to logarithmic phase in galactose, then was transferred to glucose for 4, 8, and 12 hr to deplete cells of Ssf proteins. At the indicated time points, α-factor was added to an aliquot of cells and pheromone pathway signaling was assayed by measuring *FUS1* RNA levels

Figure 3-1. Pheromone-induced transcription in *ssf* cells.

A Δ*ssf1* Δ*ssf2* strain (H50-16C.Ba) containing a plasmid with the *SSF1* gene under the control of the *GAL* promoter (pGAL-SSF1.14) was grown to log phase in galactose, then switched to glucose for the indicated periods of time. At each time point, an aliquot of cells was treated with 0.1μM α-factor for 30 min and RNA was isolated. A Northern blot prepared from the RNA was hyrbridized with a *FUS1* probe (A) and then rehybridized with a *PGK1* probe (B) as a loading control.

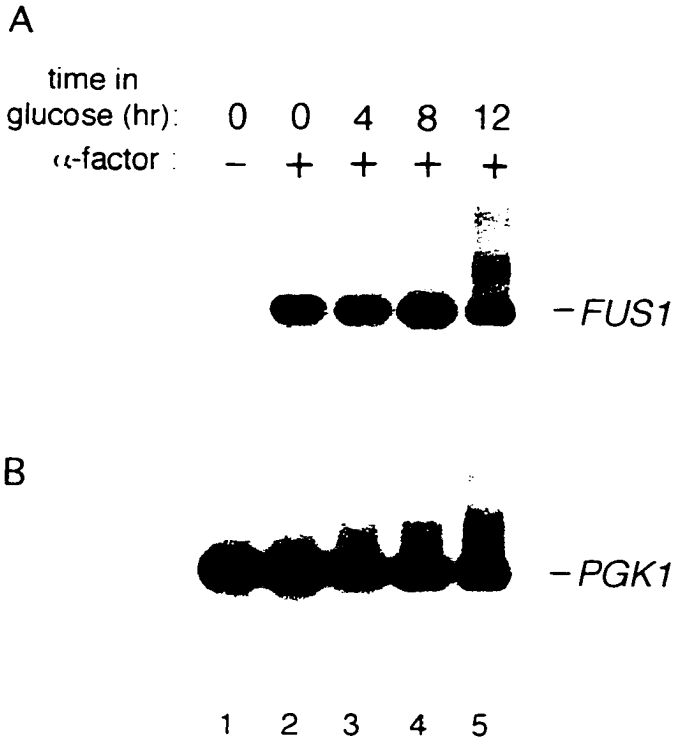

(Figure 3-1, lanes 2-5). The *FUS1* RNA levels did not appear significantly altered after *SSF* depletion in glucose-containing medium for 4, 8, or 12 hrs (Figure 3-1, lanes 3- 5). *FUS1* RNA appeared to be induced to the same extent in cells depleted of *SSF* gene products (Figure 3-1, lanes 3- 5) as in cells containing *SSF* gene products (Figure 3-1, lane 2). There was no significant difference in *FUS1* RNA levels after normalization to the control *PGK1* RNA, as quantified by PhosphorImager analysis. Depletion of *SSF* gene products for 12 hr results in an approximately 10-fold decrease in mating efficiency (157). However, this decrease in mating efficiency does not appear to be the result of the inability of *SSF*-depleted cells to induce pheromone-dependent transcription, as the signaling pathway appears to be intact in these cells. This result indicates that the decrease in mating efficiency seen in cells depleted of *SSF* gene products is probably not the result of disruption of signal transduction leading to transcriptional activation.

2. *SSF* depletion inhibits pheromone-dependent projection formation

Depletion of *SSF* gene products did not appear to disrupt signal transduction, therefore, the effect of *SSF* depletion on pheromone-dependent morphogenesis was observed. Pheromone-induced cellular morphogenesis is required to choose a suitable mating partner, and to facilitate cell and nuclear fusion. To test whether Ssf1p is involved in projection formation, cells were depleted of *SSF* gene products, treated with pheromone, and

Figure 3-2. Morphology of *SSF* and *ssf* cell treated with α-factor.

A Δ*ssf1* Δ*ssf2* strain (H50-16C.Ba) containing a plasmid with the *SSF1* gene under the control of the *GAL* promoter (pGAL-SSF1.14) was grown to log phase in galactose and then switched to glucose (A) or maintained on galactose (B) for 12 hr. The cells were then exposed to 0.1 μM α-factor for 3 hr and photographed using differential interference contrast optics.

A.

B.

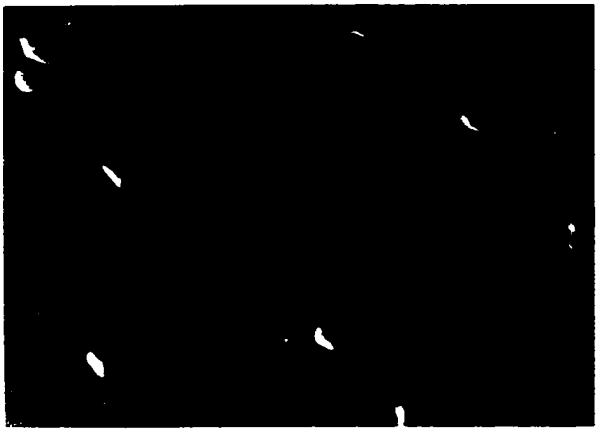

observed microscopically. The *Δssf1 Δssf2* cells containing a copy of *SSF1* under the control of the *GAL1* promoter, were incubated in glucose for 12 hr to deplete the cells of *SSF1* or incubated in galactose to express *SSF1* (control). The cells were then exposed to pheromone for 3 hr and observed microscopically. Control cells expressing *SSF1*, which were grown in galactose, were able to form normal projections (Figure 3-2B). Cells depleted of *SSF1*, by growth in glucose were not able to form projections (Figure 3-2A), however the cells continued to increase in size, which suggests that the cells were still metabolically active. A population of the cells appeared to form pointed tips at two opposing poles of the cell, but no cells formed full-length projections. Therefore, the observation that cells depleted of *SSF* gene products were unable to form projections is consistent with a function of *SSF1* in mating projection formation.

3. Overexpression of *SSF1* does not dramatically increase pheromone-dependent transcriptional activation

The results presented above suggest that depletion of *SSF* gene products did not block signal transduction, as assayed by pheromone-dependent transcriptional activation. However, overexpression of *SSF1* resulted in an increased mating efficiency of a strain containing a defective Gβ subunit (157). Therefore, it was important to determine whether *SSF1* overexpression increased mating efficiency through increasing the

pheromone pathway signaling. A strain containing the *ste4*^{ts} mutation was incubated at either the permissive temperature (30°C) or the non-permissive temperature (37°C) for 2 hr, then either treated with pheromone or left untreated. RNA was isolated from the *ste4*^{ts} cells and *FUS1* levels were measured, as described above. After treatment with pheromone at 30°C, *ste4*^{ts} cells containing a multicopy *SSF1* plasmid displayed a 1.4-fold increase in the levels of *FUS1* RNA, as compared to the same strain containing a control vector (Figure 3-3, lanes 3 and 4). At 37°C *ste4*^{ts} cells containing a multicopy *SSF1* plasmid displayed a 2.4-fold increase in *FUS1* RNA levels over the same strain containing the control vector (Figure 3-3, lanes 7 and 8). The increase in *FUS1* levels conferred by overexpression of *SSF1* in *ste4*^{ts} cells at 37°C is relatively small compared to the 17-fold increase in mating efficiency (Figure 3-5) conferred by overexpression of *SSF1* at the same temperature. These results suggest that signal transduction is not greatly affected by *SSF1* overexpression. In addition, overexpression of *SSF1* did not result in an increase in the basal level of signaling at either 30°C (Figure 3-3, lanes 1 and 2) or 37°C (Figure 3-3, lanes 5 and 6). Overexpression of some components of the signal transduction pathway, such as *STE4*, results in constitutive activation of the pheromone response pathway (151). Therefore, it is improbable that *SSF1* is a component of the signaling pathway, but may act to increase mating efficiency by modulating another response, such as mating projection formation.

Figure 3-3. Pheromone-induced transcription in *ste4*^{ts} cells overexpressing *SSF1*.

A *ste4*^{ts} strain (JH8-3510a) containing either a multicopy *SSF1* plasmid (pSSF1-2; lanes 2, 4, 6, 8) or control vector (YEp351; lanes 1, 3, 5, 7) was incubated at either 30°C (lanes 1-4) or 37°C (lanes 5-8) and either treated with 3 μM α-factor for 30 min (lanes 3, 4, 7, 8) or left untreated (lanes 1, 2, 5, 6). RNA was isolated and a Northern blot was prepared from the RNA was hyrbridized with a *FUS1* probe (A) and then rehybridized with a *TCM1* probe (B) as a loading control.

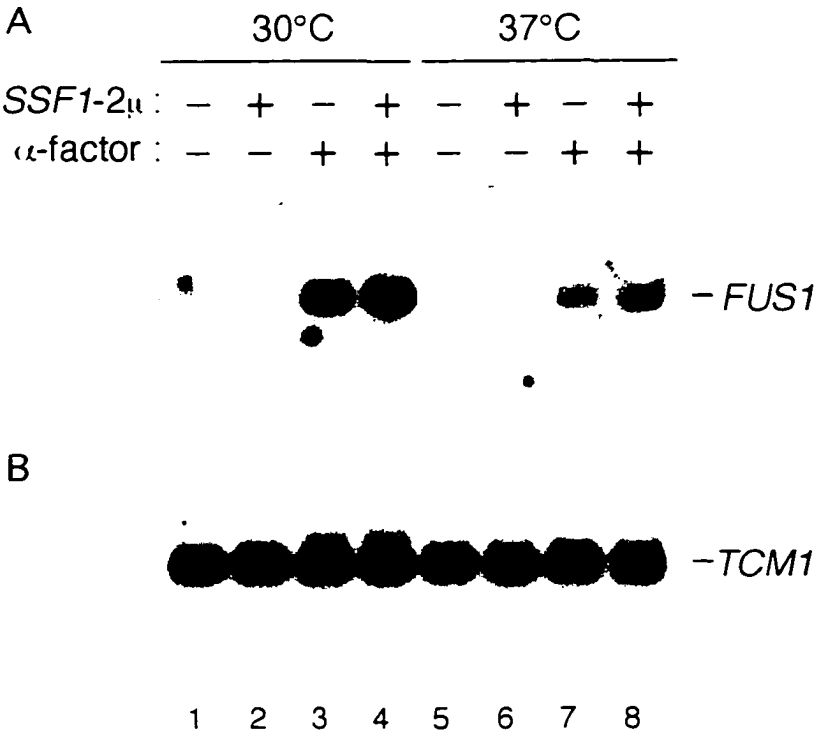

4. *SSF1* overexpression increases projection formation

Cells depleted of *SSF* gene products were incapable of forming normal mating projections and overexpression of *SSF1* did not significantly increase pheromone-induced signaling. Taken together, the results suggest that the mating-specific function of Ssf1p involves mating projection formation. To test the effect of *SSF1* overexpression on projection formation, *ste4*^{ts} cells expressing either a multicopy *SSF1* plasmid or control plasmid, were treated with α-factor and the morphological response was observed microscopically at various temperatures. Although the *ste4*^{ts} strain appeared to mate at relatively high levels at 30°C, *ste4*^{ts} cells containing vector alone were unable to form full-length mating projections after treatment for 3 hr with 3μM α-factor (Figure 3-4). This observation may indicate that this particular *ste4*^{ts} allele used encodes a protein that is at least partially defective in inducing mating projection formation.

ste4^{ts} cells grown at 30°C containing a multicopy *SSF1* plasmid which were treated with 3μM α-factor for 3 hr, displayed an increase in the percentage of cells that appeared to form small mating projections (Figure 3-4, see arrowhead). Additionally, expression of the multicopy *SSF1* plasmid in the *ste4*^{ts} strain resulted in the formation of projections that appeared to be of full-length (Figure 3-4, see arrow). No cells containing the vector alone were observed to form full-length mating projections. The results suggest that the

Figure 3-4. Effect of *SSF1* overexpression on the morphology of *ste4*^{ts} cells treated with α-factor.

A *ste4*^{ts} strain (JH8-3510a) containing either a multicopy *SSF1* plasmid (pSSF1-2; left panel) or control vector (YEp351; right panel) was treated with 3 μM α-factor for 3 hr at 30°C and photographed using differential interference contrast optics. The arrow marks a fully formed projection and the arrowhead marks a partially formed projection (left panel).

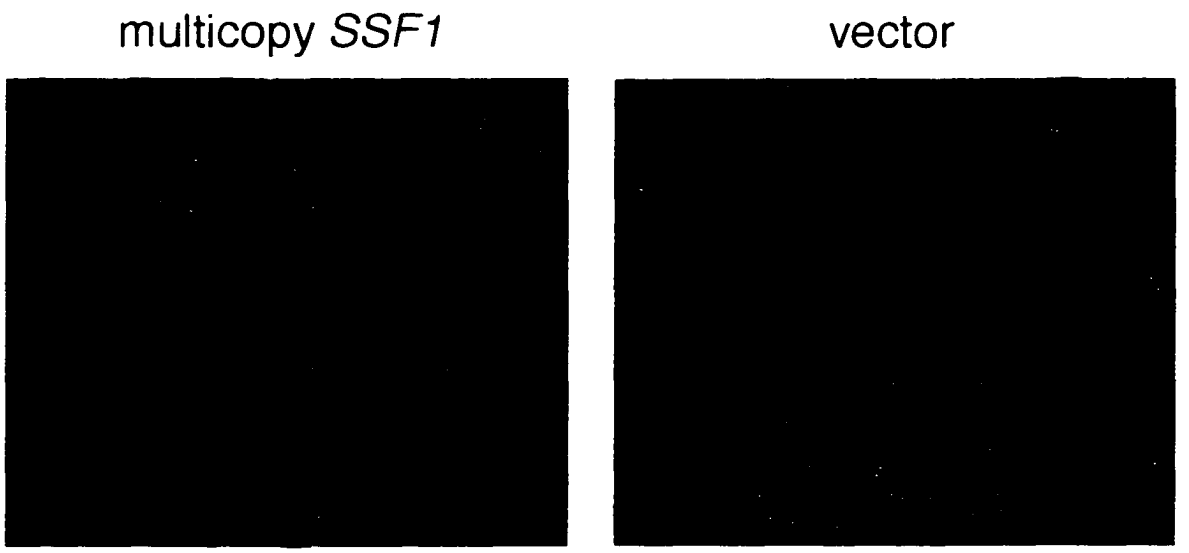

increase in mating efficiency may be the result of a role of Ssf1p in promoting mating projection formation.

5. *SSF1* overexpression preferentially increases mating efficiency in a strain defective in projection formation

The results presented above suggest that the mating function of Ssf1p is related to the morphological response, rather than to signal transduction. To better characterize the role of Ssf1p in projection formation, the effect of *SSF1* overexpression on mating was measured in strains containing defects in mating projection formation. *ste4^{ts}* strains were constructed that contained either Δ*spa2* or *far1*Δc deletion alleles. Mutations in *SPA2* and *FAR1* define two different classes of defects in mating projections. Haploid cells containing a null allele of *SPA2* are defective in projection formation (133). Cells containing a truncated allele of *FAR1* are not defective in mating projection formation, but rather are defective in directing polarity of the mating projection towards the highest concentration of pheromone and instead form the projection at the site at which the incipient bud would have formed (44, 146).

At the non-permissive temperature (37°C), the mating efficiency of the *ste4^{ts}* strain containing a multicopy *SSF1* plasmid was increased 17-fold as compared to the vector alone (Figure 3-5). At 37°C the mating frequency of strains containing the *ste4^{ts}* mutation and either the Δ*spa2* or the *far1*Δc

Figure 3-5. Effect of *SSF1* overexpression on the mating efficiency of strains defective in projection formation.

Quantitative mating assays were performed at 34°C or 37°C on *ste4*^{ts} (JH8-3510a), *ste4*^{ts} Δ*spa2* (JH8-3510a.sp), and *ste4*^{ts} *far1*Δc (JH8-3510a.fc) strains containing either a multicopy *SSF1* plasmid (pSSF1-2) or control vector (YEp351). Similar results were obtained from three independent experiments. A representative experiment is shown.

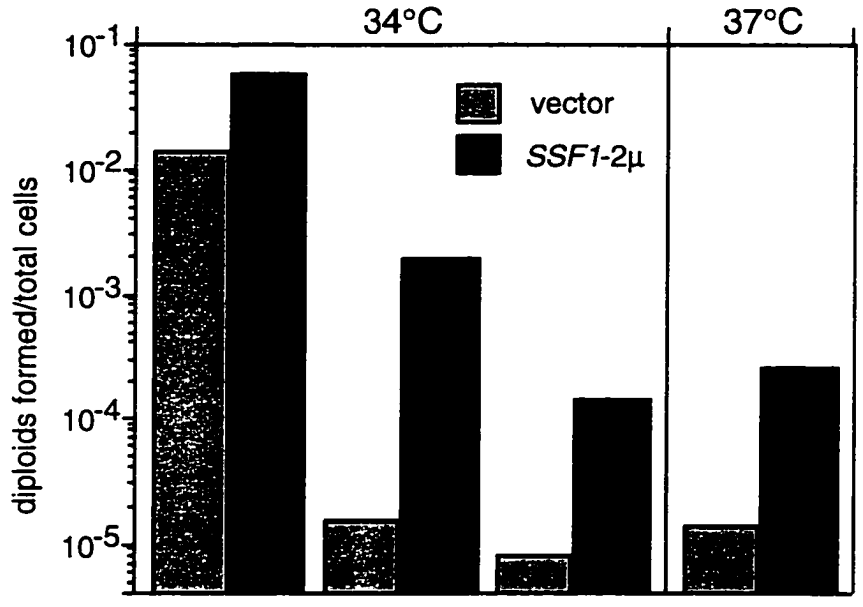

fold increase:	4.2	127	17.3	17.1

were below the level of detection (data not shown). Therefore, a semi-permissive temperature of 34°C was used to assay the mating efficiency of these double mutant strains. Introduction of either the Δ*spa2* or the *far1*Δc mutation into the *ste4*^{ts} strain resulted in a reduction in mating efficiency of approximately 1000-fold as compared to the parent *ste4*^{ts} strain at 34°C (Figure 3-5). At 34°C, the mating efficiency of the parent *ste4*^{ts} strain containing the multicopy *SSF1* plasmid was increased 4-fold as compared to vector alone (Figure 3-5). This quantity is significantly less than that observed at 37°C presumably because the mating efficiency of this strain is much higher at 34°C. The mating efficiency of the *ste4*^{ts} Δ*spa2* strain containing the multicopy *SSF1* plasmid was increased 127-fold as compared to vector alone (Figure 3-5). In contrast, the mating efficiency of the *ste4*^{ts} *far1Δc* strain containing a multicopy *SSF1* plasmid was increased by only 17-fold with respect to the vector alone (Figure 3-5). Therefore, the results indicate that *SSF1* increases mating efficiency of a strain defective in the formation of mating projections (Δ*spa2*), but has less of an effect on cells capable of forming normal projections (*SPA2* and *far1Δc*).

6. Morphology of Δ*spa2 ste4*^{ts} strains overexpressing *SSF1*

Overexpression of *SSF1* increased the mating efficiency of a strain containing a deletion in *SPA2* by approximately 127-fold. Δ*spa2* strains are

Figure 3-6. Effect of *SSF1* overexpression on the morphology of *ste4*^{ts} Δ*spa2* cell treated with α-factor.

A *ste4*^{ts} Δ*spa2* strain (JH8-3510a.sp) containing either multicopy *SSF1* plasmid (pSSF1-2; left panel) or control vector (YEp351; right panel) was treated with 6 μM α-factor for 3 hr at 30°C and photographed using differential interference contrast optics.

multicopy *SSF1*

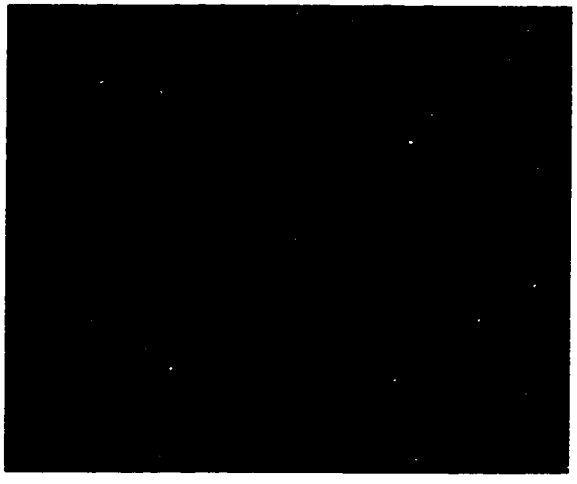

vector

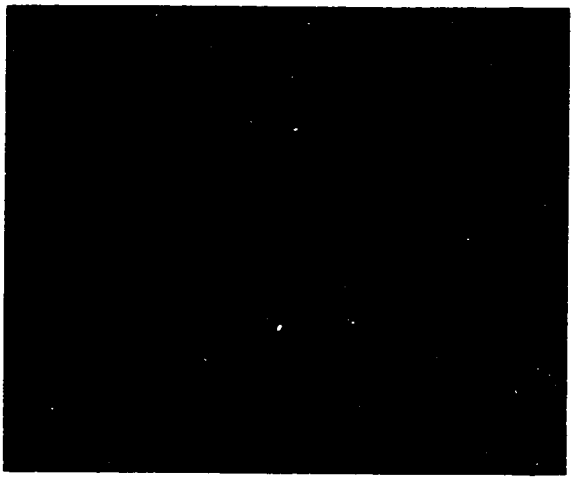

defective in mating projection formation and form peanut-shaped cells only after treatment with high concentrations of pheromone (51, 146). Therefore, it was of interest to determine if *SSF1* overexpression is able to increase projection formation in a strain that is defective in forming mating projections. To test this hypothesis, a *ste4*^{ts} *Δspa2* strain containing either a multicopy *SSF1* plasmid or vector alone was treated with α-factor for 3 hrs and its morphology was observed microscopically. Overexpression of *SSF1* was able to increase pheromone-dependent projection formation, as observed by the larger mating projections formed in cells containing a multicopy *SSF1* plasmid (Figure 3-6) compared to cells containing the vector alone (Figure 3-6). Therefore, overexpression of *SSF1* can increase the mating efficiency of a strain containing a defect in mating projection formation and can also increase the percentage and extent of projection formation in this strain. The results demonstrated that the *SSF1*-mediated increase in mating projection formation is independent of the *SPA2* gene product.

7. Overexpression of *SSF1* does not increase the abundance of Ste4p

The results presented thus far suggest that the specific role of Ssf1p in mating is to promote pheromone-dependent projection formation. However, the mechanism by which Ssf1p promotes projection formation is not known. One explanation for the increase in mating efficiency due to overexpression of *SSF1* in a strain containing a temperature-sensitive Gβ subunit may be that Ssf1p functions to increase the abundance of Ste4p. To

test this hypothesis, the total cellular abundance of Ste4p was measured in *ste4*^{ts} strains containing either the multicopy *SSF1* plasmid or vector alone by immunoblot using a polyclonal anti-Ste4p antibody (67). The *ste4*^{ts} strains were incubated at 37°C, 34°C, or 30°C for 2 hr, and then treated with pheromone. Approximately equal amounts of protein were analyzed by SDS-PAGE. Overexpression of *SSF1* did not appear to increase the abundance of Ste4p^{ts} as compared to expression of the vector alone (Figure 3-7, lanes 1-6). A strain containing a null allele of *STE4* demonstrated the specificity of the antibody (Figure 3-7B, lane 2). Although the Ste4p^{ts} protein appeared to be expressed at lower levels than the wild type Ste4p protein (Figure 3-7B, lane 1), there was no significant increase in Ste4p^{ts} associated with overexpression of *SSF1*. To test whether overexpression of *SSF1* alters the abundance of Ste4p^{ts} in response to pheromone, the *ste4*^{ts} strain containing either a multicopy *SSF1* plasmid or vector alone were incubated for 2 hr at 34°C then exposed to pheromone and assayed for Ste4p^{ts} abundance. The abundance of Ste4p^{ts} in cells overexpressing *SSF1* did not appear to be affected by treatment with pheromone for either 1 hr or 6 hr when compared to cells left untreated (Figure 3-7C, lanes 4-6). In addition, there was no observable difference in the abundance of Ste4p^{ts} in cells containing the multicopy *SSF1* plasmid or vector alone (Figure 3-7C, lanes 1-6). These results indicate that *SSF1* overexpression does not result in an increase in the abundance of Ste4p as a mechanism of promoting projection formation.

Figure 3-7. Effect of *SSF1* overexpression on the abundance of Ste4p in a *ste4^{ts}* strain.

(A) A *ste4^{ts}* strain (JH8-3510a) containing either multicopy *SSF1* plasmid (pSSF1-2; lanes 2, 4, 6) or control vector (YEp351; lanes 1, 3, 5) was incubated at either 37°C (lanes 1, 2), 34°C (lanes 3, 4), or 30°C (lanes 5, 6) for 3 hr. Cell extracts were prepared and a Western blot containing these samples was probed with anti-Ste4p polyclonal antiserum. (B) Cell extracts were prepared from strains containing either wild type *STE4* (H67-9D.Ba; lane 1) or a *ste4::HIS3* allele (AC17-7B; lane 2) and a Western blot containing these samples was probed with anti-Ste4p polyclonal antiserum. (C) A *ste4^{ts}* strain (JH8-3510a) containing either multicopy *SSF1* (pSSF1-2; lanes 4, 5, 6) or control vector (YEp351; lanes 1, 2, 3) was incubated at 34°C for 2.5 hr and then either treated with 3 μM α-factor for 1 hr (lanes 2, 5) for 6 hr (lanes 3, 6) or left untreated (lanes 1, 4). cell extracts were prepared and a Western blot containing these samples was probed with anti-Ste4p polyclonal antiserum.

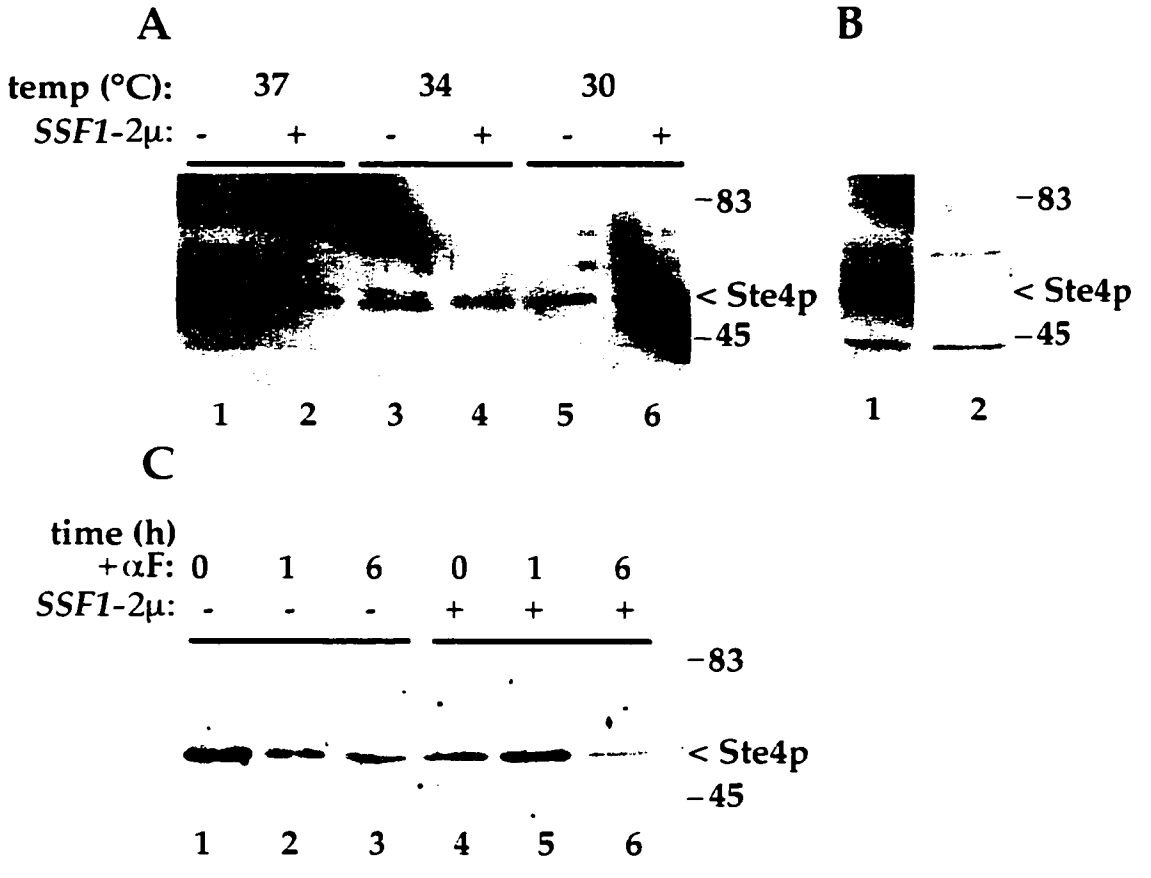

8. Localization of Ssf1p

Many proteins known to be involved in establishing polarity or promoting morphological changes reside at the projection tip of cells exposed to pheromone (reviewed in (86)). Therefore, identification of the subcellular localization of Ssf1p is relevant to determining whether Ssf1p is directly involved in promoting polarity or projection formation. To identify the subcellular localization of Ssf1p, the coding sequence of *SSF1* was fused in frame with the coding sequence of green fluorescent protein (GFP) (15). A *Δssf1 Δssf2* strain containing the plasmid encoding the Ssf1p-GFP fusion was able to complement the viability defect, therefore, the fusion protein retains Ssf1p function (data not shown). The Ssf1p-GFP fusion protein was localized to a subregion of the nucleus, which appeared to correspond to the nucleolus (Figure 3-8A-C). After these cells were treated with pheromone for 3 hr, the localization did not appear to have an altered distribution in the cell (Figure 3-8 D-F). Co-localization of Ssf1p to the nucleolus was accomplished by indirect double immunofluorescence using a monoclonal antibody directed against the yeast nucleolar protein fibrillin (Nop1p) (2) and anti-GFP polyclonal antibody as the primary antibodies. These results confirm that Ssf1p is present in a subregion of the nucleus which corresponds with the nucleolus (Figure 3-9). Proteins that are directly involved in projection

formation are observed at the plasma membrane. Therefore, these results indicate that the role of Ssf1p in projection formation is physically indirect.

Figure 3-8. Localization of Ssf1p-GFP.

An *ssf1::HIS3* (JH111-1C) containing a low copy *SSF1*-GFP plasmid (pSF-GP2) was grown to log phase and either left untreated (A, B, C) or treated with 3 μM α-factor for 3 hr (D, E, F). The cells were then strained with DAPI and viewed by fluorescence microscopy with FITC (A, D) or UV (B, E) filters or with differential interference contrast optics (C, F).

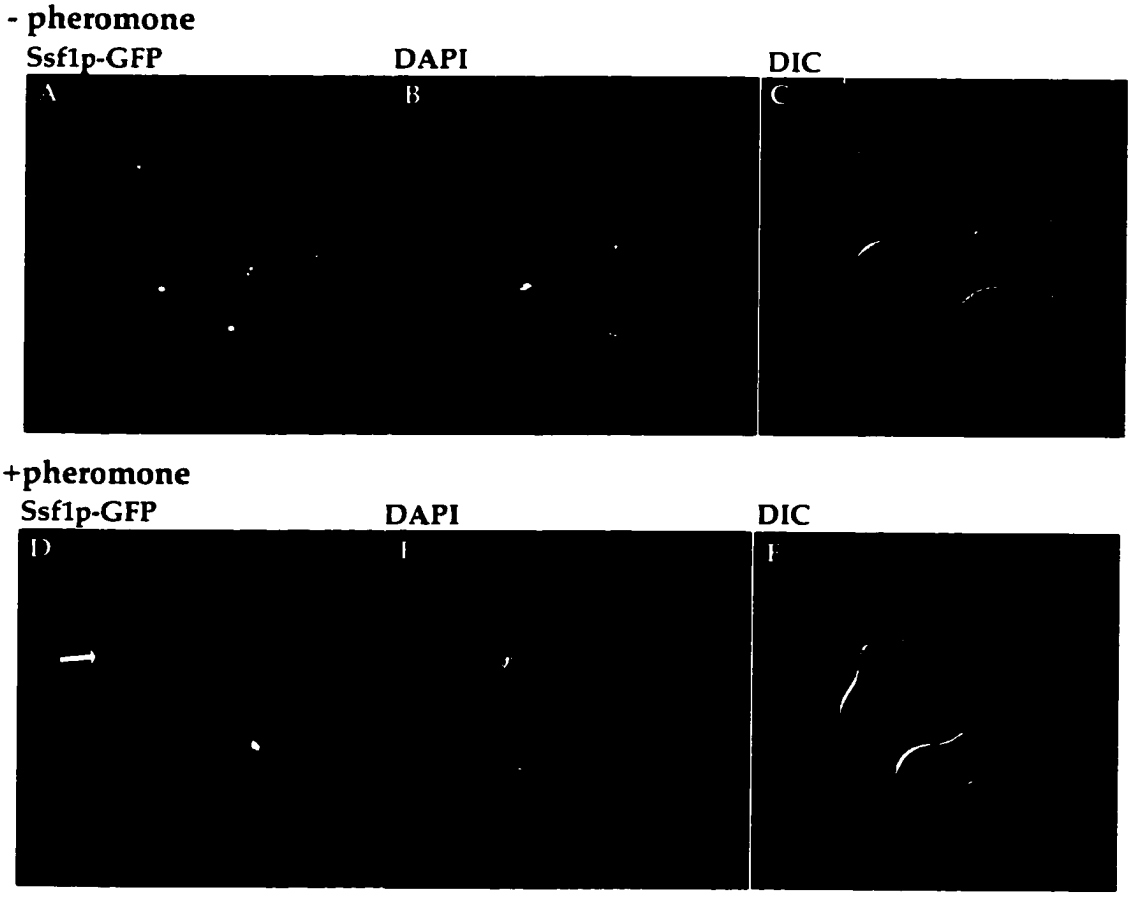

Figure 3-9. Co-localization of Ssf1p-GFP and Nop1p.

An *ssf1::HIS3* strain (JH111-1C) containing a multicopy *SSF1*-GFP plasmid (YEpSFGP) was grown to early log phase and processed for indirect immunofluorescence with anti-GFP (A) and anti-Nop1p (B) antibodies. The cells were also stained with DAPI (C).

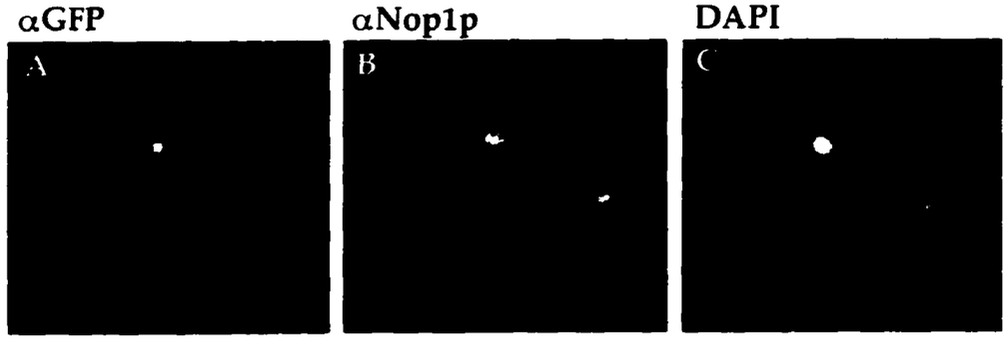

D. Discussion

The following observations suggest that the mating function of *SSF1* is primarily to promote mating projection formation: 1) depletion of Ssf proteins resulted in the inability to form pheromone-dependent projections without altering pheromone-dependent transcriptional activation; 2) overexpression of *SSF1* resulted in a significant increase in projection formation without significantly increasing pheromone pathway signaling, as measured by transcriptional activation; 3) *SSF1* overexpression was shown to greatly increase the mating efficiency of a Δ*spa2* strain, which has a specific defect in projection formation. In addition, *SSF1* overexpression was shown to promote projection formation in the Δ*spa2* cells, which is consistent with a role of *SSF1* in pheromone-dependent morphogenesis. Taken together, these results suggest that the mating function of Ssf proteins involves the morphological response to pheromone and altering the dosage of Ssf proteins has little effect on pheromone pathway signal transduction.

Depletion of Ssf proteins prevents projection formation

Cells depleted of Ssf proteins do not form pheromone-dependent projections. Some of the cells depleted of Ssf proteins, however, are capable of forming pointed tips in response to pheromone. The football-like morphology of these cells may reflect successful completion of initial steps required for polarization. However, Ssfp proteins may be required for the

synthesis, activation, or localization of specific proteins required in later steps in projection formation.

Linking the signal transduction complex to the cytoskeleton

Bem1p is required for polarized morphogenesis during budding and mating projection formation (6, 22). Cells containing null alleles of *BEM1* are unable to form projections and display resistance to pheromone, as assayed by G_1 arrest (92). The signaling complex is thought to activate the morphology complex, which is composed of proteins essential for mediating pheromone-dependent morphological changes. It has been suggested that Bem1p links the signal transduction complex to the morphology complex (92). In addition, the interaction between Ste20p and actin is dependent on Bem1p (88), which suggests that the signaling complex and the actin cytoskeleton are linked through Bem1p.

Overexpression of *BEM1* resulted in a 2.5-fold increase in the level of *FUS1* expression (92). *SSF1* overexpression results in a similar level of *FUS1* induction. Proteins involved in regulating morphological changes may increase mating efficiency by promoting projection formation. Bem1p, along with other proteins involved in controlling cellular morphology, are targeted to the projection tip in cells exposed to pheromone. The slight increase in the level of transcriptional induction may represent the level of transcriptional activation observed by overexpression of a morphology gene.

Ssf1p is a nucleolar protein

Proteins required for projection formation such as Spa2p, Cdc42p, and Bem1p are localized to the tips of mating projections (22, 133, 159). However, inconsistent with a direct role of Ssf1p in mating projection formation, Ssf1p-GFP was shown to co-localize with a nucleolar protein Nop1p. In fact, the protein sequence of Ssf1p contains many basic stretches, which may act as potential nuclear localization signals, for example at amino acids 399 to 404 (KKQRKL). In addition, the amino-terminus of Ssf1p contains a potential nucleolar localization signal (KRRQKKR) at amino acids 3 to 9, which is similar to the amino-terminal nucleolar localization signal of the $p27^{x\text{-}III}$ protein, encoded by the *pX* region of the human T cell leukemia virus type I (HTLV-I) (53, 78, 128). The nucleolar localization of Ssf1p suggests that its mating function is indirect since localization of many components that promote morphological changes are localized to the projection tips. Our immunofluorescence results can not rule out the possibility that Ssf1p, in an amount below the level of detection, may shuttle in and out of the nucleus. In this case, a fraction of Ssf1p may be localized in the cytoplasm or plasma membrane for its mating function. Proteins that shuttle into and out of the nucleus have been described previously (108, 120).

The nucleolus is the site of transcription of rDNA and processing of the rDNA transcripts, production of pre-ribosomal components, and biogenesis of ribosomal subunits (reviewed in (129)). This work demonstrated that the abundance of $Ste4p^{ts}$ did not appear to be greatly altered by overexpression of

SSF1. Therefore, it is unlikely that the mating function of Ssf1p is to increase the production of ribosomal subunits, resulting in an increase the relative abundance of proteins required for mating.

Pheromone pathway activation results in transcriptional activation and repression of many genes which requires significant reorganization of the chromatin structure. Silent information regulators (Sir2p, Sir3p, and Sir4p) and histones H3 and H4 promote silencing at telomeres and at the silent mating-type loci (*HM*), which entails stable repression of *MAT*α information at the *HML* locus and repression of *MAT***a** information at the *HMR* (reviewed in (64). Haploid strains containing null alleles of *SIR3* are defective in mating due to the simultaneous expression of genes at the *MAT* locus and the normally repressed *HM* loci (122). In addition, a member of the silencing complex, Sir2p has been demonstrated to be localized within two nuclear domains: 1) at subtelomeric sites and 2) within a subdomain of the nucleolus in yeast (75). Sir3p is also targeted to the nucleolus in a Sir2-dependent manner in strains that lack Sir4p (54). Therefore, a plausible mechanism of the role of Ssf1p in the nucleolus is to regulate the activity of the silencing complex which modulates chromatin structure resulting in transcriptional silencing.

Pheromone response pathway signal transduction promotes Sir3p hyperphosphorylation which results in increased silencing of *HM* loci (140). Ssf1p may regulate silencing through post-translational modification or redistribution of the Sir protein complex between nucleolar and genomic sites

to regulate silencing. Defects in silencing of mating-type loci have been demonstrated to result in mating defects (149). It is plausible that overexpression of *SSF1* may promote alterations of chromatin structure by interacting with components of the silencing complex which results in an increase in mating efficiency by increased silencing of the *HM* loci or by promoting transcription of genes required for projection formation.

E. Future studies

Overexpression of *SSF1* has been demonstrated in this work to promote projection formation. However, Ssf1p has also been demonstrated to reside within a subregion of the nucleus that corresponds to the nucleolus, which suggests an indirect mechanism of promoting cellular morphogenesis. To account for the ability of Ssf1p to promote projection formation from this site, it was hypothesized that Ssf1p may interact with silencing components, which control chromatin structure and regulates the accessibility of general and specific transcription factors to genomic sites. It would be of interest to determine whether any of the components of the silencing complex directly interact with Ssf1p. In addition, it would be interesting to test whether other pheromone-inducible genes, especially genes which encode proteins involved in controlling morphology, are regulated by Ssf1p overexpression.

IV. Conclusions

The focus of this work was to better understand in molecular terms the regulation of the Ste4p G-protein β subunit activity. This work demonstrated that the Ste4p Gβ subunit mediates receptor inhibition most likely through altering its localization in *MAT***a** $STE3^{DAF}$ cells. However it is unclear whether the Ste4p is associated with an internal membrane or a large protein complex during receptor inhibition. Secondly, the mating function of *SSF1*, a gene, which when overexpressed suppresses the mating defect in a strain containing a temperature sensitive Gβ subunit, was shown to promote projection formation. However, since Ssf1p did not appear to reside at the projection tip, this effect was most likely indirect.

This work utilized the pheromone response pathway of *Saccharomyces cerevisiae* as a model system to understand regulatory mechanisms of G protein signaling. The RGS family of regulators of Gα signaling has already been demonstrated to have similar activity in both *S. cerevisiae* and mammalian cells. Therefore, the identification of regulators of $G_{\beta\gamma}$ signaling, which may be conserved in mammalian systems, will be useful in understanding G protein signaling.

V. References

1. Adams, A. E. M., D. I. Johnson, R. M. Longnecker, B. F. Sloat, and J. R. Pringle. 1990. *CDC42* and *CDC43*, two additional genes involved in budding and the establishment of cell polarity in the yeast *Saccharomyces cerevisiae*. J. Cell Biol. **111**:131-142.

2. Aris, J. P., and G. Blobel. 1988. Identification and Characterization of a Yeast Nucleolar Protein That Is Similar to a Rat Liver Nucleolar Protein. Journal of Cell Biology **107**:17-31.

3. Ayscough, K. R., J. Stryker, N. Pokala, M. Sanders, P. Crews, and D. G. Drubin. 1997. High rates of actin turnover in budding yeast and roles for actin in establishment and maintenance of cell polarity revealed using the actin inhibitor Latruculin-A. Journal of Cell Biology **137**:399-416.

4. Bauer, P. H., K. Bluml, S. Schroder, J. Hegler, C. Dees, and M. J. Lohse. 1998. Interactions of Phosducin with the Subunits of G-proteins. Binding to the α as well as the $\beta\gamma$ subunits. Journal of Biological Chemistry **273**:9465-9471.

5. Bauer, P. H., S. Muller, M. Puzicha, S. Pippig, B. Obermaier, M. E.J.M., and M. J. Lohse. 1992. Phosducin is a protein-kinase A-regulated G-protien regulator. Nature **358**:73-76.

6. Bender, A., and J. R. Pringle. 1991. Use of a screen for synthetic lethal and multicopy suppressee mutants to identify two new genes involved in morphogenesis in *Saccharomyces cerevisiae*. Mol. Cell. Biol. **11**:1295-1305.

7. Bender, A., and G. F. Sprague, Jr. 1989. Pheromones and pheromone receptors are the primary determinants of mating specificity in the yeast *Saccharomyces cerevisiae*. Genetics **121**:463-476.

8. Berman, D. M., and A. G. Gilman. 1998. Mammalian RGS Proteins: Barbarians at the Gate. J. Biol. Chem. **273**:1269-1272.

9. Bluml, K., W. Schnepp, S. Schroder, M. Beyermann, M. Macias, H. Oschkinat, and M. J. Lohse. 1997. A small region in phosducin inhibitis G-protein $\beta\gamma$-subunit function. EMBO J. **16**:4908-4915.

10. Boone, C., N. G. Davis, and G. F. Sprague, Jr. 1993. Mutations that alter the third cytoplasmic loop of the a-factor receptor lead to a constitutive and hypersensitive phenotype. Proc. Natl. Acad. Sci. USA **90**:9921-9925.

11. Brown, D. A., and E. London. 1997. Structure of Detergent-Resistant Membrane Domains: Does Phase Separation Occur in Biological Membranes? Biochem. Biophys. Res. Comm. **240**:1-7.

12. Burkholder, A. C., and L. H. Hartwell. 1985. The yeast α-factor receptor: structural properties deduced from the sequence of the *STE2* gene. Nucl. Acids Res. **13**:8463-8475.

13. Casey, P. J. 1994. Lipid modifications of G proteins. Curr. Opin. Cell Biol. **6**:219-225.

14. Chaleff, D. T., and K. Tatchell. 1985. Molecular cloning and characterization of the *STE7* and *STE11* genes of *Saccharomyces cerevisiae*. Mol. Cell. Biol. **5**:1878-1886.

15. Chalfie, M., Y. Tu, G. Euskirchen, W. Ward, and D. C. Prascher. 1994. Green fluorescent protein as a marker for gene expression. Science **263**:802-805.

16. Chan, R. K., and C. A. Otte. 1982. Isolation and genetic analysis of *Saccharomyces cerevisiae* mutants supersensitive to G1 arrest by **a** factor and α factor pheromones. Mol. Cell. Biol. **2**:11-20.

17. Chan, R. K., and C. A. Otte. 1982. Physiological characterization of *Saccharomyces cerevisiae* mutants supersensitive to G1 arrest by **a** factor and α factor pheromones. Mol. Cell. Biol. **2**:21-29.

18. Chang, F., and I. Herskowitz. 1990. Identification of a gene necessary for cell cycle arrest by a negative growth factor of yeast: FAR1 is an inhibitor of a G1 cyclin, CLN2. Cell **63**:999-1011.

19. Chant, J., and I. Herskowitz. 1991. Genetic control of bud site selection in yeast by a set of gene products that comprise a morphogenetic pathway. Cell **65**:1203-1212.

20. Chen, J., M. DeVivo, J. Dingus, A. Harry, J. Li, J. Sui, D. Carty, J. Blank, J. Exton, R. Stoffel, J. Inglese, R. Lefkowitz, D. Logothetis, J. Hildebrandt, and R. Iyengar. 1995. Science **268**:1166-1169.

21. Chen, Q., and J. B. Konopka. 1996. Regulation of the G-Protein-Coupled α-Factor Pheromone Receptor by Phosphorylation. Mol. Cell. Biol. **16**:247-257.

22. Chenevert, K. Corrado, A. Bender, J. Pringle, and I. Herskowitz. 1992. A yeast gene (*BEM1*) necessary for cell polarization whose product contains two SH3 domains. Nature **356**:77-79.

23. Chenevert, J. 1994. Cell polarization directed by extracellular cues in yeast. Mol. Biol. Cell **5**:1169-1175.

24. Chenevert, J., N. Valtz, and I. Herskowitz. 1994. Identification of genes required for normal pheromone-induced cell polarization in *Saccharomyces cerevisiae*. Genetics **136**:1287-1297.

25. Choi, K. Y., B. Satterberg, D. M. Lyons, and E. A. Elion. 1994. Ste5 tethers multiple protein kinases in the MAP kinase cascade required for mating in S. cerevisiae. Cell **78**:499-512.

26. Clapham, D. E., and E. J. Neer. 1997. G protein βγ subunits. Annual Review of Pharmalogical Toxicology **37**:167-203.

27. Clark, K. L., D. Dignard, D. Y. Thomas, and M. Whiteway. 1993. Interactions among the subunits of the G protein involved in *Saccharomyces cerevisiae* mating. Mol. Cell. Biol. **13**:1-8.

28. Cole, G. M., and S. I. Reed. 1991. Pheromone-induced phosphorylation of a G protein β subunit in *S. cerevisiae* is associated with an adaptive response to mating pheromone. Cell **64**:703-716.

29. Cole, G. M., D. E. Stone, and S. I. Reed. 1990. Stoichiometry of G protein subunits affects the *Saccharomyces cerevisiae* mating pheromone signal transduction pathway. Mol. Cell. Biol. **10**:510-517.

30. Couve, A., *Receptor-mediated down regulation of the Mating Signaling Cascade in Saccharomyces cerevisiae*, in *Department of Cell Biology and Anatomy*1997, The City University of New York: New York.

31. Couve, A., and J. P. Hirsch. Unpublished data.

32. Couve, A., and J. P. Hirsch. 1996. Loss of Sustained Fus3p Kinase Activity and the G1 Arrest Response in Cells Expressing an Inappropriate Pheromone Receptor. Mol. Cell. Biol. **16**:4478-4485.

33. Cross, F. R. 1990. The *DAF2-2* mutation, a dominant inhibitor of the *STE4* step in the α-factor signalling pathway of *Saccharomyces cerevisiae MAT***a** cells. Genetics **126**:301-308.

34. Cross, F. R. 1997. 'Marker Swap' Plasmids: Convenient Tools for Budding Yeast Molecular Genetics. Yeast **13**:647-653.

35. Cross, F. R., and A. H. Tinkelenberg. 1991. A potential positive feedback loop controlling *CLN1* and *CLN2* gene expression at the start of the yeast cell cycle. Cell **65**:875-883.

36. Daugherty, B. L., J. A. DeMartin, M. F. Law, D. W. Kawka, and M. G. E. Singer II. 1991. Polymerase chain reaction facilitates the cloning, CDR-grafting, and rapid expression of a murine monoclonal antibody directed against the CD18 component of leukocyte integrins. Nucl. Acids Res. **19**:2471-2476.

37. Davis, N. G., J. L. Horecka, and G. F. Sprague. 1993. *Cis-* and *Trans-*acting functions required for endocytosis of the yeast pheromone receptors. J. Cell Biol. **122**:53-65.

38. Dharmawardhane, S., A. B. Cubitt, A. M. Clark, and R. A. Firtel. 1994. Regulatory role of the Gα1 subunit in controlling cellular morphogenesis in *Dictyostelium*. Development **120**:3549-3561.

39. Dietzel, C., and J. Kurjan. 1987. Pheromonal regulation and sequence of the *Saccharomyces cerevisiae SST2* gene: a model for desensitization to pheromone. Mol. Cell. Biol. **7**:4169-4177.

40. Dietzel, C., and J. Kurjan. 1987. The yeast *SCG1* gene: a Gα-like protein implicated in the **a**- and α-factor response pathway. Cell **50**:1001-1010.

41. Dohlman, H. G., J. Thorner, M. G. Caron, and R. J. Lefkowitz. 1991. Model systems for the study of seven-transmembrane-segment receptors. Ann. Rev. Biochem. **60**:653-688.

42. Doi, K., A. Gartner, G. Ammerer, B. Errede, H. Shinkawa, K. Sugimoto, and K. Matsumoto. 1994. MSG5, a novel protein phosphatase promotes adaptation to pheromone response in *S. cerevisiae*. EMBO J. **13**:61-70.

43. Dolan, J. W., C. Kirkman, and S. Fields. 1989. The yeast STE12 protein binds to the DNA sequence mediating pheromone induction. Proc. Natl. Acad. Sci. **86**:5703-5707.

44. Dorer, R., P. M. Pryciak, and L. H. Hartwell. 1995. *Saccharomyces cerevisiae* cells execute a default pathway to select a mate in the absence of pheromone gradients. J. Cell Biol. **131**:845-861.

45. Elion, E. A., P. L. Grisafi, and G. R. Fink. 1990. *FUS3* encodes a cdc2+/CDC28-related kinase required for the transition from mitosis into conjugation. Cell **60**:649-664.

46. Elion, E. A., B. Satterberg, and J. E. Kranz. 1993. FUS3 phosphorylates multiple components of the mating signal transduction cascade: Evidence for STE12 and FAR1. Mol. Biol. Cell **4**:495-510.

47. Errede, B., and G. Ammerer. 1989. STE12, a protein involved in cell-type-specific transcription and signal transduction in yeast, is part of protein-DNA complexes. Genes Dev. **3**:1349-1361.

48. Errede, B., A. Gartner, Z. Zhou, K. Nasmyth, and G. Ammerer. 1993. MAP kinase-related FUS3 from *S. cerevisiae* is activated by STE7 *in vitro*. Nature **362**:261-264.

49. Errede, B., and D. E. Levin. 1993. A conserved kinase cascade for MAP kinase activation in yeast. Curr. Opin. Cell Biol. **5**:254-260.

50. Freedman, N. J., and R. J. Lefkowitz. 1996. Desensitization of G protein-coupled receptors. Recent Progress in Hormone Research **51**:319-353.

51. Gehrung, S., and M. Snyder. 1990. The *SPA2* gene of *Saccharomyces cerevisiae* is important for pheromone-induced morphogenesis and efficient mating. J. Cell Biol. **111**:1451-1464.

52. Gietz, R. D., and A. Sugino. 1988. New yeast-*Escherichia coli* shuttle vectors constructed with *in vitro* mutagenized yeast genes lacking six-base pair restriction sites. Gene **74**:527-534.

53. Goh, W. C., J. Sodroski, C. Rosen, M. Essex, and W. A. Haseltine. 1985. Subcellular localization of the product of the long open reading frame of human T-cell leukemia virus type I. Science **227**:1227-1228.

54. Gotta, M., S.-B. S., H. Renauld, T. Laroche, B. K. Kennedy, M. Grunstein, and S. M. Gasser. 1997. Localization of Sir2p: the nucleolus as a compartment for silent information regulators. EMBO J. **16**:3243-3255.

55. Graeser, D., and R. R. Neubig. 1993. Compartmentation of receptors and G proteins in NG108-15 cells: lack of cross-talk in agoinst binding among the alpha2 adrenergic, muscarinic and opiate receptors. Mol. Pharm. **43**:434-443.

56. Grishin, A. V., J. L. Weiner, and K. J. Blumer. 1994. Biochemical and Genetic Analysis of Dominant-Negative Mutations Affecting a Yeast G-Protein γ Subunit. Mol. Cell. Biol. **14**:4571-4578.

57. Guthrie, C., and G. Fink. 1991. *Guide to Yeast Genetics and Molecular Biology*, in *Methods in Enzymology*. Academic Press, Inc., San Diego, CA. p. 77-93.

58. Hagen, D. C., G. McCaffrey, and G. F. Sprague, Jr. 1986. Evidence the *STE3* gene encodes a receptor for the peptide pheromone a factor: gene sequence and implications for the structure of the presumed receptor. Proc. Natl. Acad. Sci. USA **83**:1418-1422.

59. Hamm, H. E. 1998. The Many Faces of G Protein Signaling. J. Biol. Chem. **273**:669-672.

60. Hartwell, L. H. 1980. Mutants of *Saccharomyces cerevisiae* unresponsive to cell division control by polypeptide mating hormone. J. Cell Biol. **85**:811-822.

61. Hasson, M. S., D. Blinder, J. Thorner, and D. D. Jenness. 1994. Mutational activation of the *STE5* gene product bypasses the requirement for G protein β and γ subunits in the yeast pheromone response pathway. Mol. Cell. Biol. **14**:1054-1065.

62. Heasley, L. E., J. Zamarripa, B. Storey, B. Helfrich, M. F.M., B. P. A. Jr, and G. L. Johnson. 1996. Discordant signal transduction and growth inhibition of small cell lung carcinomas induced by expression of GTPase-deficient Gα16. J. Biol. Chem. **271**:349-354.

63. Heim, R., A. B. Cubitt, and R. Y. Tsien. 1995. Improved green fluorescence. Nature **373**:663-664.

64. Herskowitz, I., J. Rine, and J. Strathern. 1992. *Mating-type Determination and Mating-type Interconversion in Saccharomyces cerevisiae,* in *The Molecular and Cellular Biology of the Yeast Saccharomyces cerevisiae.* Cold Spring Harbor Laboratory Press, Cold Spring Harbor. p. 583-655.

65. Hicke, L., and H. Riezman. 1996. Ubiquitination of a yeast plama membrane receptor signals its ligand-stimulated endocytosis. Cell **84**:277-287.

66. Hirsch, J. P., and F. R. Cross. 1993. The pheromone receptors inhibit the pheromone response pathway in *Saccharomyces cerevisiae* by a process that is independent of their associated Gα protein. Genetics **135**:943-953.

67. Hirschman, J. E., G. S. De Zutter, W. F. Simonds, and D. D. Jenness. 1997. The Gβγ complex of the yeast pheromone response pathway. J. Biol. Chem. **272**:240-248.

68. Holtzman, D. A., S. Yang, and D. G. Drubin. 1993. Synthetic-lethal interactions identify two novel genes, *SLA1* and *SLA2*, that control membrane cytoskeleton assembly in *Saccharomyces cerevisiae*. J. Cell Biol. **122**:635-644.

69. Inouye, C., N. Dhillon, T. Durfee, P. C. Zambryski, and J. Thorner. 1997. Mutational Analysis of *STE5* in the Yeast *Saccharomyces cerevisiae*:

Application of a Differential Interaction Trap Assay for Examining Protein-Protein Interactions. Genetics **147**:479-492.

70. Inouye, C., N. Dhillon, and J. Thorner. 1997. Ste5 RING-H2 Domain: Role in Ste4-Promoted Oligomerization for Yeast Pheromone Signaling. Science **278**:103-106.

71. Ito, H., Y. Fukuda, K. Murata, and A. Kimura. 1983. Transformation of intact yeast cells with alkali cations. J. Bact. **153**:163-168.

72. Jackson, C. L., J. B. Konopka, and L. H. Hartwell. 1991. S. cerevisiae α pheromone receptors activate a novel signal transduction pathway for mating partner discrimination. Cell **67**:389-402.

73. Jenness, D. D., and P. Spatrick. 1986. Down regulation of the α-factor pheromone receptor in *S. cerevisiae*. Cell **46**:345-353.

74. Kao, L., J. Peterson, R. Ji, L. Bender, and A. Bender. 1996. Interactions between the ankyrin repeat-containing protein Akr1p and the pheromone response pathway in *Saccharomyces cerevisiae*. Mol. Cell. Biol. **16**:168-178.

75. Kennedy, B. K., M. Gotta, D. A. Sinclair, K. Mills, D. S. McNabb, M. Murthy, S. M. Pak, T. Laroche, S. M. Gasser, and L. Guarente. 1997. Redistribution of Silencing Proteins from Telomeres to the Nucleolus Is Associated with Extension of Life Span in *S. cerevisiae*. Cell **89**:381-391.

76. Kim, J., and J. P. Hirsch. Unpublished data.

77. Kim, J., and J. P. Hirsch. 1998. A Nucleolar Protein That Affects Mating Efficiency in *Saccharomyces cerevisiae* by Altering the Morphological Response to Pheromone. Genetics **149**:795-805.

78. Kiyokawa, T., M. Seiki, S. Iwashita, K. Imagawa, F. Shimizu, and M. Yoshida. 1985. $p27^{x\text{-}III}$ and $p21^{x\text{-}III}$, proteins encoded by the *pX* sequence of human T-cell leukemia virus type I. Proceedings of the National Academy of Science **82**:8359-8363.

79. Kleuss, C., H. Scherubl, J. Hescheler, G. Schultz, and B. Wittig. 1992. Different β-subunits determine G-protein interactions wih transmembrane receptors. Nature **358**:424-426.

80. Kleuss, C., H. Scherubl, J. Hescheler, G. Schultz, and B. Wittig. 1993. Selectivity in Signal Transduction determined by gamma subunits of heterotrimeric G proteins. Science **259**:832-834.

81. Konopka, J. B., D. D. Jenness, and L. H. Hartwell. 1988. The C-terminus of the *S. cerevisiae* α-pheromone receptor mediates an adaptive response to pheromone. Cell **54**:609-620.

82. Kubler, E., H. G. Dohlman, and M. P. Lisanti. 1996. Identification of Triton X-100 Insoluble Membrane Domains in the Yeast *Saccharomyces cerevisiae*. J. Biol. Chem. **271**:32975-32980.

83. Kurjan, J. 1992. Pheromone response in yeast. Annu. Rev. Biochem. **61**:1097-1129.

84. Lambright, D. G., J. Sondek, A. Bohm, N. P. Skiba, H. E. Hamm, and P. B. Sigler. 1996. The 2.0A crystal structure of a heterotrimeric G protein. Nature **379**:311-319.

85. Leberer, E., D. Dignard, D. Harcus, D. Y. Thomas, and M. Whiteway. 1992. The protein kinase homologue Ste20p is required to link the yeast pheromone response G-protein βγ subunits to downstream signalling components. EMBO J. **11**:4815-4824.

86. Leberer, E., D. Y. Thomas, and M. Whiteway. 1997. Pheromone signaling and polarized Morphogenesis in yeast. Curr. Opin. Gen. Dev. **7**:59-66.

87. Lee, R. H., T. D. Ting, B. S. Lieberman, D. E. Tobias, R. N. Lolley, and Y.-K. Ho. 1992. Regulation of retinal cGMP cascade by phosducin in bovine rod photoreceptor cells. Interaction of phosducin and transducin. J. Biol. Chem. **267**:25104-25112.

88. Leeuw, T., A. Fourest-Lieuvin, C. Wu, J. Chenevert, K. Clark, M. Whiteway, D. Y. Thomas, and E. Leberer. 1995. Pheromone response in yeast: Association of Bem1p with proteins of the MAP kinase cascade and actin. Science **270**:1210-1213.

89. Leeuw, T., C. Wu, J. D. Schrag, M. Whiteway, D. Y. Thomas, and E. Leberer. 1998. Interaction of a G-protein β-subunit with a conserved sequence in Ste20/PAK family of protein kinases. Nature **391**:191-198.

90. Lehrach, H., D. Diamond, J. M. Wozney, and H. Boedtker. 1977. RNA molecular weight determinations by gel electrophoresis under denaturing conditions, a critical reexamination. Biochem. **16**:4743-4751.

91. Li, E., E. Meldrum, H. F. Stratton, and D. E. Ston. 1998. Substitutions in the pheromone-responsive Gβ protein of *Saccharomyces cerevisiae* confer a defect in recovery from pheromone treatment. Genetics **148**:947-961.

92. Lyons, D. M., S. K. Mahanty, K. Choi, M. Manandhar, and E. A. Elion. 1996. The SH3-Domain Protein Bem1 Coordinates Mitogen-Activated Protein Kinase Cascade Activation with Cell Cycle Control. Mol. Cell. Biol. **16**:4095-4106.

93. MacKay, V. L., S. K. Welch, M. Y. Insley, T. R. Manney, J. Holly, G. C. Saari, and M. L. Parker. 1988. The *Saccharomyces cerevisiae BAR1* gene encodes an exported protein with homology to pepsin. Proc. Natl. Acad. Sci. **85**:55-59.

94. Manser, E., T. Leung, H. Salihuddin, Z. Zhao, and L. Lim. 1994. A brain serine/threonine protein kinase activated by Cdc42 and Rac1. Nature **367**:40-46.

95. Marcus, S., B. Polverino, M. Barr, and M. Wigler. 1994. Complexes between STE5 and components of the pheromone-responsive mitogen-activated protein kinase module. Proc. Natl. Acad. Sci. **91**:7762-7766.

96. Marcus, S., C.-B. Xue, F. Naider, and J. M. Becker. 1991. Degradation of **a**-factor by a *Saccharomyces cerevisiae* α-mating-type-specific endopeptidase: evidence for a role in recovery of cells from G1 arrest. Mol. Cell. Biol. **11**:1030-1039.

97. McCaffrey, G., F. J. Clay, K. Kelsay, and G. F. Sprague, Jr. 1987. Identification and regulation of a gene required for cell fusion during mating of the yeast *Saccharomyces cerevisiae*. Mol. Cell. Biol. **7**:2680-2690.

98. McKinney, J. D., and F. R. Cross. 1995. *FAR1* and the G_1 phase specificity of cell cycle arrest by mating factor in *Saccharomyces cerevisiae*. Mol. Cell. Biol. **15**:2509-2516.

99. Miyajima, I., M. Nakafuku, N. Nakayama, C. Brenner, A. Miyajima, K. Kaibuchi, K. I. Arai, Y. Kaziro, and K. Matsumoto. 1987. *GPA1*, a haploid-specific essential gene, encodes a yeast homolog of mammalian G protein which may be involved in mating factor signal transduction. Cell **50**:1011-1019.

100. Nakayama, N., A. Miyajima, and K. Arai. 1985. Nucleotide sequences of *STE2* and *STE3*, cell type-specific sterile genes from *Saccharomyces cerevisiae*. EMBO J. **4**:2643-2648.

101. Neiman, A. M., and I. Herskowitz. 1994. Reconstitution of a yeast protein kinase cascade *in vitro*: activation of the yeast MEK homologue STE7 by STE11. Proc. Natl. Acad. Sci. **91**:3398-3402.

102. Nobes, C. D., and A. Hall. 1995. Rho, rac, and Cdc42 GTPases regulate the assembly of multimolecular focal complexes associated with actin stress fibers, lamellipodia, and filopodia. Cell **81**:53-62.

103. Nomoto, S., N. Nakayama, K. Arai, and K. Matsumoto. 1990. Regulation of the yeast pheromone response pathway by G protein subunits. EMBO J. **9**:691-696.

104. Parma, J., L. Duprez, J. Van Sande, P. Cochaux, C. Gervy, J. Mokel, J. Dumont, and G. Vassart. 1993. Somatic Mutations in the Thyrotropin Receptor Gene Cause Hyperfunctioning Thyroid Adenomas. Nature **365**:649-651.

105. Peter, M., A. Gartner, J. Horecka, G. Ammerer, and I. Herskowitz. 1993. FAR1 links the signal transduction pathway to the cell cycle machinery in yeast. Cell **73**:747-760.

106. Peter, M., and I. Herskowitz. 1994. Direct inhibition of the yeast cyclin-dependent kinase Cdc28-Cln by Far1. Science **265**:1228-1231.

107. Phillips, W. J., and R. A. Cerione. 1992. Rhodopsin/Transducin Interactions I. Characterization of the binding of the Transducin-βγ subunit complex to Rhodopsin using fluorescence spectroscopy. J. Biol. Chem.

108. Pinol-Roma, S., and G. Dreyfuss. 1992. Shuttling of pre-mRNA binding proteins between nucleus and cytoplasm. Nature **355**:730-732.

109. Pitcher, J. A., J. Inglese, J. B. Higgins, J. L. Arriza, P. J. Casey, C. Kim, J. L. Benovic, M. M. Kwatra, M. G. Caron, and R. J. Lefkowitz. 1992. Role of βγ subunits of G proteins in targeting the β-adrenergic receptor kinase to membrane-bound receptors. Science **257**:1264-1267.

110. Pringle, J. R., and L. H. Hartwell. 1981. *The Saccharomyces cerevisiae life cycle*, in *The Molecular Biology of the Yeast Saccharomyces cerevisiae*, J. Strathern, E.W. Jones, andJ.R. Broach, Editors. Cold Spring Harbor Laboratory, Cold Spring Harbor, NY. p. 97-142.

111. Pringle, J. R., R. A. Preston, A. E. Adams, T. Stearns, D. G. Drubin, B. K. Haarer, and E. W. Jones. 1989. Fluorescent Microscopic Methods for Yeast. Meth. Cell Biol. **31**:357-435.

112. Printen, J. A., and G. F. Sprague, Jr. 1994. Protein-protein interactions in the yeast pheromone response pathway: Ste5p interacts with all members of the MAP kinase cascade. Genetics **138**:609-619.

113. Pryciak, P. M., and L. H. Hartwell. 1996. *AKR1* encodes a candidate effector of the Gβγ complex in the *Saccharomyces cerevisiae* pheromone response pathway and contributes to control of both cell shape and signal transduction. Mol. Cell. Biol. **16**:2614-2626.

114. Ramer, S. W., and R. W. Davis. 1993. A dominant trucation allele identifies a gene, *STE20*, that encodes a putative protein kinase necessary for mating in *Saccharomyces cerevisiae*. Proc. Natl. Acad. Sci. USA **90**:452-456.

115. Rasenick, M. M., N. Wang, and K. Yan. 1990. Specific associations between tubulin and G proteins: participation of cytoskeletal elements in celular signal transduction. Adv. Second Messenger Phosphoprotein Res. **24**:381-386.

116. Raths, S., J. Rohrer, F. Crausaz, and H. Riezman. 1993. *end3* and *end4*: Two mutants defective in receptor-mediated and Fluid-phase endocytosis in *Saccharomyces cerevisiae*. J. Cell Biol. **120**:55-65.

117. Rehm, A., and H. L. Ploegh. 1997. Assembly and Intracellular Targeting of the βγ Subunits of Heterotrimeric G Proteins. J. Cell Biol. **137**:305-317.

118. Reid, B. J., and L. H. Hartwell. 1977. Regulation of mating in the cell cycle of *Saccharomyces cerevisiae*. J. Cell Biol. **75**:355-365.

119. Reneke, J. E., K. J. Blumer, W. E. Courchesne, and J. Thorner. 1988. The carboxy-terminal segment of the yeast α-factor receptor is a regulatory domain. Cell **55**:221-234.

120. Richard, N., S. Iacampo, and A. Cochrane. 1994. HIV-1 Rev is capable of shuttling between the nucleus and cytoplasm. Virology **204**:123-131.

121. Richardson, H. E., C. Wittenberg, F. Cross, and S. I. Reed. 1989. An essential G1 function for cyclin-like proteins in yeast. Cell **59**:1127-1133.

122. Rine, J., and I. Herskowitz. 1987. Four genes responsible for a position effect on expression from *HML* and *HMR* in *Saccharomyces cerevisiae*. Genetics **116**:9-22.

123. Rosenthal, W., A. Antaramian, S. Gilbert, and M. Birnbaumer. 1993. Nephrogenic Diabetes Insipidus. J. Biol. Chem. **268**:13030-13033.

124. Roth, A., and N. G. Davis. 1996. Ubiquitination of the yeast a-Factor receptor. J. Cell Biol. **134**:661-674.

125. Schandel, K. A., and D. D. Jenness. 1994. Direct evidence for ligand-induced internalization of the yeast α-factor pheormone receptor. Mol. Cell. Biol. **14**:7245-7255.

126. Schultz, L. D., and J. D. Friesen. 1983. Nucleotide sequence of the *tcm1* gene (ribosomal protein L3) of *Saccharomyces cerevisiae*. J. Bacteriol. **155**:8-14.

127. Segall, J. E. 1993. Polarization of yeast cells in spatial gradients of α mating factor. Proc. Natl. Acad. Sci. USA **90**:8332-8336.

128. Seiki, M., S. Hattori, Y. Hirayama, and M. Yoshida. 1983. Human adult T-cell leukemia virus: complete nucleotide sequence of the provirus genome integrated in leukemia cell DNA. Proc. Natl. Acad. Sci. **80**:3618-3622.

129. Shaw, P. J., and E. G. Jordan. 1995. *The Nucleolus*, in *Annu. Rev. Cell Dev. Biol.* p. 93-121.

130. Shenker, A., L. Laue, S. Kosugi, J. J. Merendino, T. Minegishi, and G. B. Cutler. 1993. A Constitutively Activating Mutation of the Luteinizing Hormone Receptor in Familial Male Precocious Puberty. Nature **365**:652-654.

131. Shenoy-Scaria, A. M., D. J. Dietzen, J. Kwong, D. C. Link, and D. M. Lublin. 1994. Cysteine of src family kinases determined palmitoylation and localization in caveolae. J. Cell Biol. **126**:

132. Sherman, F., G. R. Fink, and J. B. Hicks. 1989. *Laboratory course manual for methods in yeast genetics*. Cold Spring Harbor Laboratory, Plainview, NY.

133. Snyder, M. 1989. The SPA2 protein of yeast localizes to sites of cell growth. J. Cell Biol. **108**:1419-1429.

134. Snyder, M., and R. W. Davis. 1988. *SPA1*: A gene important for chromosome segregation and other mitotic functions in *S. cerevisiae*. Cell **54**:743-754.

135. Sondek, J., A. Bohm, D. Lambright, H. Hamm, and P. Sigler. 1996. Crystal structure of a G_A protein βγ dimer at 2.1 A resolution. Nature **379**:369-374.

136. Spain, B. H., D. Koo, M. Ramakrishnan, B. Dzudzor, and J. Colicelli. 1995. Truncated forms of a Novel Yeast Protein Suppress the Lethality of a G protein α Subunit Deficiency by Interacting with the β subunit. J. Biol. Chem. **270**:25435-25444.

137. Sprague, G. F., Jr., R. Jensen, and I. Herskowitz. 1983. Control of yeast cell type by the mating type locus: positive regulation of the α-specific *STE3* gene by the *MATα1* product. Cell **32**:409-415.

138. Sprague, G. F., Jr., and J. W. Thorner. 1992. *Pheromone response and signal transduction during the mating process of Saccharomyces cerevisiae*, in *The Molecular and Cellular Biology of the Yeast Saccharomyces: Gene Expression*, E.W. Jones, J.R. Pringle, andJ.R. Broach, Editors. Cold Spring Harbor Laboratory Press, Plainview, NY. p. 657-744.

139. Stevenson, B. J., N. Rhodes, B. Errede, and G. F. Sprague, Jr. 1992. Constitutive mutants of the protein kinase STE11 activate the yeast pheromone response pathway in the absence of the G protein. Genes Dev. **6**:1293-1304.

140. Stone, E. M., and L. Pillus. 1996. Activation of an MAP Kinase Cascade Leads to Sir3p Hyperphosphorylation and Strengthens Transcriptional Silencing. J. Cell Biol. **135**:571-583.

141. Taylor, J. M., G. G. Jacob-Mosier, R. G. Lawton, A. E. Remmers, and R. R. Neubig. 1994. Binding of an α_2 Adrenergic Receptor Third Intracellular Loop Peptide to Gβ and the Amino Terminus of Gα*. J. Biol. Chem. **269**:27618-27624.

142. Taylor, J. M., G. G. Jacob-Mosier, R. G. Lawton, M. VanDort, and R. R. Neubig. 1996. Receptor and Membrane Interaction sites on Gβ. J. Biol. Chem. **271**:3336-3339.

143. Teague, M. A., D. T. Chaleff, and B. Errede. 1986. Nucleotide sequence of the yeast regulatory gene *STE7* predicts a protein homologous to protein kinases. Proc. Natl. Acad. Sci. USA **83**:7371-7375.

144. Trueheart, J., J. D. Boeke, and G. R. Fink. 1987. Two genes required for cell fusion during yeast conjugation: evidence for a pheromone-induced surface protein. Mol. Cell. Biol. **7**:2316-2328.

145. Tyers, M., and B. Futcher. 1993. Far1 and Fus3 link the mating pheromone signal transduction pathway to three G_1-phase Cdc28 kinase complexes. Mol. Cell Biol. **13**:5659-5669.

146. Valtz, N., M. Peter, and I. Herskowitz. 1995. *FAR1* is required for oriented polarization of yeast cells in response to mating pheromones. J. Cell Biol. **131**:863-873.

147. Wesp, A., L. Hicke, J. Palecek, R. Lombardi, T. Aust, A. L. Munn, and H. Riezman. 1997. End4p/Sla2p interacts with actin-associated proteins for endocytosis in *Saccharomyces cerevisiae*. Molecular Biology of the Cell **8**:2291-2306.

148. Whiteway, M., K. L. Clark, E. Leberer, D. Dignard, and D. Y. Thomas. 1994. Genetic Identification of Residues Involved in Association of α and β G-protein Subunits. Mol. Cell. Biol. **14**:3223-3229.

149. Whiteway, M., R. Freedman, S. Van Arsdell, J. W. Szostak, and J. Thorner. 1987. The yeast *ARD1* gene product is required for repression of cryptic mating-type information at the *HML* locus. Mol. Cell. Biol. 7:3713-3722.

150. Whiteway, M., L. Hougan, D. Dignard, D. Y. Thomas, L. Bell, G. C. Saari, F. J. Grant, P. O'Hara, and V. L. MacKay. 1989. The *STE4* and *STE18* genes of yeast encode potential β and γ subunits of the mating factor receptor-coupled G protein. Cell **56**:467-477.

151. Whiteway, M., L. Hougan, and D. Y. Thomas. 1990. Overexpression of the *STE4* gene leads to mating response in haploid *Saccharomyces cerevisiae*. Mol. Cell. Biol. **10**:217-222.

152. Whiteway, M. S., and D. Y. Thomas. 1994. Site-directed mutations altering the CAAX box of Ste18, the yeast pheromone-response pathway Gγ subunit. Genetics **137**:967-976.

153. Whiteway, M. S., C. Wu, T. Leeuw, K. Clark, A. Fourest-Lieuvin, D. Y. Thomas, and E. Leberer. 1995. Association of the yeast pheromone response G protein βγ subunits with the MAP kinase scaffold Ste5p. Science **269**:1572-1575.

154. Wittenberg, C., K. Sugimoto, and S. I. Reed. 1990. G1-specific cyclins of S. cerevisiae: Cell cycle periodicity, regulation by mating pheromone, and association with the $p34^{CDC28}$ protein kinase. Cell **62**:225-237.

155. Wu, C., M. Whiteway, D. Y. Thomas, and E. Leberer. 1995. Molecular characterization of Ste20p, a potential mitogen-activated protein or extracellular signal-regulated kinase kinase (MEK) kinase kinase from *Saccharomyces cerevisiae*. J. Biol. Chem. **270**:15984-15992.

156. Yablonski, D., I. Marbach, and A. Levitzki. 1996. Dimerization of Ste5, a mitogen-activated protein kinase cascade scaffold protein, is required for signal transduction. Proc. Natl. Acad. Sci. **93**:13864-13869.

157. Yu, Y., and J. P. Hirsch. 1995. An essential gene pair in *Saccharomyces cerevisiae* with a potential role in mating. DNA Cell Biol. **14**:411-418.

158. Zanolari, B., S. Raths, B. Singer-Kruger, and H. Riezman. 1992. Yeast pheromone receptor endocytosis and hyperphosphorylation are independent of G protein-mediated signal transduction. Cell **71**:755-763.

159. Ziman, M., D. Preuss, J. Mulholland, J. M. O'Brien, D. Botstein, and D. I. Johnson. 1993. Subcellular localization of Cdc42p, a *Saccharomyces cerevisiae* GTP-binding protein involved in the control of cell polarity. Mol. Biol. Cell **4**:1307-1316.

160. Zwaal, R. R., J. Ahringer, H. G. A. M. van Luenen, A. Rushforth, P. Anderson, and R. H. A. Plasterk. 1996. G proteins are required for spatial orientation of early cell cleavages in C. elegans embryos. Cell **86**:619-629.

IMAGE EVALUATION
TEST TARGET (QA-3)

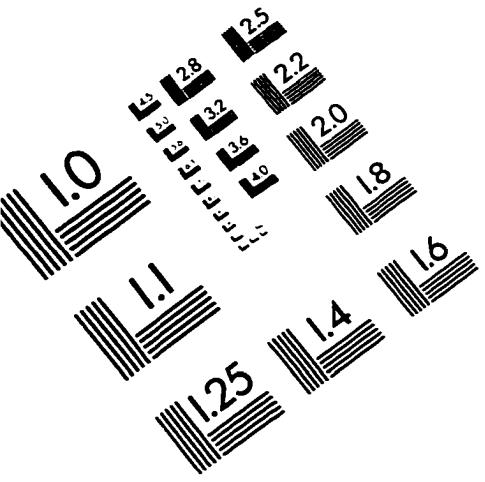

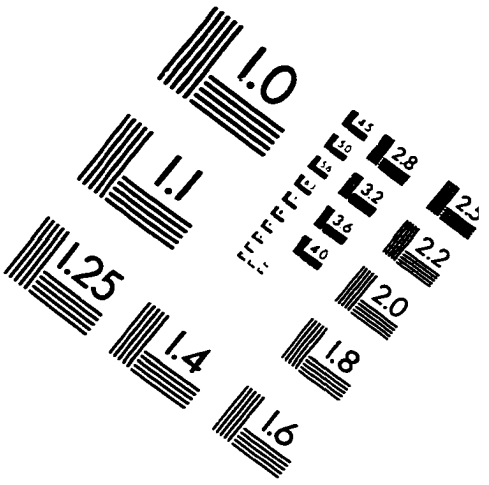

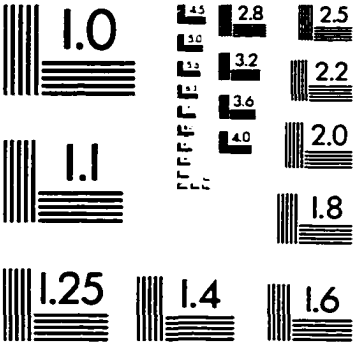

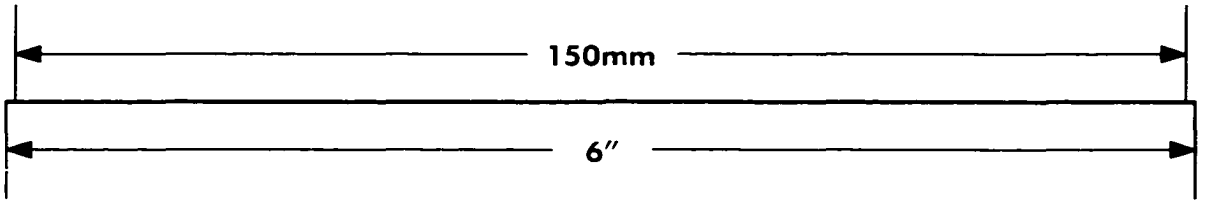

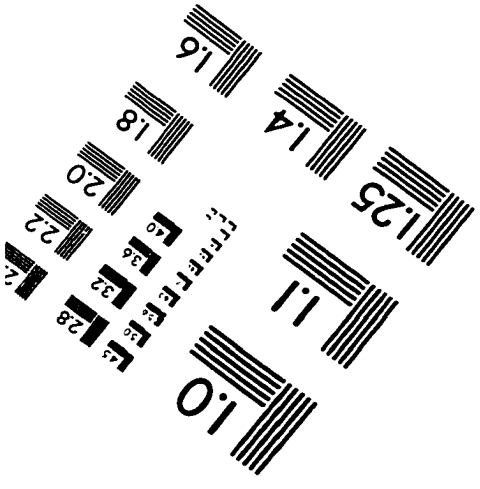

APPLIED IMAGE, Inc
1653 East Main Street
Rochester, NY 14609 USA
Phone: 716/482-0300
Fax: 716/288-5989